Study on Libration Points of the Sun and the Interstellar Medium for Interstellar Travel

Authors: Elena Fantino, Stefano Casotto
Academic Institution: Centro Interdipartimentale Studi ed Attivitá Spaziali (CISAS) “G.Colombo”. Universtitá di Padova.
Approved by: Dario Izzo, Advanced Concepts Team (ESTEC)

Contacts:

Stefano Casotto
Tel: +39-049-8298224
Fax: +39-049-8759840.
e-mail: casotto@pd.astro.it

Dario Izzo
Tel: ++31 (0)71565 – 3511
Fax: ++31 (0)71565 – 8018
e-mail: act@esa.int

Ariadna id: 03/4102
Study length: 2 months.
Contract Number: 18141/04/NL/MV

Available on the ACT net (www.esa.int/act)

1 INTRODUCTION

The subject of the present study is the analysis of the applicability of recent advances in transfer trajectory design in multi-body systems to the exploration of stars in the Solar Neighborhood. The new design techniques make use of Dynamical Systems Theory and have been recently given some publicity under the general term of "Interplanetary Superhighways" (Koon et al., 2001; Howell et al., 1997). The main advantage of these new techniques is that they exploit the dynamical characteristics of multi-body systems to identify transfer trajectories requiring very low energy input, which would otherwise go unobserved if classical two-body transfer techniques were applied.

The approach adopted in this study has been to first identify the dynamical character of the possible targets of stellar exploration both as subsystems (double, triple, etc. stellar systems) and possibly in combination with our Sun. The second part of the study was then addressed to investigating the applicability of the new techniques to the different contexts.

The study was conducted over a period of two months during April and May, 2004. Given this constraint, the study constitutes only a first attempt at the definition of analysis and design techniques applicable to interstellar exploration carried out using only the software tools accessible to the study team and not requiring further major development.

The first part of this report addresses the preliminary phase in which information about the Solar Neighborhood has been collected. This part has been particularly time consuming since the data sources are many and generally incomplete in several respects, making it necessary to merge information of differing quality, scope and accuracy. It must be realized, however, that stellar catalogues are a difficult business, since they have to extract information from the original observation records, published papers, other repertories, etc. which themselves suffer from the same inconsistencies and limitations just mentioned. This first task has at times required our intervention in terms of making the data consistent. This may happen for instance when the masses and the periods of double stars have to be merged from different sources, in which case either the periods must be recomputed or the masses redetermined, under the assumption that the mutual distance (or semimajor axis) is correct.

A list of all stars and star systems within a sphere of 6.7 parsecs has been produced. All binary, triple, quadruple and quintuple systems present in these first 77 objects have been identified. Specific information regarding the dynamical characteristics of 13 binaries, 2 triples and 2 planetary systems have been collected and discussed. In order to generate the initial conditions for numerical integration of the orbits of the individual stars and star systems, the position and velocity information have been appropriately processed and transformed into the required form. This finally brought to an understanding of the dynamical behaviour of the stars in the Solar Neighbourhood.

The second phase of the study addresses the design of transfer orbits to the nearby stars or star systems as well as transfers within target multi-body systems. The analysis is carried out with a view to the applicability in each case of the known paradigms, like the Circular Restricted Three-Body Problem, the Problem of the Two Fixed Centers (Whittaker, 1937), etc., clarifying when these are indeed an acceptable approximation and when the models have to be left aside and new directions explored.

Space missions to the stars have been considered for a long time and studies have been carried out even recently tryng to define the actual possibilities for the exploration of the Solar Neighborhood (McNutt, 2003). One of the fundamental questions, apart from the necessary technological advancements, is the limitations to be imposed on the length of the mission. Current wisdom holds that an acceptable duration is limited to a few human generations. This makes it possible for the designers and all involved in planning the mission to enjoy the wealth of information sent back to Earth by an automatic probe.

2 THE SOLAR NEIGHBOURHOOD

2.1 Catalogue comparisons: completeness of the data, accuracies, magnitude limits, sky coverage

For the purpose of the present study we define the solar neighbourhood as the volume of space centered at the Sun and occupied by stars with parallax > 150 mas (i.e. within 6.7 pc from the Sun) (approximately represented in Figure 1).

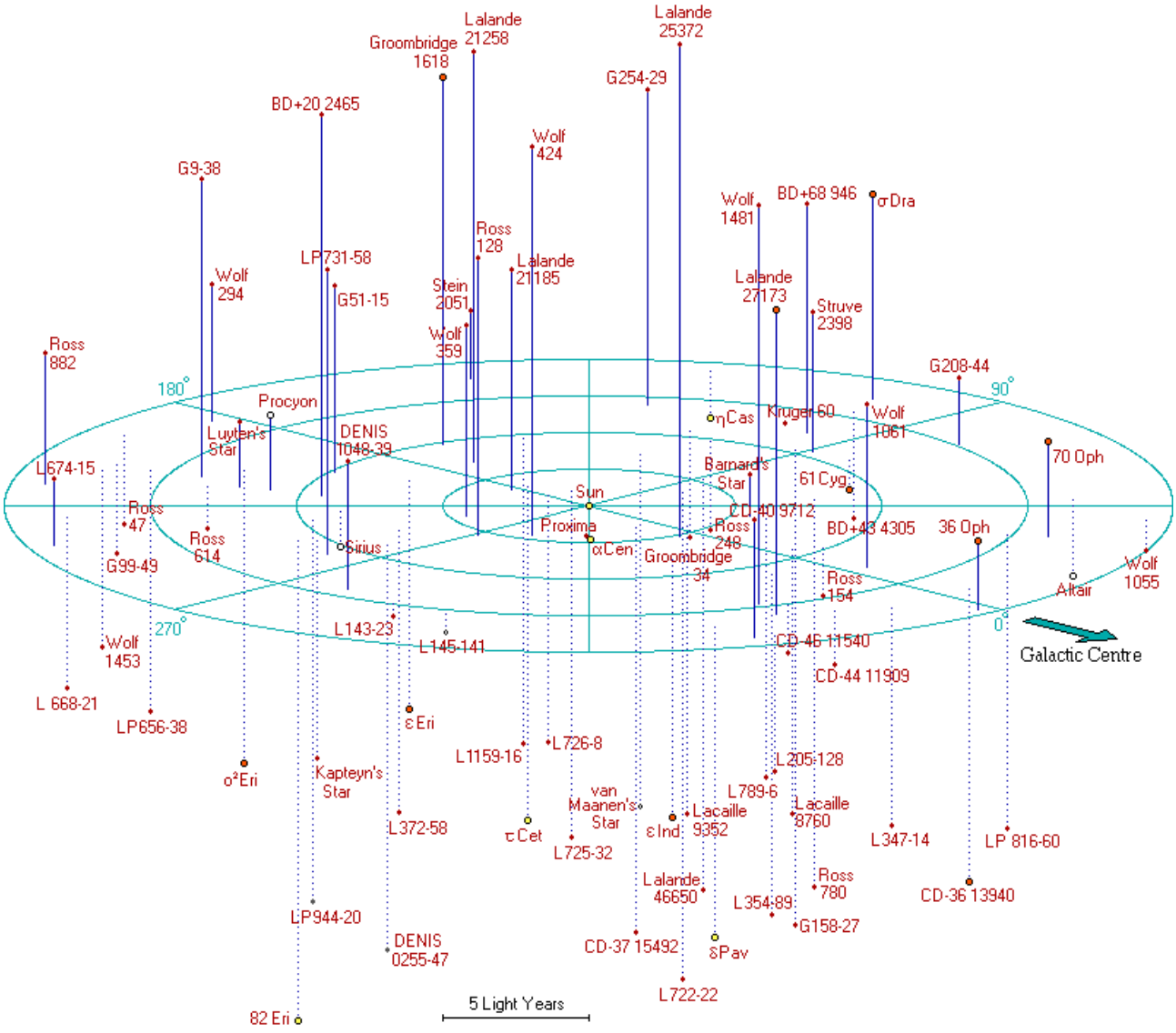

Figure 1: The stars within 20 ly (= 6.13 parsecs) from the Sun (Hipparcos and Tycho Catalogue, 3rd Gliese Catalogue).

We looked for a star catalogue capable of providing the most complete and accurate information for the largest number of stars within the given volume. In particular we were interested in: positional information (coordinates, parallaxes), kinematic data (proper motions, radial velocities) and stellar masses. We compared the following catalogues:

- Nearby Stars, Preliminary 3rd Version (Jahreiss & Gliese, 1985; Gliese & Jahreiss, 1989; Jahreiss & Gliese, 1989; Gliese & Jahreiss, 1991a; Gliese & Jahreiss, 1991b; Jahreiss & Gliese, 1993) which contains photometric, astrometric and spectroscopic data for stars within 25 parsecs of the Sun. It largely depends on a preliminary version (Spring 1989) of the new General Catalogue of Trigonometric Parallaxes (YPC) prepared by Dr. William F. van Altena (Yale University). The Gliese Catalogue lists 122 objects in the parallax range > 150 mas.
- Hipparcos & Tycho: the Hipparcos satellite mission provided for 118,300 pre-selected stars the five astrometric parameters with an average formal error of 1.6 milli arcsec. For a full description of the data products the reader is referred to ESA (1997) and to the review published by van Leeuwen (1997). Here we would like to recall the limiting magnitude (V ≈ 12.4 mag) and the completeness (up to V = 7.3-9.0 mag) of the main (Hipparcos) catalogue. The number of entries in the parallax range > 150 mas is 84.
- Zakhozhaj Catalogue of Nearest stars until 10 pc (Zakhozhaj, 1998): it presents the stars with trigonometric, photometric and spectral parallaxes > 100 mas. The catalogue also contains data on components of multiple visual systems, on components of spectral-binary systems and on invisible components with masses > 0.08 solar masses. The catalogue provides the main characteristics of stars such as the positions, proper motions, radial velocities, parallaxes, photometrical data and also masses and radii of stars. The completeness of the catalogue is about 70%. It lists 122 objects with parallax larger than 150 mas. We were unable to identify the source of the data and the information on the errors.
- NStars Database (Henry et al., 2000): the NStars research project was initiated in 1998 and is based at the Northern Arizona University. Its objective is to provide the most current, complete and accurate source of scientific data about all stellar objects within the radius of 25 parsecs. At present this includes approximately 2,600 stars. The RECONS programme is part of the NStars project and constitutes the most complete dataset of stars within 10 parsecs of the Sun. The information listed in the RECONS database is obtained by combining data from different catalogues and authors, most noticeably: the Hipparcos Catalogue (ESA, 1997), the Yale Parallax Catalog (Van Altena & Hoffleit, 1996), Söderhjelm (1999) and Tinney (1996) for the parallaxes; other quantities (proper motions, masses) are derived from the works published by Ducourant et al. (1998), Geballe et al. (2002), Scholz et al. (2003) and by the work of the RECONS research group itself. The RECONS database contains 140 objects closer than 6.7 pc.

The comparison among the above catalogues and databases suggested the adoption of the NStars Database to collect positions, parallaxes, proper motions and mass data, and the Gliese Catalogue for radial velocities. We compiled a database (see Table 1) that we used for all later computations. Missing data (always radial velocities and/or mass determinations) in Table 1 are replaced by large numbers (999) for computational reasons, flagged in red and excluded from subsequent reductions. Errors are explicitly reported only for parallax determinations; for the proper motions one should recover the sources of each entry among those cited above; the estimated mass (in units of the Sun's mass) of a star is based upon the M_V (absolute magnitude) value and the empirical mass-luminosity relations of Henry & McCarthy (1993): when an object is too faint for the relations to be applicable (fainter than Mv = 20.00) a mass of 0.5 is always listed (this is typically the case of white dwarfs).

The NStars Project web page offers some statistics regarding the astrometric properties of the nearby stars which we report in Figure 2, Figure 3, Figure 4 and Figure 5.

We have not been able to identify the typical or the average standard errors of the radial velocities published by the Gliese Catalogue.

GLIESE	HIP	common name	n	α (J2000.0)	δ (J2000.0)	Π	Δ Π	μ	PA	M	R_V
				(h m s)	(° ' ")	(")	(")	("/yr)	(°)	(M_{sun})	(Km/s)
-		SUN	1	-	-	-		-	-	1.000	-
GL 551	70890	Proxima Centauri	1	14 29 43.0	-62 40 46	0.77199	0.00225	3.853	281.5	0.107	-16.000
GL 559	71683	alpha Centauri A	2	14 39 36.5	-60 50 02	0.74723	0.00117	3.710	277.5	1.144	-26.200
GL 559	71681	alpha Centauri B	2	14 39 35.1	-60 50 14	0.74723	0.00117	3.724	284.8	0.916	-18.100
GL 699	87937	Barnard's Star	1	17 57 48.5	04 41 36	0.54698	0.00100	10.358	355.6	0.166	-111.000
GL 406		Wolf 359	1	10 56 29.2	07 00 53	0.41910	0.00210	4.696	234.6	0.092	13.000
GL 411	54035	Lalande 21185	1	11 03 20.2	35 58 12	0.39342	0.00070	4.802	186.9	0.464	-84.300
GL 244	32349	Sirius A	2	06 45 08.9	-16 42 58	0.38002	0.00128	1.339	204.1	1.991	-9.400
GL 244		Sirius B	2	06 45 08.9	-16 42 58	0.38002	0.00128	1.339	204.1	0.500	-9.400
GL 65		UV Ceti	2	01 39 01.3	-17 57 01	0.37370	0.00270	3.368	80.4	0.109	29.000
GL 65		BL Ceti	2	01 39 01.3	-17 57 01	0.37370	0.00270	3.368	80.4	0.102	32.000
GL 729	92403	Ross 154	1	18 49 49.4	-23 50 10	0.33690	0.00178	0.666	106.8	0.171	-12.100
GL 905		Ross 248	1	23 41 54.7	44 10 30	0.31600	0.00110	1.617	177.0	0.121	-77.700
GL 144	16537	epsilon Eridani A	2	03 32 55.8	-09 27 30	0.30999	0.00079	0.977	271.1	0.850	16.900
GJ 144		epsilon Eridani B	2	03 32 55.8	-09 27 30	0.30999	0.00079	0.977	271.1	999.000	16.900
GJ 887	114046	Lacaille 9352	1	23 05 52.0	-35 51 11	0.30364	0.00087	6.896	78.9	0.529	9.500
GL 447	57548	Ross 128	1	11 47 44.4	00 48 16	0.29872	0.00135	1.361	153.6	0.156	-31.100
GL 866		EZ Aquarii A	3	22 38 33.4	-15 18 07	0.28950	0.00440	3.254	46.6	0.105	-60.000
GL 866		EZ Aquarii B	3	22 38 33.4	-15 18 07	0.28950	0.00440	3.254	46.6	0.106	-60.000
GL 866		EZ Aquarii C	3	22 38 33.4	-15 18 07	0.28950	0.00440	3.254	46.6	0.095	-60.000
GL 280	37279	Procyon A	2	07 39 18.1	05 13 30	0.28605	0.00081	1.259	214.7	1.569	-4.000
GL 280		Procyon B	2	07 39 18.1	05 13 30	0.28605	0.00081	1.259	214.7	0.500	-4.000
GL 820	104214	61 Cygni A	2	21 06 53.9	38 44 58	0.28604	0.00056	5.281	51.9	0.703	-64.800
GL 820	104217	61 Cygni B	2	21 06 55.3	38 44 31	0.28604	0.00056	5.172	52.6	0.630	-64.300
GL 725	91768	DM+59 1915 A	2	18 42 46.7	59 37 49	0.28300	0.00169	2.238	323.6	0.351	-0.800
GL 725	91772	DM+59 1915 B	2	18 42 46.9	59 37 37	0.28300	0.00169	2.313	323.0	0.259	1.200
GL 15	1475	GX Andromedae	2	00 18 22.9	44 01 23	0.28059	0.00095	2.918	81.9	0.486	12.000
GL 15		GQ Andromedae	2	00 18 22.9	44 01 23	0.28059	0.00095	2.918	81.9	0.163	11.300
GL 845	108870	Eps Indi A	3	22 03 21.7	-56 47 10	0.27584	0.00069	4.704	122.7	0.766	-40.400
GL 845		Eps Indi B	3	22 04 10.5	-56 46 58	0.27584	0.00069	4.823	121.1	0.044	-40.400
GL 845		Eps Indi C	3	22 04 10.5	-56 46 58	0.27584	0.00069	4.823	121.1	0.028	-40.400
GJ 1111		DX Cancri	1	08 29 49.5	26 46 37	0.27580	0.00300	1.29	242.2	0.087	-5.000
GL 71	8102	Tau Ceti	1	01 44 04.1	-15 56 15	0.27439	0.00076	1.922	296.4	0.921	-17.000
GJ 1061		RECONS 1	1	03 36 00.0	-44 30 46	0.27200	0.00140	0.814	117.3	0.113	-20.000
GJ 54.1		YZ Ceti	1	01 12 30.6	-16 59 57	0.26884	0.00295	1.372	61.9	0.136	28.000
GJ 273	36208	Luyten's Star	1	07 27 24.5	05 13 33	0.26376	0.00125	3.738	171.2	0.257	18.200
GJ 191	24186	Kapteyn's Star	1	05 11 40.6	-45 01 06	0.25527	0.00086	8.67	131.4	0.393	245.500
GJ 825	105090	AX Microscopium	1	21 17 15.3	-38 52 03	0.25343	0.00112	3.455	250.6	0.600	28.200
GJ 860	110893	Kruger 60 A	2	22 27 59.5	57 41 45	0.24806	0.00139	0.99	241.6	0.279	-33.300
GJ 860		Kruger 60 B	2	22 27 59.5	57 41 45	0.24806	0.00139	0.99	241.6	0.160	-31.700
DEN1048-3956		RECONS 2	1	10 48 14.7	-39 56 06	0.24790	0.00240	1.515	229.6	0.113	999.000
GJ 234	30920	Ross 614 A	2	06 29 23.4	-02 48 50	0.24434	0.00201	0.93	131.7	0.170	16.700
GJ 234		Ross 614 B	2	06 29 23.4	-02 48 50	0.24434	0.00201	0.93	131.7	0.097	16.700
GJ 628	80824	Wolf 1061	1	16 30 18.1	-12 39 45	0.23601	0.00167	1.189	184.5	0.261	-13.000
GJ 35	3829	WD 0046+051	1	00 49 09.9	05 23 19	0.23188	0.00179	2.978	155.5	0.500	54.000
GJ 1		-	1	00 05 24.4	-37 21 27	0.22920	0.00107	6.1	112.5	0.481	22.900
GJ 473		Wolf 424 A	2	12 33 17.2	09 01 15	0.22790	0.00460	1.811	277.4	0.118	-553.700
GJ 473		Wolf 424 B	2	12 33 17.2	09 01 15	0.22790	0.00460	1.811	277.4	0.118	-553.700
GJ 83.1		TZ Arietis	1	02 00 13.2	13 03 08	0.22480	0.00290	2.097	147.8	0.140	-31.000
LHS 288		-	1	10 44 31.8	-61 11 38	0.22250	0.01130	1.657	348.1	0.105	999.000
GJ 687		-	1	17 36 25.9	68 20 21	0.22049	0.00082	1.309	194.2	0.390	-23.200
LHS 292		-	1	10 48 12.6	-11 20 14	0.22030	0.00360	1.644	158.5	0.083	-7.000
GJ 674		-	1	17 28 39.9	-46 53 43	0.22025	0.00159	1.05	146.9	0.361	-10.200
GJ 1245		G 208-044 A	3	19 53 54.2	44 24 55	0.22020	0.00100	0.731	143.1	0.114	999.000
GJ 1245		G 208-045	3	19 53 55.2	44 24 56	0.22020	0.00100	0.731	143.1	0.104	999.000
GJ 1245		G 208-044 B	3	19 53 54.2	44 24 55	0.22020	0.00100	0.731	143.1	0.074	999.000
GJ 440		WD 1142-645	1	11 45 42.9	-64 50 29	0.21657	0.00201	2.688	97.4	0.500	999.000
GJ 1002		-	1	00 06 43.8	-07 32 22	0.21300	0.00360	2.041	203.6	0.109	-42.000
GJ 876	113020	Ross 780	3	22 53 16.7	-14 15 49	0.21259	0.00196	1.174	125.1	0.273	-1.500
GJ 876		-	3	22 53 16.7	-14 15 49	0.21259	0.00196	1.174	125.1	999.000	-1.500
GJ 876		-	3	22 53 16.7	-14 15 49	0.21259	0.00196	1.174	125.1	999.000	-1.500
GJ 412		-	2	11 05 28.6	43 31 36	0.20602	0.00108	4.511	282.1	0.483	68.800
GJ 412		WX Ursae Majoris	2	11 05 30.4	43 31 18	0.20602	0.00108	4.531	281.9	0.099	68.800
GJ 380		-	1	10 11 22.1	49 27 15	0.20581	0.00067	1.452	249.7	0.642	-25.400

GJ 388		-	1	10 19 36.4	19 52 10	0.20460	0.00280	0.506	264.0	0.393	12.300
GJ 832		-	1	21 33 34.0	-49 00 32	0.20278	0.00132	0.819	183.2	0.503	4.100
LP 944-020		-	1	03 39 35.2	-35 25 41	0.20140	0.00420	0.439	47.6	0.066	999.000
GJ 682		-	1	17 37 03.7	-44 19 09	0.19965	0.00230	1.176	217.1	0.213	-60.000
GJ 166	19849	omicron 2 Eridani	3	04 15 16.3	-07 39 10	0.19900	0.00077	4.088	213.2	0.887	-42.700
GJ 166		-	3	04 15 22.0	-07 39 35	0.19900	0.00077	4.073	212.4	0.500	-21.000
GJ 166		-	3	04 15 22.0	-07 39 35	0.19900	0.00077	4.073	212.4	0.195	-45.900
GJ 873	112460	EV Lacertae	1	22 46 49.7	44 20 02	0.19804	0.00161	0.841	236.9	0.285	-0.500
GJ 702	88601	70 Ophiuchi A	2	18 05 27.3	02 30 00	0.19596	0.00087	0.971	172.6	0.924	-6.900
GJ 702		70 Ophiuchi B	2	18 05 27.3	02 30 00	0.19596	0.00087	0.971	172.6	0.701	-10.000
GJ 768	97649	Altair	1	19 50 47.0	08 52 06	0.19497	0.00086	0.661	54.3	1.710	-26.100
GJ 1116		EI Cancri	2	08 58 14.9	19 45 43	0.19120	0.00250	0.874	267.7	0.108	-34.000
GJ 1116		-	2	08 58 14.9	19 45 49	0.19120	0.00250	0.874	267.7	0.095	-34.000
G 099-049		-	1	06 00 03.6	02 42 20	0.18620	0.01010	0.241	108.0	0.195	999.000
GJ 445		-	1	11 47 41.4	78 41 28	0.18584	0.00139	0.885	57.1	0.240	-112.200
GJ 1005	1242	-	2	00 15 28.1	-16 08 02	0.18582	0.00297	0.955	130.3	0.177	-29.000
GJ 1005		-	2	00 15 28.1	-16 08 02	0.18582	0.00297	0.955	130.3	0.105	-29.000
GJ 526		-	1	13 45 43.8	14 53 29	0.18421	0.00116	2.298	129.3	0.526	16.100
LHS 1723		RECONS 3	1	05 01 57.0	-06 56 47	0.18270	0.00330	0.786	226.7	0.157	999.000
LP 816-060		-	1	20 52 33.0	-16 58 29	0.18215	0.00368	0.308	275.7	0.193	999.000
GJ 169.1	21088	Stein 2051	2	04 31 11.8	58 58 38	0.18063	0.00078	2.427	147.6	0.224	17.000
GJ 169.1		-	2	04 31 11.8	58 58 38	0.18063	0.00078	2.427	147.6	0.500	17.000
GJ 251		-	1	06 54 49.0	33 16 05	0.17958	0.00161	0.831	241.3	0.334	999.000
2MA1835+3259		-	1	18 35 37.9	32 59 54	0.17650	0.00050	0.759	186.1	999.000	999.000
GJ 754		-	1	19 20 48.0	-45 33 27	0.17520	0.01010	2.945	167.3	0.158	16.000
GJ 205	25878	Wolf 1453	1	05 31 27.4	-03 40 38	0.17517	0.00105	2.228	160.0	0.566	8.500
GJ 764	96100	sigma Draconis	1	19 32 21.6	69 39 40	0.17359	0.00041	1.839	161.0	0.892	28.200
GJ 229	29295	-	2	06 10 34.6	-21 51 53	0.17317	0.00110	0.727	190.9	0.556	5.200
GJ 229		-	2	06 10 34.6	-21 51 53	0.17317	0.00110	0.727	190.9	0.050	5.200
GJ 693		-	1	17 46 34.2	-57 19 09	0.17169	0.00214	1.756	219.6	0.262	-115.000
GJ 752	94761	Wolf 1055	2	19 16 55.3	05 10 08	0.17101	0.00062	1.452	203.5	0.494	36.300
GJ 752		van Biesbroeck 10	2	19 16 58.3	05 09 01	0.17101	0.00062	1.461	203.1	0.073	36.300
GJ 213	26857	Ross 47	1	05 42 09.3	12 29 22	0.17037	0.00309	2.542	128.2	0.196	105.600
GJ 300		-	1	08 12 40.8	-21 33 10	0.16990	0.01500	0.707	177.5	0.166	999.000
GJ 570		-	4	14 57 28.0	-21 24 56	0.16985	0.00082	2.012	149.1	0.764	29.100
GJ 570		-	4	14 57 26.5	-21 24 41	0.16985	0.00082	1.937	149.4	0.548	27.900
GJ 570		-	4	14 57 26.5	-21 24 41	0.16985	0.00082	1.937	149.4	0.346	27.900
GJ 570		-	4	14 57 15.0	-21 21 50	0.16985	0.00082	2.012	149.1	0.050	27.900
GJ 908		-	1	23 49 12.5	02 24 04	0.16851	0.00140	1.388	134.2	0.507	-71.300
GJ 34	3821	eta Cassiopei A	2	00 49 06.3	57 48 55	0.16838	0.00059	1.223	117.2	1.105	8.200
GJ 34		eta Cassiopei B	2	00 49 06.3	57 48 55	0.16838	0.00059	1.223	117.2	0.604	10.500
GJ 588		-	1	15 32 12.9	-41 16 32	0.16836	0.00138	1.564	228.9	0.464	15.400
GJ 285	37766	Ross 882	1	07 44 40.2	03 33 09	0.16754	0.00228	0.568	217.4	0.225	26.800
GJ 663	84405	36 Ophiuchi A	3	17 15 21.0	-26 36 10	0.16751	0.00075	1.238	202.5	0.850	0.500
GJ 663		36 Ophiuchi B	3	17 15 21.0	-26 36 10	0.16751	0.00075	1.238	202.5	0.849	0.900
GJ 664	84478	36 Ophiuchi C	3	17 16 13.4	-26 32 46	0.16751	0.00075	1.222	203.1	0.707	-0.100
GJ 783	99461	-	2	20 11 11.9	-36 06 04	0.16533	0.00090	1.64	163.8	0.822	-129.800
GJ 783		-	2	20 11 11.9	-36 06 04	0.16533	0.00090	1.64	163.8	0.202	-129.800
GJ 139	15510	82 Eridani	1	03 19 55.6	-43 04 11	0.16501	0.00055	3.124	76.6	0.971	86.700
GJ 1221		-	1	17 48 06.7	70 52 29	0.16470	0.00240	1.651	311.0	0.500	999.000
GJ 780	99240	delta Pavonis	1	20 08 43.6	-66 10 55	0.16378	0.00065	1.656	133.0	1.095	-21.700
GJ 268		QY Aurigae A	2	07 10 01.8	38 31 46	0.16293	0.00177	1.045	204.9	0.170	37.900
GJ 268		QY Aurigae B	2	07 10 01.8	38 31 46	0.16293	0.00177	1.045	204.9	0.156	37.900
GJ 555		HN Librae	1	14 34 16.8	-12 31 10	0.16286	0.00261	0.694	329.0	0.220	9.000
GJ 338		-	2	09 14 22.8	52 41 12	0.16213	0.00237	1.634	249.8	0.601	13.700
GJ 338		-	2	09 14 24.7	52 41 11	0.16213	0.00237	1.684	247.1	0.595	14.700
GJ 2130		-	3	17 46 12.6	-32 06 13	0.16177	0.01129	0.324	188.9	0.304	999.000
GJ 2130		-	3	17 46 14.4	-32 06 08	0.16177	0.01129	0.281	196.0	0.187	999.000
GJ 2130		-	3	17 46 14.4	-32 06 08	0.16177	0.01129	0.281	196.0	0.147	999.000
GJ 784		-	1	20 13 53.4	-45 09 50	0.16118	0.00107	0.794	101.6	0.577	-31.100
GJ 581	74995	Wolf 562	1	15 19 26.8	-07 43 20	0.15929	0.00210	1.229	265.4	0.300	-9.400
GJ 896	116132	EQ Pegasi	2	23 31 52.2	19 56 14	0.15772	0.00243	0.558	96.4	0.339	1.100
GJ 896		-	2	23 31 52.2	19 56 14	0.15772	0.00243	0.558	96.4	0.160	-1.200
GJ 661		-	2	17 12 07.9	45 39 57	0.15632	0.00128	1.625	168.4	0.389	-30.000
GJ 661		-	2	17 12 07.9	45 39 57	0.15632	0.00128	1.625	168.4	0.330	-30.000
LHS 3003		-	1	14 56 38.5	-28 09 51	0.15630	0.00300	0.965	210.1	0.077	999.000

G 180-060		-	1	16 31 18.4	40 51 54	0.15600	0.00400	0.358	330.0	0.103	999.000
GJ 223.2		WD 0552-041	1	05 55 09.7	-04 10 17	0.15500	0.00210	2.377	166.6	0.500	999.000
GJ 644		Wolf 630 A	5	16 55 28.8	-08 20 11	0.15497	0.00056	1.208	223.3	0.425	12.100
GJ 644		Wolf 630 B	5	16 55 28.8	-08 20 11	0.15497	0.00056	1.208	223.3	0.309	12.100
GJ 644		van Biesbroeck 8	5	16 55 35.8	-08 23 40	0.15497	0.00056	1.19	222.5	0.080	20.000
GJ 644		Wolf 630 C	5	16 55 28.8	-08 20 11	0.15497	0.00056	1.208	223.3	0.299	20.000
GJ 643	82809	Wolf 629	5	16 55 25.2	-08 19 21	0.15497	0.00056	1.21	222.3	0.194	999.000
GJ 892		-	1	23 13 17.0	57 10 06	0.15341	0.00054	2.095	81.9	0.812	999.000
GJ 1156		GL Virginis	1	12 19 00.3	11 07 31	0.15290	0.00300	1.301	279.1	0.123	999.000
GJ 625		-	1	16 25 24.6	54 18 15	0.15179	0.00101	0.465	111.5	0.372	-12.600
GJ 408		Ross 104	1	11 00 04.3	22 49 59	0.15016	0.00149	0.51	236.7	0.389	999.000

Table 1: Our database of stars with parallax > 150 mas, as listed in the RECONS dataset. For each star the following entries are reported: Gliese index, Hipparcos index, common name (when available), number of components of the system, right ascension and declination (J2000.0), parallax and associated error, proper motion, position angle of proper motion, mass, radial velocity. All data come from the RECONS dataset, except the radial velocity measurements which have been taken from the Gliese Catalogue.

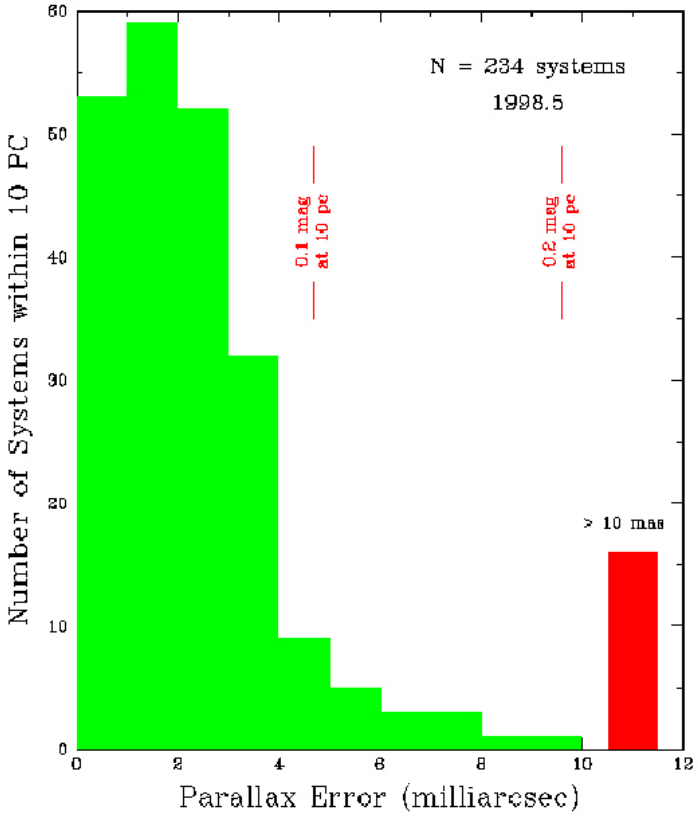

Figure 2: The number of stellar systems within 10 parsecs (234 as of 1998.5) with various errors in the measured trigonometric parallaxes (NStars Project): less than 20 parallax determinations are affected by errors larger than 10 mas which corresponds to a maximum relative error of 10% for stars as far as at 10 pc (i.e., at the edge of the selected volume).

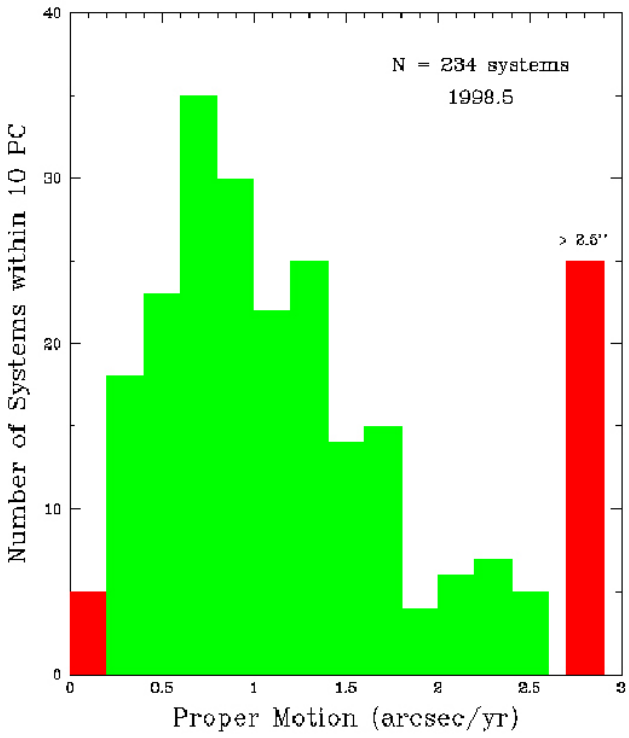

Figure 3: The number of stellar systems within 10 parsecs (234 as of 1998.5) with various amounts of proper motion (NStars Project).

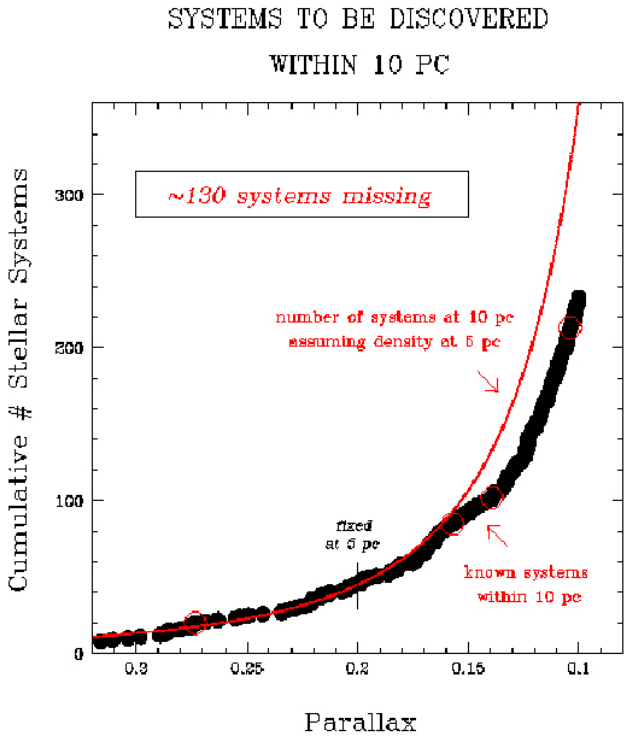

Figure 4: Assuming that the density of stars in a sphere of space surrounding the Sun with a 5 pc radius carries out to 10 pc, 130 systems in the larger sphere are anticipated to be missing from present catalogs (NStars Project). According to this figure within 6.7 pc of the Sun (i.e., parallaxes larger than 150 mas) only a few (of the order of 10) objects are missing.

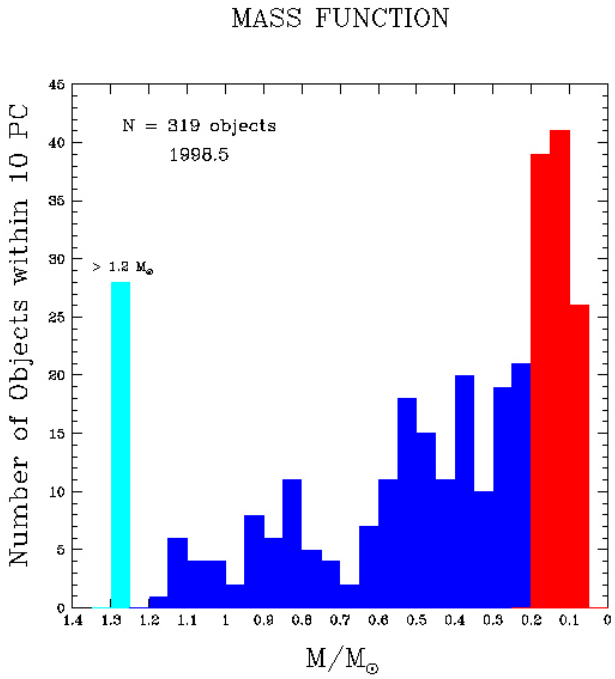

Figure 5: The number of objects known within 10 parsecs (319 as of 1998.5) with various masses in units of the Sun's mass (NStars Project).

name	distance from the Sun		name	distance from the Sun	
	pc	ly		pc	ly
Proxima Centauri	1.2954	4.2229	GJ 380	4.8589	15.8399
alpha Centauri	1.3383	4.3628	GJ 388	4.8876	15.9335
Barnard's Star	1.8282	5.9600	GJ 832	4.9315	16.0765
Wolf 359	2.3861	7.7786	GJ 682	5.0088	16.3286
Lalande 21185	2.5418	8.2863	omicron 2 Eri	5.0251	16.3819
Sirius	2.6314	8.5785	EV Lacertae	5.0495	16.4613
UV Ceti	2.6759	8.7236	70 Ophiuchi	5.1031	16.6360
Ross 154	2.9682	9.6765	Altair	5.1290	16.7205
Ross 248	3.1646	10.3165	EI Cancri	5.2301	17.0502
epsilon Eri	3.2259	10.5165	GJ 445	5.3810	17.5420
Lacaille 9352	3.2934	10.7364	GJ 1005	5.3816	17.5439
Ross 128	3.3476	10.9132	GJ 526	5.4286	17.6972
EZ Aquarii	3.4542	11.2608	Stein 2051	5.5362	18.0479
Procyon	3.4959	11.3966	GJ 754	5.7078	18.6073
61 Cygni	3.4960	11.3970	Wolf 1453	5.7087	18.6105
DM+59 1915	3.5336	11.5194	sigma Draconi	5.7607	18.7799
GX Andromedae	3.5639	11.6184	GJ 229	5.7747	18.8254
Eps Indi	3.6253	11.8184	GJ 693	5.8245	18.9877
DX Cancri	3.6258	11.8202	Wolf 1055	5.8476	19.0632
Tau Ceti	3.6444	11.8809	Ross 47	5.8696	19.1348
RECONS 1	3.6765	11.9853	GJ 570	5.8875	19.1934
YZ Ceti	3.7197	12.1262	GJ 908	5.9344	19.3460
Luyten's Star	3.7913	12.3597	eta Cassiopei	5.9389	19.3610
Kapteyn's Star	3.9174	12.7708	GJ 588	5.9397	19.3633
AX Microscopium	3.9459	12.8635	Ross 882	5.9687	19.4580
Kruger 60	4.0313	13.1420	36 Ophiuchi	5.9698	19.4615
Ross 614	4.0927	13.3421	GJ 783	6.0485	19.7181
Wolf 1061	4.2371	13.8130	82 Eridani	6.0602	19.7564
WD 0046+051	4.3126	14.0590	delta Pavonis	6.1058	19.9048
GJ 1	4.3630	14.2234	QY Aurigae	6.1376	20.0086
Wolf 424	4.3879	14.3045	HN Librae	6.1402	20.0172
TZ Arietis	4.4484	14.5018	GJ 338	6.1679	20.1073
GJ 687	4.5354	14.7853	GJ 784	6.2042	20.2258
LHS 292	4.5393	14.7980	Wolf 562y	6.2779	20.4658
GJ 674	4.5403	14.8014	EQ Pegasi	6.3403	20.6695
GJ 1002	4.6948	15.3052	GJ 661	6.3971	20.8547
Ross 780	4.7039	15.3347	Wolf 630	6.4529	21.0363
WX Ursae Maj	4.8539	15.8237	GJ 625	6.5880	21.4770

Table 2: Star distances from the Sun, expressed in parsecs (pc) and light years (ly).

2.2 Double and multiple stellar systems information

Of the 140 + 1 (= the Sun) stars that constitute our database, 33 form multiple systems (24 binaries, 7 triples, 1 quadruple and 1 quintuple system). In many cases the source catalogues do not resolve the astrometric parameters of the system members and one must search for the required information in the specialized literature. Unfortunately, as we shall discuss later, many systems do not yet have accurate determinations of their astrometric parameters, and in some cases these cannot be distinguished from those of their companions.

The Gliese Catalogue does not always provide radial velocity determinations for the companions of the main star within a multiple system: under these circumstances we have assigned to the companions the radial velocity of the corresponding primary (and the value is coloured in blue in Table 1).

Orbital parameters for 235 binary systems are published in the Hipparcos Catalogue, 1811 in the Sixth Orbit Catalog of Visual Binary Stars of the U.S. Naval Observatory (Hartkopf, Mason & Worley, 2001) which combines, merges and classifies data from various catalogues and authors. We have been able to extract from the latter catalogue orbital elements[1] for 13 binaries of our database.

Table 3 reports the period P, the semi-major axis a, the inclination i with respect to the tangent plane to the celestial sphere through the object, the position of the ascending node Ω, the epoch T, the eccentricity e and the argument of perigee ω of these systems. Individual values for the masses of the components are not provided; however, the total mass of the system, as derived by applying the third Kepler's law to the given period and semi-major axis (after transformation from angular to linear units by means of the parallax value contained in our database), in general is not consistent with the sum of the masses provided by NStars and included in our database. We removed this difficulty by ignoring the published value of the period and by computing a new one on the basis of the semi-major axis and our values of the masses (see

Table 4, which reports the semi-major axes in linear units, the masses of the system members as in our database and the derived values of the period).

HIP	Name	P	a	i	Ω	T	e	ω	SOURCE
		years	arcsec	deg	deg	year		deg	
71683	alpha Centauri	79.914	17.575	79.21	204.85	1875.663	0.5179	231.651	6th Orbit Catalogue
32349	Sirius	50.090	7.500	136.53	44.57	1894.130	0.5923	147.270	6th Orbit Catalogue
	UV Ceti = L 726-8	26.520	1.950	127.30	150.50	1971.910	0.6200	285.300	Geyer et al., 1988
37279	Procyon	40.820	4.271	31.10	97.30	1967.970	0.4070	92.200	6th Orbit Catalogue
104214	61 Cygni	4.900	0.140	134.00	94.00	1953.200	0.5000	295.000	6th Orbit Catalogue
91768	DM+59 1915	408.000	13.880	66.00	136.90	1775.000	0.5300	234.600	6th Orbit Catalogue
1475	GX Andromedae	2600.000	41.150	61.40	45.30	1745.000	**0.0000**	0.000	6th Orbit Catalogue
110893	Kruger 60	44.670	2.383	167.20	154.50	1970.220	0.4100	211.000	6th Orbit Catalogue
30920	Ross 614	16.124	1.040	51.80	30.70	1999.380	0.3710	223.000	6th Orbit Catalogue
88601	70 Ophiuchi	88.380	4.554	121.16	302.12	1895.940	0.4992	14.000	6th Orbit Catalogue
1242	GJ 1005	4.566	0.304	146.00	62.60	1995.366	0.3640	346.400	6th Orbit Catalogue
3821	eta Cassiopei	480.000	11.994	34.76	278.42	1889.600	0.4970	268.590	6th Orbit Catalogue
116132	EQ Pegasi	359.000	6.870	123.50	82.10	2008.000	0.2000	354.000	6th Orbit Catalogue

Table 3: Orbital elements of 13 binary systems present in our dataset. The source is the Sixth Orbit Catalog of Visual Binary Stars of the U.S. Naval Observatory, except for the case of UV Ceti (L 726-8) for which data have been obtained from the paper published by Geyer et al. (1988).

[1] The Sixth Orbit Catalog of Visual Binaries lists orbital parameters of binary stars according to their HIP index. The relation with indices of other catalogues is also provided but the link to the Gliese Catalogue (of which RECONS adopts the numbering) does not appear. Therefore the identification of the binary systems which appear in our database depends on the existence (and availability) of a correspondence between HIP and Gliese numbers.

Name	m_1	m_2	a	P
	M_{sun}	M_{sun}	AU	years
alpha Centauri	1.144	0.916	23.52	79.475
Sirius	1.991	0.500	19.74	55.551
UV Ceti = L 726-8	0.109	0.102	5.22	25.949
Procyon	1.569	0.500	14.93	40.297
61 Cygni	0.703	0.630	0.50	0.297
DM+59 1915	0.351	0.259	49.05	439.784
GX Andromedae	0.486	0.163	146.66	2204.571
Kruger 60	0.279	0.160	9.61	44.939
Ross 614	0.170	0.097	4.23	16.994
70 Ophiuchi	0.924	0.701	23.24	87.884
GJ 1005	0.177	0.105	1.64	3.940
eta Cassiopei	1.105	0.604	71.23	459.874
EQ Pegasi	0.339	0.160	43.56	406.963

Table 4: The masses of the members of the 13 binary systems of the previous table, the semi-major axes in linear units and the orbital periods as obtained by applying the third Kepler's law.

2.3 From catalogue data to space positions and velocities

Starting from the raw data of Table 1 and by means of basic astrometric formulas (Zagar, 1984; Smart, 1931), we computed the stellar distances from the Sun and the cartesian components of the heliocentric positions (x_E,y_E,z_E) and velocities (u_E,v_E,w_E) in the J2000.0 equatorial reference system expressed in parsecs and in km/s respectively:

$$\begin{aligned} x_E &= \frac{1}{\pi}\cos\delta\cos\alpha \\ y_E &= \frac{1}{\pi}\cos\delta\sin\alpha \\ z_E &= \frac{1}{\pi}\sin\delta \end{aligned} \qquad (1)$$

$$\begin{aligned} u_e &= -\frac{k}{\pi}\mu_\alpha\sin\alpha\cos\delta - \frac{k}{\pi}\mu_\delta\cos\alpha\sin\delta + v_R\cos\alpha\cos\delta \\ v_e &= +\frac{k}{\pi}\mu_\alpha\cos\alpha\cos\delta - \frac{k}{\pi}\mu_\delta\sin\alpha\sin\delta + v_R\sin\alpha\cos\delta \\ w_e &= +\frac{k}{\pi}\mu_\delta\cos\delta + v_R\sin\delta \end{aligned} \qquad (2)$$

μ_α and μ_δ are the proper motion in right ascension and declination respectively (in arcsec/yr), π is the parallax (arcsec) and v_R is the radial velocity (km/s). k (approximately equal to 4.74) is a conversion factor from AU/yr to km/s.

Following the derivation made by Murray (1989), the direction to the galactic pole in the J2000.0 equatorial system is $\alpha_G = 12^h51^m26.2755^s$; $\delta_G = 27^\circ7'41.704''$. By pre-multiplying the vector (x_E,y_E,z_E) of equatorial position by the matrix N_{J2000} of the direction cosines of the principal galactic axes in the equatorial system referred to equinox and equator of J2000

$$N_{J2000} = \begin{bmatrix} -0.054875539 & -0.873437105 & -0.483834992 \\ +0.494109454 & -0.444829594 & +0.746982249 \\ -0.867666136 & -0.198076390 & +0.455983795 \end{bmatrix}, \qquad (3)$$

we obtained the J2000.0 galactic components (x_G, y_G, z_G) of the star's position. In the same way we computed the J2000.0 galactic components (u_G, v_G, w_G) of the star's velocity from (u_E, v_E, w_E).

The results are summarized in Table 5, which gives the name, the mass and the cartesian heliocentric galactic components of position and velocity of each star. In this respect note that each multiple system has been treated as a single object (with the total mass of the system concentrated in its barycentre) in the context of the overall kinematics and dynamics of the solar neighbourhood; individual members of a stellar system are resolved only when dealing with the internal dynamics of the system.

Star name	Mass	x_G	y_G	z_G	u_G	v_G	w_G
	(Msun)	(pc)	(pc)	(pc)	(km/s)	(km/s)	(km/s)
Sun	1.000	0.0000	0.0000	0.0000	0.0000	0.0000	0.0000
Proxima Centauri	0.107	0.8983	-0.9322	-0.0436	-25.0535	-2.5416	13.5058
alpha Centauri	2.060	0.9583	-0.9340	-0.0159	-29.5921	1.7868	13.6440
Barnard's Star	0.166	1.5200	0.9136	0.4442	-141.5593	4.5502	18.1865
Wolf 359	0.092	-0.5819	-1.1961	1.9809	-26.1342	-44.2696	-18.7476
Lalande 21185	0.464	-1.0526	-0.0943	2.3117	46.0142	-53.6332	-73.9268
Sirius	2.491	-1.7654	-1.9085	-0.4067	15.5544	0.9537	-11.1752
UV Ceti	0.211	-0.6589	0.0520	-2.5930	-44.1600	-19.5149	-20.5939
Ross 154	0.171	2.8639	0.5726	-0.5299	-13.5685	-1.3087	-6.9666
Ross 248	0.121	-1.0348	2.8448	-0.9222	32.9478	-74.4376	0.0299
epsilon Eri	0.850	-2.0745	-0.5888	-2.3993	-3.8814	7.0210	-21.0898
Lacaille 9352	0.529	1.3365	0.1193	-3.0076	-93.5769	-13.4950	-52.5199
Ross 128	0.156	0.0498	-1.7663	2.8433	17.3102	6.1051	-33.1272
EZ Aquarii	0.306	1.2822	1.3781	-2.8963	-69.3906	-1.0633	40.3337
Procyon	2.069	-2.8336	-1.8899	0.7876	5.3590	-8.4515	-18.7556
61 Cygni	1.333	0.4648	3.4468	-0.3544	-93.3822	-53.7889	-8.7272
DM+59 1915	0.610	0.0400	3.2220	1.4502	-24.8910	-11.5070	26.3745
GX Andromedae	0.649	-1.5178	3.0209	-1.1277	-49.1588	-12.0400	-3.4556
Eps Indi	0.838	2.2174	-0.9784	-2.6960	-80.8710	-40.7147	2.6005
DX Cancri	0.087	-2.9267	-0.8955	1.9440	-5.8515	-6.3244	-21.0490
Tau Ceti	0.921	-1.0312	0.1248	-3.4933	18.8275	29.3881	13.2274
RECONS 1	0.113	-0.6900	-2.1074	-2.9324	3.4566	-0.0283	24.2814
YZ Ceti	0.136	-0.6260	0.3658	-3.6483	-28.4306	-0.3083	-23.7000
Luyten's Star	0.257	-3.1507	-1.9952	0.6827	15.9714	-65.6236	-17.0081
Kapteyn's Star	0.393	-1.0562	-2.9880	-2.3027	19.8737	-288.1694	-52.8391
AX Microscopium	0.600	2.8196	0.1924	-2.7537	63.7112	-19.1513	23.4878
Kruger 60	0.439	-1.0221	3.8996	-0.0002	26.5830	-26.8544	1.0008
Ross 614	0.267	-3.4152	-2.2118	-0.4411	-5.3850	-23.5284	4.7228
Wolf 1061	0.261	3.8737	0.2269	1.7017	-5.4938	-20.3976	-17.1433
WD 0046+051	0.500	-1.2245	1.9688	-3.6363	-11.1414	-28.1933	-75.5553
GJ 1	0.481	1.0192	-0.3009	-4.2316	-75.5562	-97.6697	-34.8649
Wolf 424	0.236	0.4503	-1.3258	4.1585	-91.2845	152.0808	-525.8738
TZ Arietis	0.140	-2.5876	1.6383	-3.2263	14.4017	-51.8465	4.8645
GJ 687	0.390	-0.5755	3.8044	2.4010	29.7659	-20.7592	-3.7954
LHS 292	0.083	-0.5338	-3.3687	2.9953	28.8531	-11.4821	-18.3804
GJ 674	0.361	4.3117	-1.3179	-0.5358	-14.6958	-5.0792	-19.3314
GJ 1002	0.109	-0.0766	1.7778	-4.3445	36.9629	-41.0218	27.9485
Ross 780	0.273	1.4640	1.8742	-4.0584	-12.4088	-19.8262	-11.8934
WX Ursae Maj	0.582	-2.1541	0.4381	4.3276	-123.4714	-5.3758	16.2542
GJ 380	0.642	-2.8914	0.7281	3.8364	-9.4993	-20.4585	-35.4461
GJ 388	0.393	-2.2783	-1.6832	3.9830	-14.8095	-7.6173	3.4032
GJ 832	0.503	3.3434	-0.6394	-3.5682	2.7508	-19.3951	0.3865
GJ 682	0.213	4.8271	-1.2048	-0.5787	-64.2773	-12.6363	9.4609
omicron 2 Eri	1.582	-3.7005	-1.4022	-3.0971	92.4081	-14.6632	-44.9881
EV Lacertae	0.285	-0.9054	4.8346	-1.1418	19.8896	2.8337	-1.5609
70 Ophiuchi	1.625	4.3374	2.4934	1.0058	4.9236	-19.4927	-14.7022
Altair	1.710	3.4073	3.7504	-0.7943	-28.8439	-10.0468	-2.6361
EI Cancri	0.203	-3.7292	-1.9456	3.1084	10.3411	12.7053	-36.8489
GJ 445	0.240	-2.5446	3.3956	3.3090	68.3978	-54.8595	-73.5618
GJ 1005	0.282	0.1360	1.2764	-5.2262	-9.0405	-29.0936	22.5213
GJ 526	0.526	1.6226	-0.2403	5.1748	61.2546	-1.8119	-2.4011
Stein 2051	0.724	-4.6620	2.9015	0.7046	-48.6837	-43.5563	-9.1808
GJ 754	0.158	5.1720	-0.6937	-2.3126	-9.8112	-69.8542	-40.4774
Wolf 1453	0.566	-4.7991	-2.4384	-1.9007	22.2908	-55.7710	-10.2644

sigma Draconi	0.892	-1.0478	5.2422	2.1465	31.2701	44.7722	-18.3956
GJ 229	0.606	-3.6219	-4.1100	-1.8265	11.4974	-12.0743	-12.0693
GJ 693	0.262	5.1243	-2.3564	-1.4537	-118.8336	2.3256	38.1066
Wolf 1055	0.567	4.4428	3.7874	-0.3349	53.5316	-7.1941	-5.0166
Ross 47	0.196	-5.6288	-1.3730	-0.9396	-89.6115	-89.7823	8.3586
GJ 570	1.708	4.6027	-1.8370	3.1787	48.8315	-22.3839	-30.9629
GJ 908	0.507	-0.2015	3.2363	-4.9702	-8.9380	-70.4216	39.6402
eta Cassiopei	1.709	-3.1890	4.9827	-0.5233	-29.7678	-10.0696	-16.7593
GJ 588	0.464	5.1591	-2.6657	1.2480	-6.0376	-46.2846	-0.6094
Ross 882	0.225	-4.7048	-3.4002	1.3891	-19.8001	-22.8652	-7.8753
36 Ophiuchi	2.406	5.9242	-0.1780	0.7149	0.3522	-34.1454	-7.3472
GJ 783	1.024	5.1671	0.4733	-3.1084	-118.7923	-52.2212	47.1550
82 Eridani	0.971	-1.1153	-3.1929	-5.0287	-78.7168	-92.6964	-28.1705
delta Pavonis	1.095	4.4533	-2.5953	-3.2731	-48.6311	-13.4271	-15.0397
QY Aurigae	0.326	-5.7700	0.1053	2.0896	-43.2565	-21.0019	-7.0644
HN Librae	0.220	4.1654	-1.6475	4.1997	-6.6258	2.9830	20.9004
GJ 338	1.196	-4.3794	1.1787	4.1802	-43.6621	-15.1028	-20.5324
GJ 784	0.577	5.1834	-0.4711	-3.3768	-38.7821	1.5610	-2.6084
Wolf 562y	0.300	4.7821	-0.4961	4.0369	-25.0412	-25.6807	11.8899
EQ Pegasi	0.499	-0.7333	4.8625	-4.0023	-13.7274	-7.0423	-6.6151
GJ 661	0.719	1.6569	4.9054	3.7570	39.7425	-31.0176	-28.1099
Wolf 630	1.307	5.9071	1.1530	2.3273	15.5671	-28.5408	9.5466
GJ 625	0.372	0.5715	4.8011	4.4750	8.0238	-2.0662	-17.3578

Table 5: Initial conditions of the motion of the 77 stars of our database derived from the raw astrometric data: positions and velocities are referred to the heliocentric galactic reference frame (J2000.0).

With these data we have analysed various aspects of the stellar distribution in the solar neighbourhood: the mass distribution (Figure 6) shows that only a handful of objects are more massive than the Sun (with Sirius A+B showing the highest mass = 2.7 M_{sun}) and that most stars occupy the mass range below 0.6 M_{sun}.

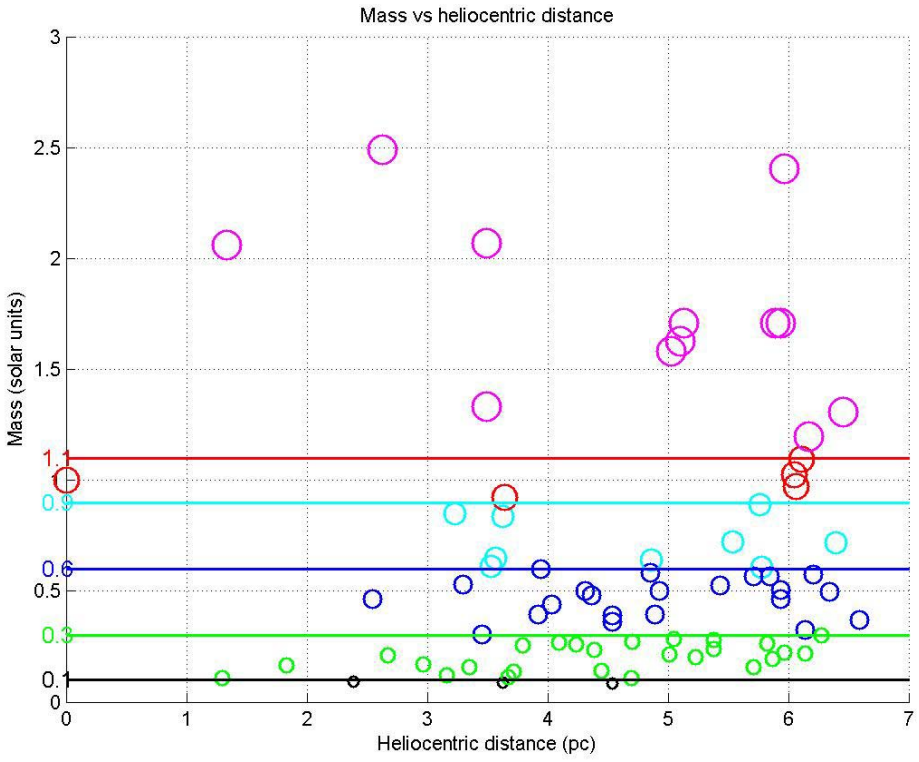

Figure 6: Stellar masses versus heliocentric distances.

The minimum relative distances among the stars (Table 6) range between 0.0661 parsecs (between Alpha Centauri and Proxima) and 2.8300 parsecs (between Stein 2051 and eta Cassiopeiae) with an average of 1.3873 parsecs.

Star name	Closest star	d (pc)		Star name	Closest star	d (pc)
Sun	Proxima Centauri	1.2954		GJ 380	WX Ursae Maj	0.9322
Proxima Centauri	**alpha Centauri**	**0.0661**		GJ 388	EI Cancri	1.7143
alpha Centauri	Proxima Centauri	0.0661		GJ 832	AX Microscopium	1.2766
Barnard's Star	Ross 154	1.6945		GJ 682	GJ 674	0.5295
Wolf 359	Ross 128	1.2116		omicron 2 Eri	Wolf 1453	1.9266
Lalande 21185	Wolf 359	1.2429		EV Lacertae	Kruger 60	1.4803
Sirius	Procyon	1.6023		70 Ophiuchi	Wolf 1055	1.8663
UV Ceti	Tau Ceti	0.9769		Altair	Wolf 1055	1.1334
Ross 154	Barnard's Star	1.6945		EI Cancri	GJ 388	1.7143
Ross 248	GX Andromedae	0.5537		GJ 445	GJ 687	2.2066
epsilon Eri	UV Ceti	1.5659		GJ 1005	GJ 1002	1.0363
Lacaille 9352	EZ Aquarii	1.2649		GJ 526	Wolf 424	1.8936
Ross 128	Wolf 359	1.2116		**Stein 2051**	**eta Cassiopei**	**2.8300**
EZ Aquarii	Lacaille 9352	1.2649		GJ 754	GJ 784	1.0873
Procyon	Luyten's Star	0.3502		Wolf 1453	Ross 47	1.6574
61 Cygni	Kruger 60	1.5942		sigma Draconi	GJ 687	1.5346
DM+59 1915	GJ 687	1.2736		GJ 229	Wolf 1453	2.0459
GX Andromedae	Ross 248	0.5537		GJ 693	GJ 682	1.4765
Eps Indi	AX Microscopium	1.3178		Wolf 1055	Altair	1.1334
DX Cancri	Procyon	1.5280		Ross 47	Wolf 1453	1.6574
Tau Ceti	YZ Ceti	0.4963		GJ 570	HN Librae	1.1268
RECONS 1	Kapteyn's Star	1.1429		GJ 908	GJ 1002	1.5919
YZ Ceti	Tau Ceti	0.4963		eta Cassiopei	EV Lacertae	2.3706
Luyten's Star	Procyon	0.3502		GJ 588	GJ 570	2.1734
Kapteyn's Star	RECONS 1	1.1429		Ross 882	Luyten's Star	2.2109
AX Microscopium	GJ 832	1.2766		36 Ophiuchi	GJ 682	1.9827
Kruger 60	Ross 248	1.4009		GJ 783	GJ 784	0.9819
Ross 614	Luyten's Star	1.1746		82 Eridani	RECONS 1	2.3987
Wolf 1061	36 Ophiuchi	2.3113		delta Pavonis	GJ 693	1.9538
WD 0046+051	GJ 1002	1.3622		QY Aurigae	GJ 338	2.7307
GJ 1	Lacaille 9352	1.3324		HN Librae	GJ 570	1.1268
Wolf 424	Ross 128	1.4436		GJ 338	GJ 380	1.5923
TZ Arietis	WD 0046+051	1.4613		GJ 784	GJ 783	0.9819
GJ 687	DM+59 1915	1.2736		Wolf 562y	HN Librae	1.3163
LHS 292	Ross 128	1.7122		EQ Pegasi	GJ 908	1.9657
GJ 674	GJ 682	0.5295		GJ 661	GJ 625	1.3055
GJ 1002	GJ 1005	1.0363		Wolf 630	36 Ophiuchi	2.0909
Ross 780	EZ Aquarii	1.2766		GJ 625	GJ 661	1.3055
WX Ursae Maj	GJ 380	0.9322				

Table 6: The minimum relative distances among the stars.

2.4 The local interstellar medium

For the sake of completeness, we wish to mention the constituents of the local interstellar medium: gas, dust and dark matter. The gas component is mainly dominated by neutral hydrogen atoms, with a typical number density of 0.10 cm^{-3} around the Sun (Spitzer, 1985). Recent mass density determinations based on Hipparcos data and observations of the line-of-sight velocities of stars suggest that dark matter does not contribute significantly to the local density in the solar neighbourhood (Creze et al., 1998; Kuijken & Gilmore, 1991).

Table 7 summarizes the properties of the local interstellar medium.

Component	Property	Value
Neutral component	Flow speed	25±2 km/s
	Flow direction	λ=75.4° β= -7.5° (ecliptic coordinates)
	Hydrogen density	0.10±0.01 cm^{-3}
	Helium density	0.010±0.003 cm^{-3}
	Hydrogen temperature	(7±2) ·1000° K
	Helium temperature	(7±2) ·1000° K
Ionized component	Electron density	< 0.3 cm^{-3}
	Flow speed	assumed as neutral component
	Flow direction	assumed as neutral component
	Ion temperature	assumed as neutral component
Magnetic field	Magnitude	0.1 – 0.5 nT
	Direction	Unknown
Cosmic rays	Total pressure	(1.3±0.2) 10^{-12} dynes cm^{-2}

Table 7: The main components of the local interstellar medium and their properties (from Axford & Suess, http://web.mit.edu/space/www/helio.review/axford.suess.html).

3 THE DYNAMICS OF THE NEARBY STARS

3.1 N-body motion

The trajectories of the 77 stellar systems of our database were numerically integrated as an isolated system of *N* bodies subject only to their mutual gravitational attractions. The data contained in Table 5 have been used as initial conditions for the numerical integration of the equations of motion. The gravitational effects of the Galaxy as a whole were not included. Computations were run at various step sizes (0.6, 1.0, 10, 100, 1000 years) and over time intervals of variable length (from a few years to million years) . The results conistently show (Figure 7 and Figure 8) that all stars move with constant speed (relative to the Sun). This means that the nearby stars behave as a collisionless system of particles, as predicted by the theorems of galactic hydrodynamics: "[...] a star's galactic orbit is not appreciably disturbed by the gravitational attraction of individual stars [...]" (Roy, 1972); and " [...] the probability of close binary encounters[2] is of the order of 10^{-6}; multiple encounters hardly ever occur and can be neglected [...]".

[2] Roy (1972) defines "close encounters" those which cause a deflection larger than 90 degrees to the initial direction of motion of the two stars. By introducing average values for the star density and peculiar velocity in the Galaxy of 10^{-1} stars per cubic parsec and 20 km/s, he finds that the average time interval between encounters of this type is $3 \cdot 10^{14}$ years, 4 orders of magnitude larger than the age of the Galaxy.

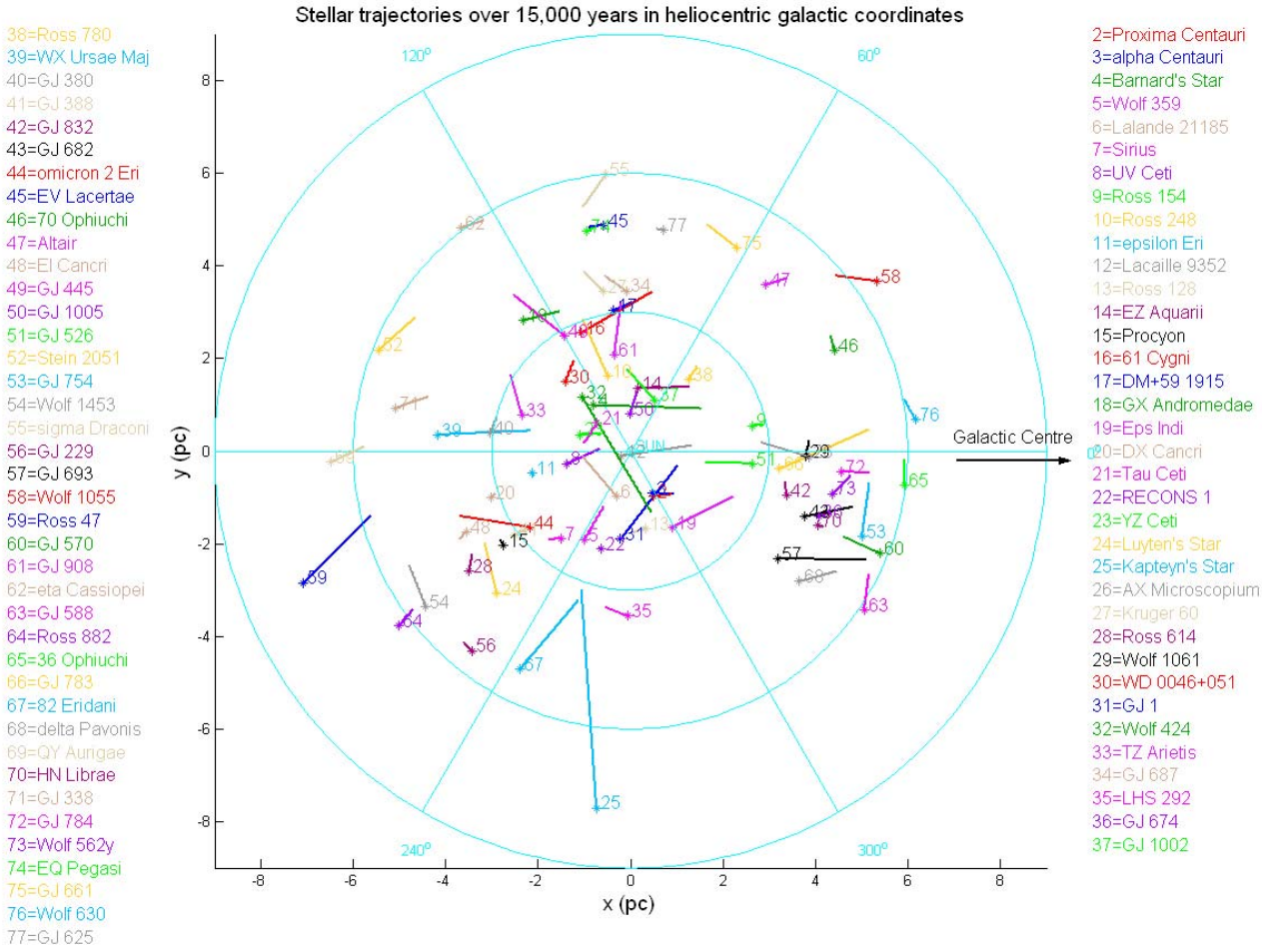

Figure 7: Stellar trajectories as obtained by integration of the N-body equations of motion over 15,000 years. Projected view on the galactic plane.

We did not push our integrations further (in terms of total integration time) because we know that (Binney & Tremaine, 1988) one cannot neglect collisions in a globular cluster which contains 10^5 stars, while for a galaxy of 10^{11} stars the collisional relaxation time turns out to be much larger than the age of the universe and collisions can be neglected.

The most common formalism to describe the large scale stellar dynamic properties in the Galaxy makes use of the collisionless Boltzmann equation which, by means of its moment equations (Jeans equations), approximates the density and velocity distribution of the stars (Binney & Tremaine, 1988).

Figure 9 shows the distances of the nearby stars as a function of time over the next 15,000 years: in a few thousand years Proxima will be “overtaken” by Alpha Cen and for a short time by Barnard’s Star and will cease to be the closest star to our Sun.

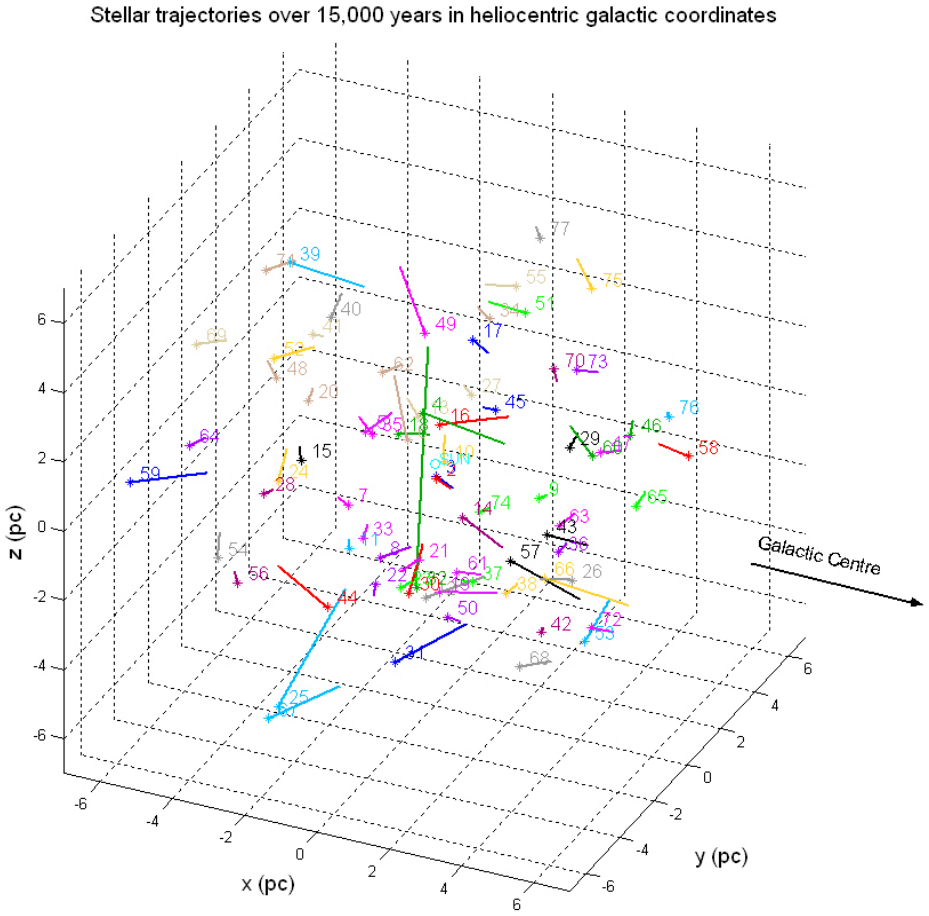

Figure 8: Stellar trajectories as obtained by integration of the N-body equations of motion over 15,000 years. 3-dimensional view in galactic coordinates.

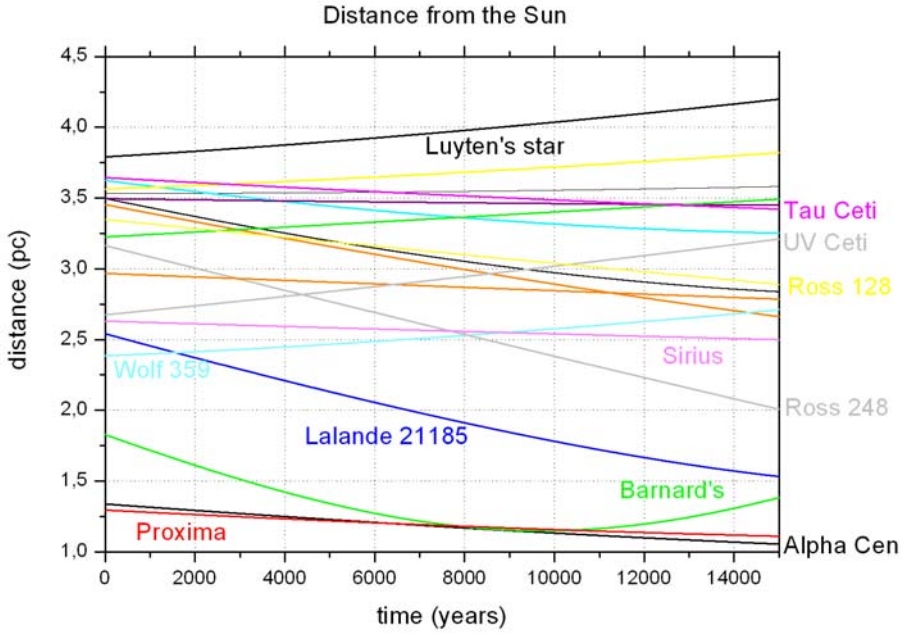

Figure 9: Stellar distances from the Sun as a function of time as obtained from the integration of the N-body equations of motion over 15,000 years.

We determined the relative contributions of the *N* stars to the gravitational acceleration at various positions in the volume of space of 6.7 pc radius around the Sun. We performed the computation over several planes parallel to the galactic plane and equally spaced by 0.5 pc. On each plane the computation grid is 0.05 pc. Figure 10 and Figure 11 show, in terms of a 2D contour map and 3D surface respectively, the acceleration field in the galactic plane ($z = 0$). The plots on several other parallel planes are placed in the Appendix to this report.

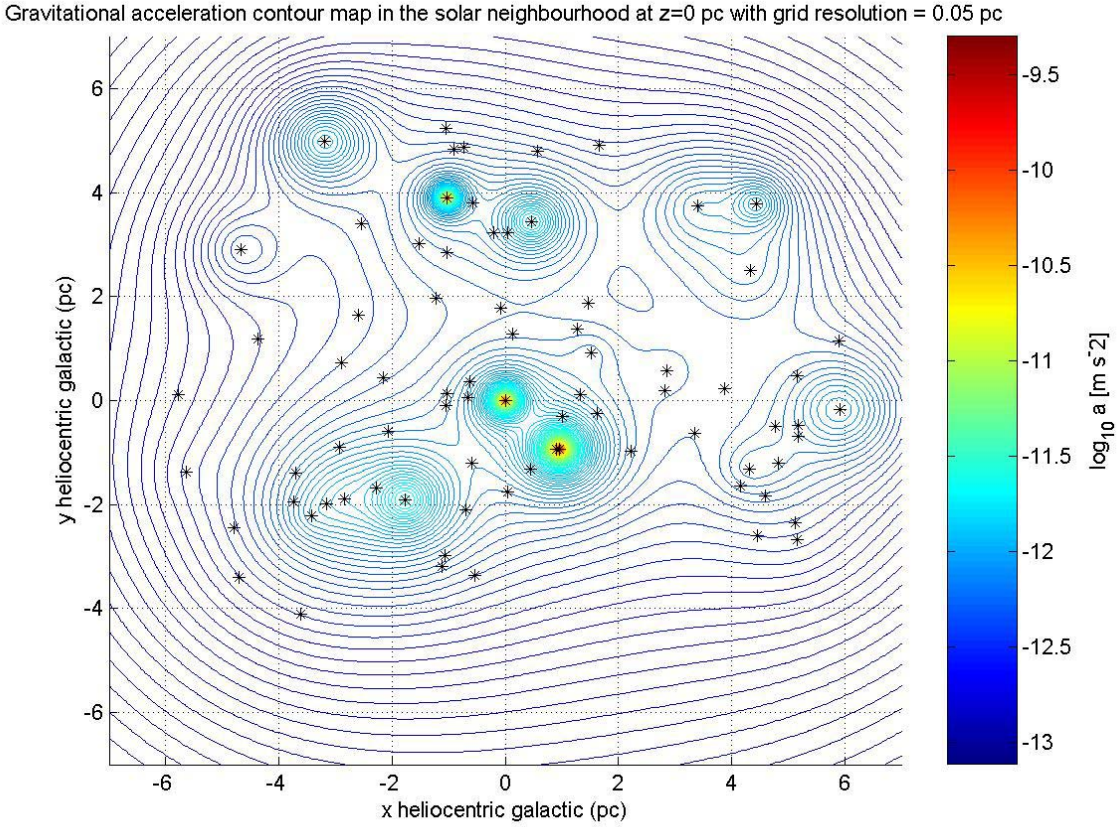

Figure 10: Contour map of the gravitational acceleration caused by the 77 stars on the galactic plane. The projected positions of the stars are also indicated.

Most[3] graphs exhibit two common features: high sharp peaks (the top part of which has been cut in order to reduce the range of values and smooth the color range of the figure) over a smooth continuum below 10^{-11}-10^{-12} m/s^2. The peaks are centered at the locations of the stars (or near their projections onto the plane under evaluation), as can be seen by looking at the contour maps where the stars have been positioned according to their *x* and *y* coordinates. Each star exerts its gravitational attraction (i.e., the peak) over a small "region of influence" around it, the boundaries of which are identified by the speed of a test particle becoming constant (within a given tolerance). In the case of the Sun, the integration of the equations of motion of the *N* bodies + a spacecraft leaving the Solar System toward Proxima Centauri has shown that the speed of the particle becomes constant at a distance of 45,000 AU from the Sun, where the order of magnitude of the gravitational acceleration is approximately 10^{-11} m/s^2. Therefore we can conclude that when the 3D surface becomes smooth (blue in the example figure above and in most figures shown in the Appendix), interstellar space is reached and the motion is uniform and rectilinear. The regions of influence of the stars in general do not intersect each other. Note that these regions should not

[3] The plots drawn at the boundaries of the region occupied by the N stars (i.e., at z = ±7.0 pc) do not exhibit peaks but a very low continuum as if there were no stars. This is a selection effect because the stars outside the volume are excluded from the computations while the effect of stars within the region gets weaker and weaker.

be mistaken for "spheres of influence", the definition of which requires the presence of a dominant central body: at this stage the body of the Galaxy has been neglected and *N* point-like bodies in empty space are being considered.

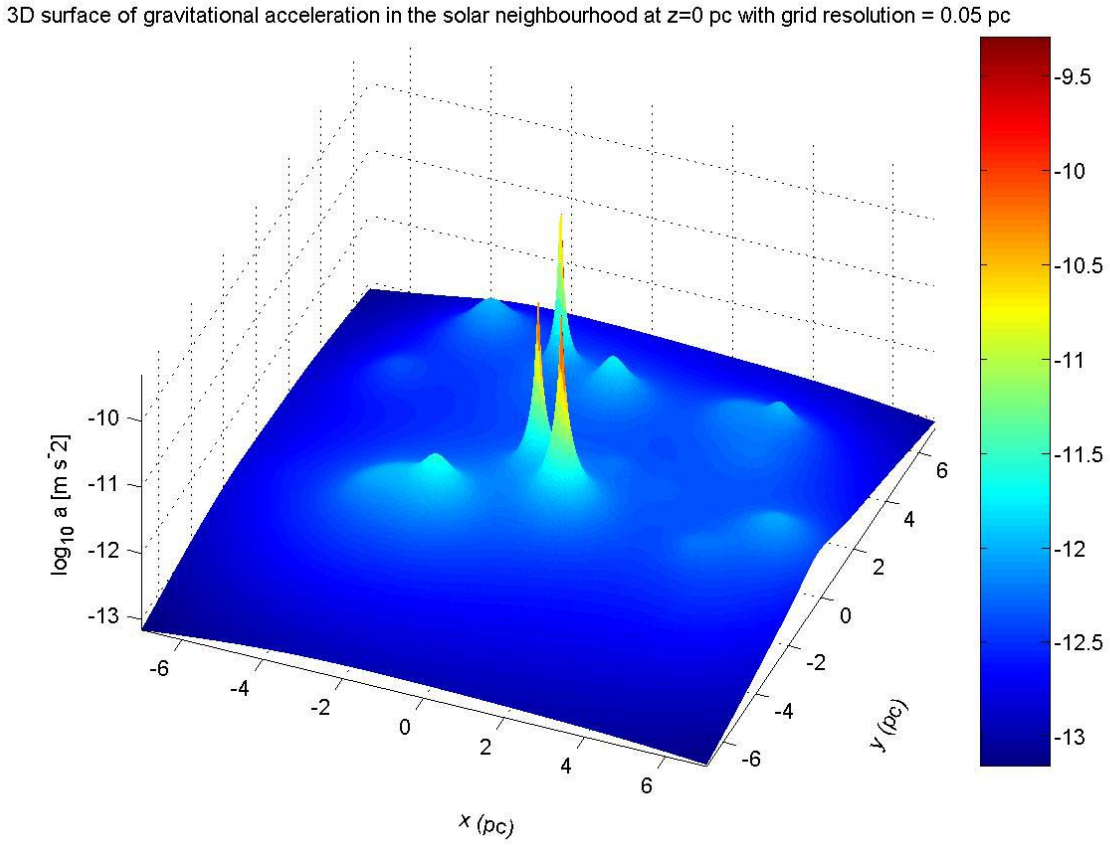

Figure 11: Surface of acceleration levels (in logarithmic scale) in the solar neighbourhood on the galactic plane. The three sharp peaks are due to Sun, Alpha Centauri and Kruger 60.

The outcome of this experiment yields further evidence that the nearby stars do not perturb each other, their gravitational acceleration peaks being well separated.

The original idea of plotting the gravitational hierarchies, defined as maps of the gravitational potential domains of the n stars, turned out not to be meaningful: the gradient of the gravitational potential (i.e., the acceleration) is the most appropriate means to measure the relative contributions of a system of *N* bodies to the motion of a test particle. The acceleration domains are nothing but spherical regions surrounding each star, as suggested by plots like Figure 10 and Figure 11.

3.2 Motion in the field of the Galactic potential

Motions in the Milky Way are commonly expressed with respect to the

- **FSR**: the "fundamental" standard of rest with respect to the galactic center, or
- **LSR**: the "local" standard of rest with respect to a circular orbit at the Sun's radius.

The FSR is a non-rotating reference frame centered at the galactic center and is used when describing the Galaxy as a whole. The LSR is more useful for describing motions near the Sun. The usual notation for the velocity expressed in the Fundamental Standard of Rest is through a vector (Π, Θ, Z), where Π is the velocity component directed radially away from the centre, Z is the velocity component perpendicular to the galactic plane, taken as positive in the direction of the North Galactic Pole, and lastly Θ is the

tangential component normal to the other two, positive in the direction of galactic rotation (clockwise as seen from the North Galactic pole). Suppose now that the mass distribution in our Galaxy is axisymmetric, so that the gravitational forces at any position in the galactic plane are directed radially toward the centre and that the forces are independent of time. Then at each position in the galactic plane there will be a particular velocity vector with components (Π, Θ, Z) = (0, Θ_0, 0) such that a star moving with this velocity follows a circular orbit around the centre of the Galaxy. A point moving with just this velocity defines the Local Standard of Rest (LSR) and Θ_0 is called the *circular velocity* (Mihalas & Binney, 1981). The relation between the LSR, the FSR and the heliocentric galactic reference frame is shown in Figure 12. Note that both the FSR and the LSR are left-handed systems, while the heliocentric galactic system is right-handed.

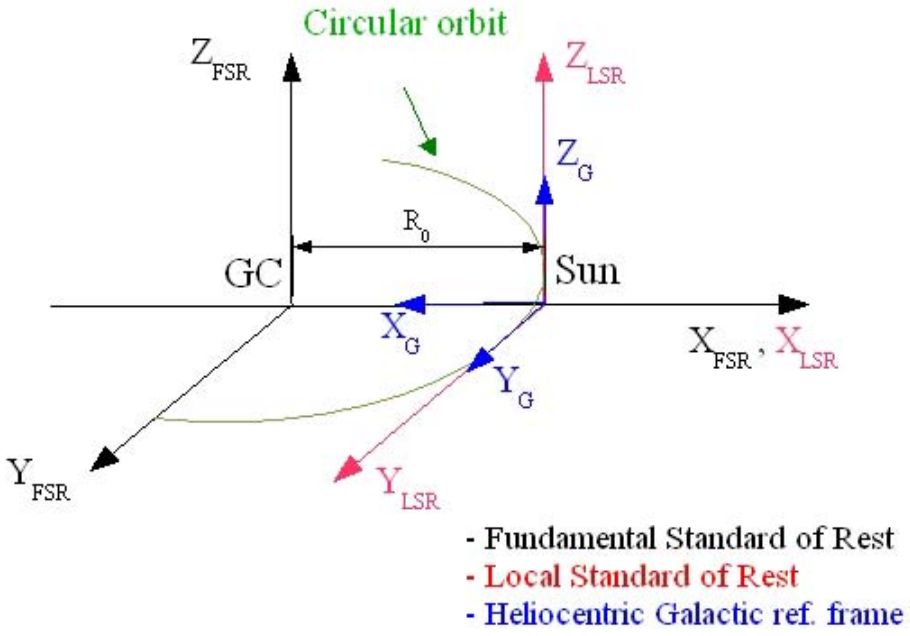

Figure 12: The three basic reference frames for describing stellar motions: the Heliocentric Galactic reference frame, the Local Standard of Rest and the Fundamental Standard of Rest.

The Sun's speed relative to the LSR is determined on the basis of the space motions (radial velocities and proper motions) of the stars relative to the Sun. The result depends on the types and numer of objects involved in the computation. In agreement with Carraro & Chiosi (1994), we adopted the Standar Solar Motion (u_S,v_S,w_S) defined to be the solar motion relative to the stars most commonly listed in general catalogues of radial velocity and proper motion, which are typically of spectral types A through G including dwarfs, giants and supergiants (Mihalas & Binney, 1981): u_S = -10.4 km/s, v_S = 14.8 km /s, w_S = 7.3 km/s.

Direct measurements of Θ_0 based on radial velocities of globular clusters or spheroidal-component stars in our Galaxy or of external galaxies in the Local Group, yield values in the range $200 \leq \Theta_0 \leq 300$ km/s. Following Allen & Santillán (1991) and Carraro & Chiosi (1994), we adopted the values 220 km/s and 8.5 kpc respectively for Θ_0 and for the distance R_0 of the Sun from the galactic centre.

A higher level of precision is reached when the motions of the stars are computed by taking into account the force field produced by Galaxy. A simple, yet realistic model of the potential of the Galaxy can be found in Allen & Santillán (1991) and Carraro & Chiosi (1994). This model is implemented in the

GRINTON software tool, kindly made available to us by Dr. Carraro. This galactic model consists of three mass components: a spherical central bulge, a flattened disk and a massive spherical halo. The total mass of the model is $2 \cdot 10^{11}$ M_{sun}. Each component provides its own contribution to the analytical representation of the overall gravitational potential, the gradient of which provides the radial and vertical components of the gravitational force. The second order differential equations that describe the motion of a star are numerically integrated using the Everhardt Radau integrator.

We applied the model to the 77 selected stars and performed an integration over 200 million years with time steps of 1 My. As expected, the resulting orbits shown in Figure 13 are very different from the straight lines obtained from the *N*-body integrations. Figure 13 also shows the important fact that the configuration of stars currently constituting the Solar Neighborhood is bound to disrupt, not being gravitationally bound as a subsystem. The solar companions are thus totally accidental and vary dramatically on a timescale much shorter than the period of galactic rotation.

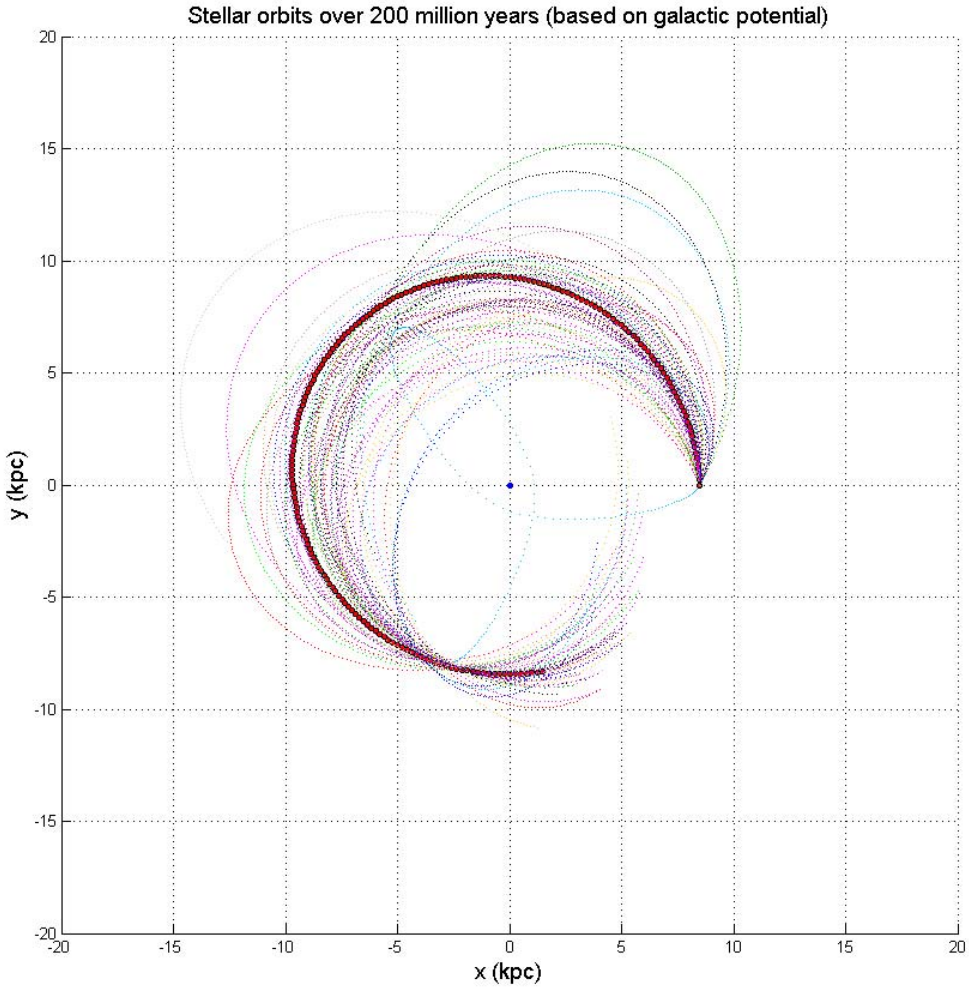

Figure 13: The orbits of the nearby stars during a period of 200 My driven by the galactic potential. The thick line indicates the orbit of the Sun.

The "*N*-body" approach presented in the previous section is obviously highly inadequate to describe stellar motions over time intervals longer than, say, 100 Ky. However, for shorter periods the isolated *N*-body scheme is a sufficient approximation which covers typical to extreme transfer times of interstellar travel. Figure 14 and Figure 15 show the orbits of the stars in the solar neighborhood over a period of 15,000 years as determined by numerical integration respectively of an isolated *N*-body system and the same system of non-interacting particles each moving under the driving acceleration of the galactic potential. No appreciable differences can be observed in the evolution of the system.

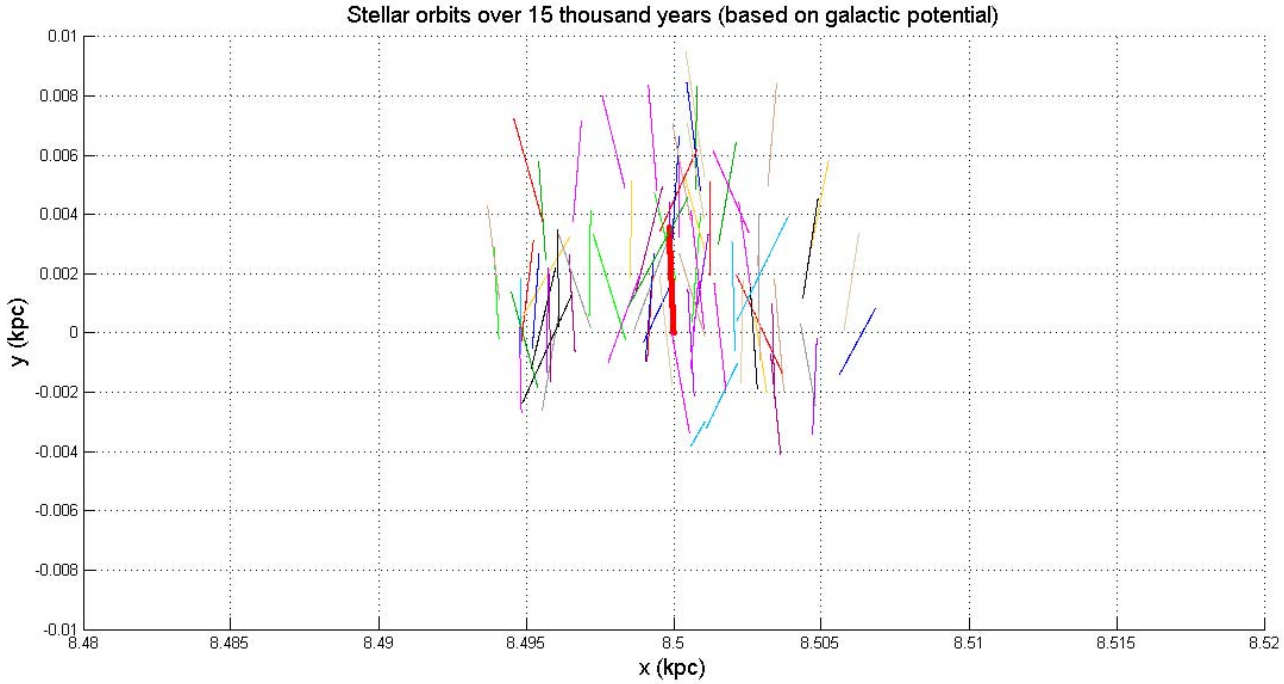

Figure 14: Stellar orbits over 15,000 years as determined by integration of the equations of motion with respect to the galactic potential.

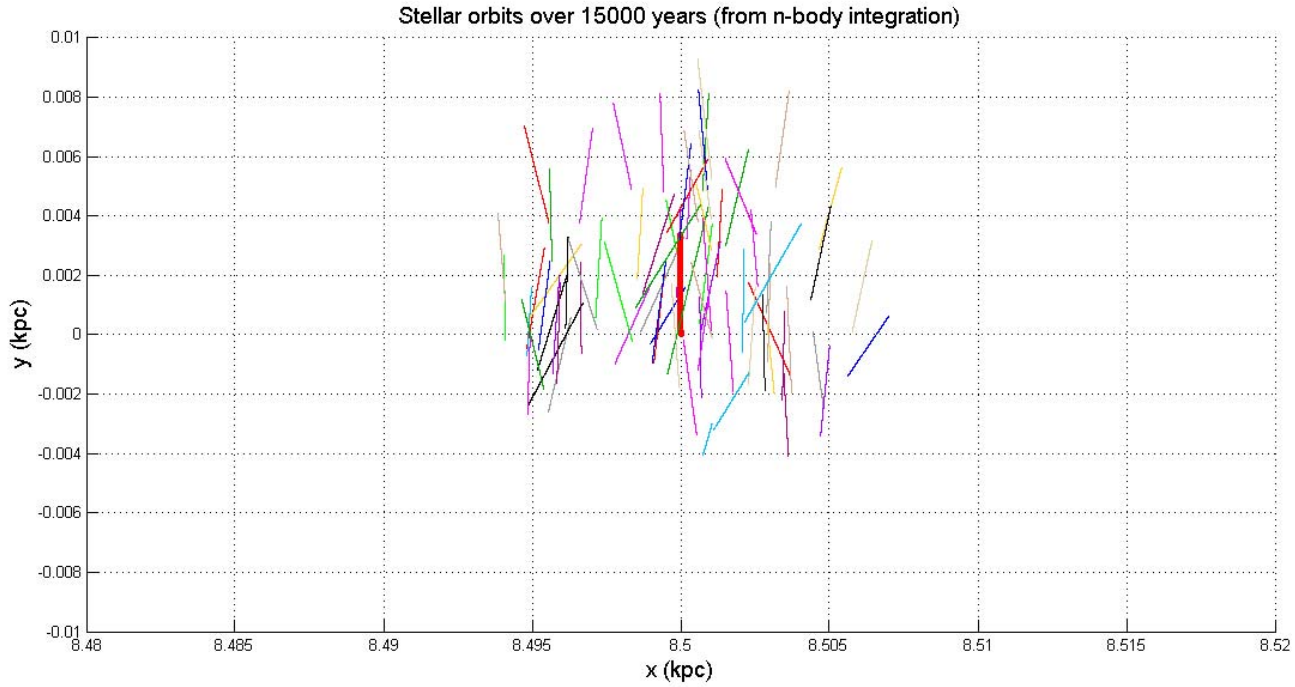

Figure 15: Stellar orbits over 15,000 years as determined by integration of the equations of motion of the N-body problem.

3.3 The spheres of influence

As a further comparison between the "*N*-body" and the "galactic potential" approaches, we computed the radii R_{SI} of the spheres of influence for each star in the database according to the well-known formula (Roy, 1972):

$$R_{SI} = r\left(\frac{m_*}{M_G}\right)^{2/5} \tag{4}$$

written for a star of mass m_* orbiting at a distance r from the galactic centre, M_G being the total mass of the Galaxy set equal to $2 \cdot 10^{11}$ M_{sun}. The results are reported in Table 8 and illustrated in Figure 16: the computations show (blue circles in the plot) that there are only two cases of intersection, i.e., Alpha Centauri with Proxima Centauri and Procyon with Luyten Star. As we shall discuss later, this observation is not sufficient to conclude, for example, that Proxima is bound to Alpha Cen.

Name	M	r	R_{SI}		Name	M	r	R_{SI}
	Msun	Kpc	pc			Msun	Kpc	pc
Sun	1.000	8.50000	0.25645		GJ 380	0.642	8.50289	0.21487
Proxima Centauri	0.107	8.49910	0.10489		GJ 388	0.393	8.50228	0.17656
alpha Centauri	2.060	8.49904	0.34238		GJ 832	0.503	8.49666	0.19474
Barnard's Star	0.166	8.49848	0.12502		GJ 682	0.213	8.49517	0.13807
Wolf 359	0.092	8.50058	0.09875		omicron 2 Eri	1.582	8.50370	0.30823
Lalande 21185	0.464	8.50105	0.18865		EV Lacertae	0.285	8.50091	0.15524
Sirius	2.491	8.50177	0.36953		70 Ophiuchi	1.625	8.49566	0.31126
UV Ceti	0.211	8.50066	0.13764		Altair	1.710	8.49659	0.31771
Ross 154	0.171	8.49714	0.12649		EI Cancri	0.203	8.50373	0.13558
Ross 248	0.121	8.50104	0.11020		GJ 445	0.240	8.50255	0.14495
epsilon Eri	0.850	8.50207	0.24037		GJ 1005	0.282	8.49987	0.15456
Lacaille 9352	0.529	8.49866	0.19876		GJ 526	0.526	8.49838	0.19830
Ross 128	0.156	8.49995	0.12197		Stein 2051	0.724	8.50466	0.22550
EZ Aquarii	0.306	8.49872	0.15967		GJ 754	0.158	8.49483	0.12252
Procyon	2.069	8.50283	0.34313		Wolf 1453	0.566	8.50480	0.20435
61 Cygni	1.333	8.49954	0.28768		sigma Draconi	0.892	8.50105	0.24502
DM+59 1915	0.610	8.49996	0.21044		GJ 229	0.606	8.50362	0.20998
GX Andromedae	0.649	8.50152	0.21577		GJ 693	0.262	8.49488	0.14999
Eps Indi	0.838	8.49778	0.23889		Wolf 1055	0.567	8.49556	0.20427
DX Cancri	0.087	8.50293	0.09660		Ross 47	0.196	8.50563	0.13372
Tau Ceti	0.921	8.50103	0.24818		GJ 570	1.708	8.49540	0.31752
RECONS 1	0.113	8.50069	0.10722		GJ 908	0.507	8.50020	0.19544
YZ Ceti	0.136	8.50063	0.11547		eta Cassiopei	1.709	8.50319	0.31788
Luyten's Star	0.257	8.50315	0.14898		GJ 588	0.464	8.49484	0.18852
Kapteyn's Star	0.393	8.50106	0.17653		Ross 882	0.225	8.50471	0.14129
AX Microscopium	0.600	8.49718	0.20899		36 Ophiuchi	2.406	8.49408	0.36410
Kruger 60	0.439	8.50102	0.18452		GJ 783	1.024	8.49483	0.25874
Ross 614	0.267	8.50342	0.15128		82 Eridani	0.971	8.50112	0.25348
Wolf 1061	0.261	8.49613	0.14978		delta Pavonis	1.095	8.49555	0.26579
WD 0046+051	0.500	8.50123	0.19438		QY Aurigae	0.326	8.50577	0.16390
GJ 1	0.481	8.49898	0.19134		HN Librae	0.220	8.49584	0.13988
Wolf 424	0.236	8.49955	0.14393		GJ 338	1.196	8.50438	0.27563
TZ Arietis	0.140	8.50259	0.11684		GJ 784	0.577	8.49482	0.20569
GJ 687	0.390	8.50058	0.17598		Wolf 562y	0.300	8.49522	0.15835
LHS 292	0.083	8.50053	0.09477		EQ Pegasi	0.499	8.50074	0.19422
GJ 674	0.361	8.49569	0.17053		GJ 661	0.719	8.49835	0.22471
GJ 1002	0.109	8.50008	0.10568		Wolf 630	1.307	8.49409	0.28524
Ross 780	0.273	8.49854	0.15254		GJ 625	0.372	8.49943	0.17266
WX Ursae Maj	0.582	8.50216	0.20658					

Table 8: Size of the sphere of influence, mass and distance from the galactic centre of the 77 stars in the solar neighbourhood.

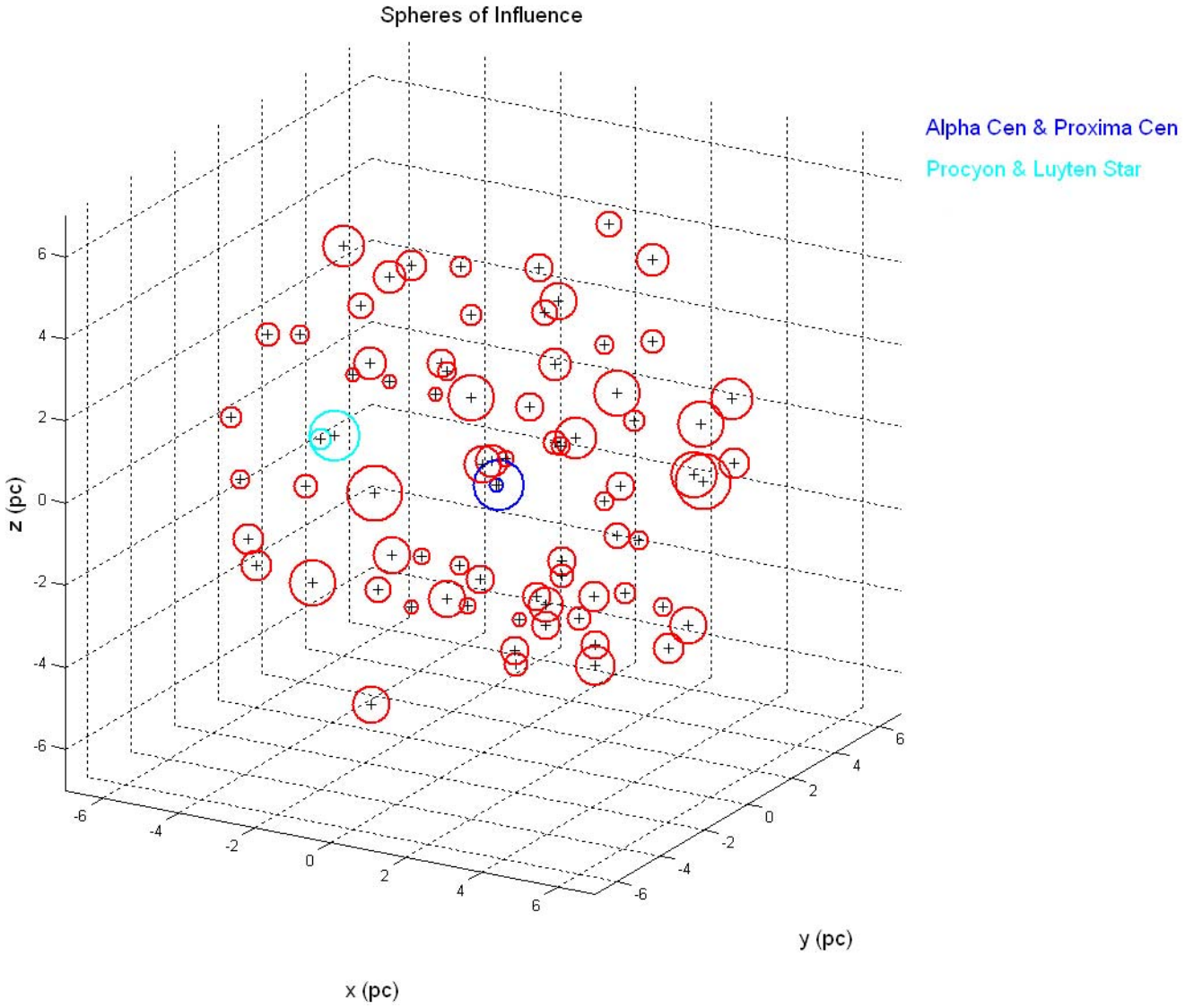

Figure 16: 3D representation of the size of the spheres of influence of the 77 stars in the solar neighbourhood. The pairs of spheres coloured in blue (Alpha Centauri AB and Proxima Centauri) and cyan (Procyon and Luyten star) are the only cases of intersection in the whole system.

The analysis presented in this section shows that the motion of the stars is dominated by the galactic potential and not by local gravitational interactions, except in the case of multiple systems which have been determined to be closely bound or happening to interact due to fortuitous close encounters (intersecting influence spheres).

Admittedly, the analysis carried out through numerical simulations is rather unsophisticated, and more detailed and modern models of the galactic potential could be used, including the perturbations due to the compressional waves forming the spiral arms. However, it is felt that the purpose of the present research is well served even under such restrictions.

4 INTERNAL KINEMATICS AND DYNAMICS OF MULTI-STAR SYSTEMS

In this section we give an overview of the major findings concerning the internal dynamics of some of the closest double and triple systems and of two known planetary systems. This will serve as a background for the subsequent considerations on the trajectory design for a space mission to the nearby stars.

4.1 Is Proxima in orbit about Alpha Cen A/B?

Proxima Centauri is the closest star to the Sun. The similarity of its distance, angular coordinates and proper motion to those of the binary system Alpha Centauri A/B has always led to questions about the relationship between these two objects. The question of whether or not Proxima is gravitationally bound to Alpha Cen A/B has long been settled in the affirmative, which led to refer to Proxima as Alpha Cen C. Unfortunately, the available measurements of the kinematic properties of this two objects do not support this conclusion. Matthews & Gilmore (1993) give a very clear view of the arguments in favour of one and the other hypothesis: the fact that Proxima Cen is located inside the sphere of influence of Alpha Cen A/B does not necessarily mean that the two are bound, the alternative being that Proxima is following a hyperbolic trajectory relative to Alpha Cen. Besides, despite the close similarity between the proper motions, the radial velocities do differ significantly. The result of a numerical search performed by the same authors within a six-dimensional space of astrometric parameters would impose that, in order for the relative velocity of Proxima to be smaller than the escape speed from Alpha Cen, the difference in radial velocity between the two stars must not exceed 0.18 km/s. During an observing programme carried out at ESO Chile in 1984 a value of –21.7 ± 1.8 km/s for the radial velocity of Proxima Cen was measured. This determination falls within the required range for the bound statement to be justified but has not yet been confirmed.

Anosova & Orlov (1995) proposed the hypothesis that this system is part of a stellar *moving group* and that what we see is nothing but a slow passage of Proxima close to the A/B pair.

We have performed the numerical integration of the equations of motion of the three stars with initial conditions taken from Table 5 and the relative motion of A and B derived from the orbital parameters listed in Table 3 and Table 4. According to our results (Figure 17), Proxima is performing a hyperbolic passage relative to Alpha Cen A/B. A further confirmation comes from evaluation of the gravitational energy per unit mass E relative to the barycentre of Alpha Cen A/B:

$$E = \frac{v_{PAB}^{\ 2}}{2} - \frac{G(m_{AB} + m_P)}{r_{PAB}} = 117 \text{ km}^2\text{s}^{-2} \tag{5}$$

where m_{AB} is the mass of the A/B system, m_P is the mass of Proxima, r_{PAB} and v_{PAB} are the relative distance and speed. The positive value of E indicates that Proxima and Alpha Cen A/B are not bound. If this will be validated by future observations, then the Circular Restricted Three-Body Problem paradigm to the system composed by Alpha Cen A and Proxima cannot be applied.

Our computations show (Figure 17, Figure 18, Figure 19 and Figure 20) that the motion of Proxima is affected by perturbations which exhibit the same frequency as the orbital motion of B around A (Figure 21).

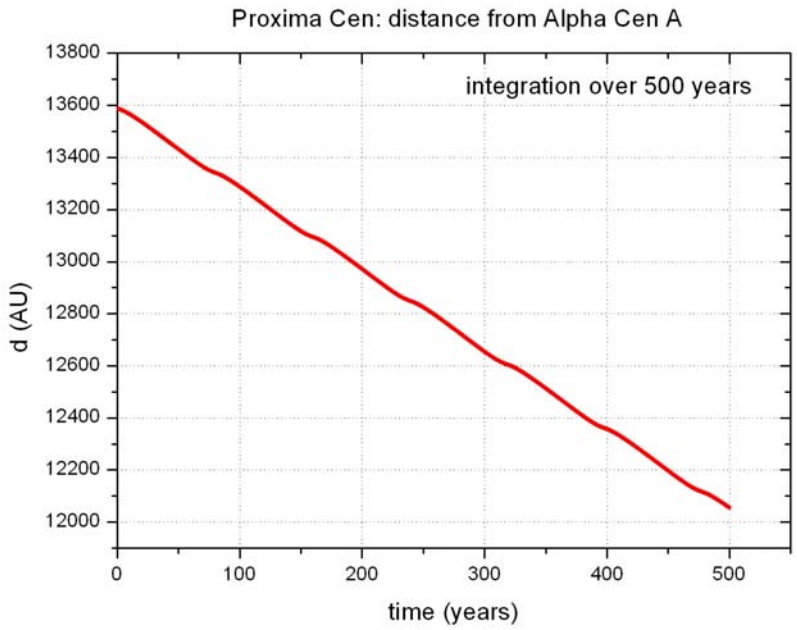

Figure 17: Distance between Proxima Centauri and Alpha Centauri A as a function of time as resulting from integration of the equations of motion of the triple system over 500 years with integration step of 0.1 years.

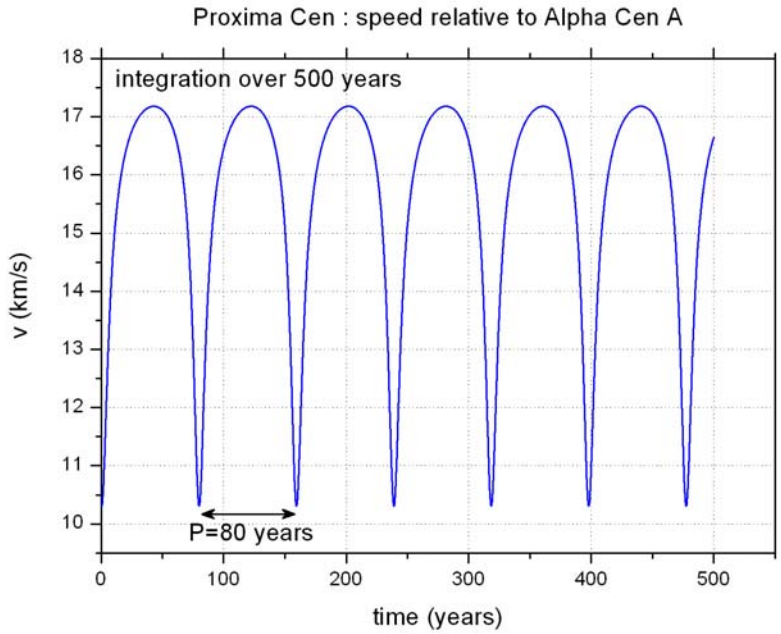

Figure 18: Speed of Proxima Centauri relative to Alpha Centauri A as a function of time as resulting from integration of the equations of motion of the triple system over 500 years with integration step of 0.1 years. The perturbation is due to the relative orbital motion of stars A and B. The perturbation is correlated with the relative orbital motion of stars A and B as indicated by the periodicity of the variations which is equal to the orbital period of the two stars.

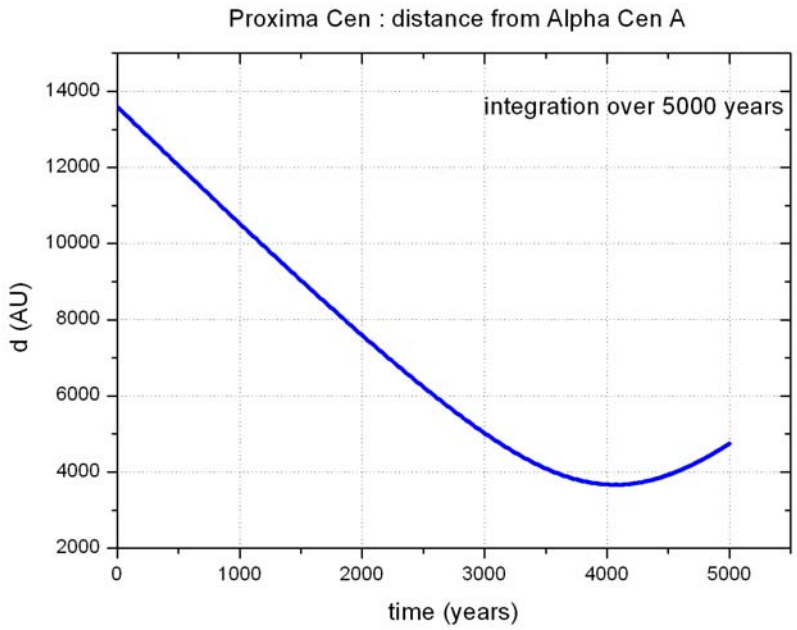

Figure 19: Distance between Proxima Centauri and Alpha Centauri A as a function of time as resulting from integration of the equations of motion of the triple system over 5,000 years with integration step of 1 year. In 4,000 years Proxima will reach the point of closest approach to Alpha Cen A.

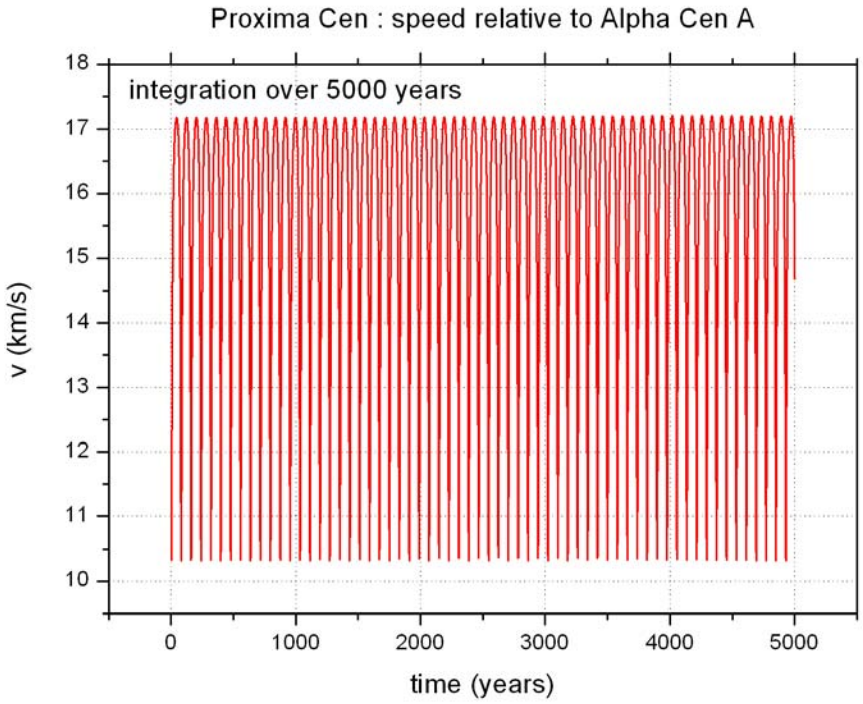

Figure 20: Speed of Proxima Centauri relative to Alpha Centauri A as a function of time as resulting from integration of the equations of motion of the triple system over 5,000 years with integration step of 1 year. The perturbation is due to the relative orbital motion of stars A and B.

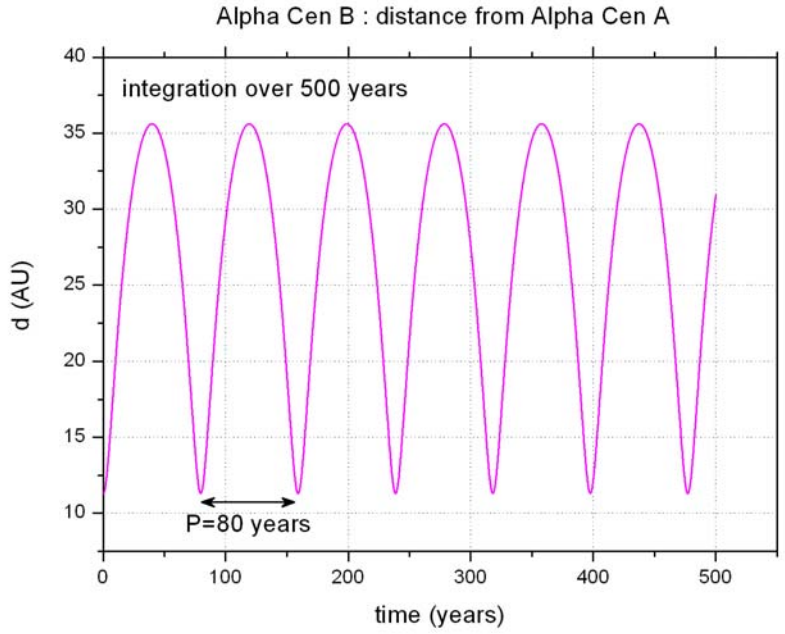

Figure 21: Relative distance between Alpha Cen A and B as a function of time as resulting from integration of the equations of motion of the triple system over 500 years with integration step of 0.1 years.

Since the results of our computations and the energy evaluation critically depend on the initial conditions determined from rather imprecise observations, at this stage we cannot make any final statement concerning the dynamical relationship between Proxima and Alpha Cen. The available measurements lead to controversial conclusions which can only be settled by further, more precise and accurate determinations of the their kinematic properties.

From precise radial velocities (Figure 22) obtained of both Alpha Cen A and B, the mass ratio of the double system was determined by Murdoch & Hearnshaw (1993) to be $m_B/m_A = 0.75 \pm 0.09$, which agrees with the estimate of 0.80 adopted in the present study.

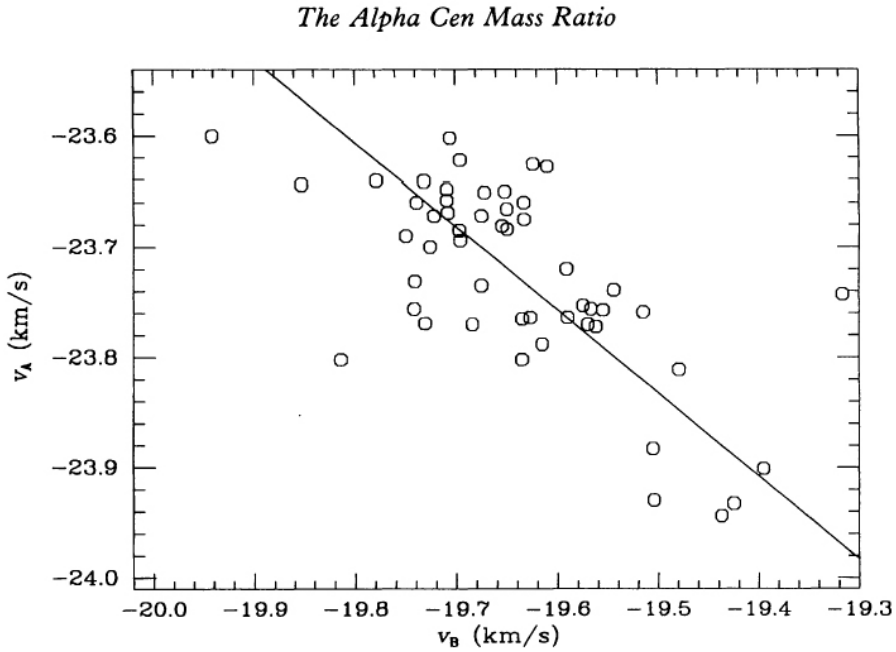

Figure 22: Radial velocities v_A of Alpha Cen A plotted versus radial velocities v_B of Alpha Cen B in order to derive the mass ratio of the two stars (Murdoch & Hearnshaw, 1993).

4.2 Binary systems

Sirius: Sirius has been known as a double star for about 140 years. However, since the beginning of the 20th century observational, physical and dynamical indications have led to the hypothesis of the existence of a third body in the system. This fact has been reported and discussed by Benest & Duvent (1995): the authors present an orbital analysis, supported by numerical simulations, of the binary Sirius A/B, whose perturbed motion is better explained by introducing a tiny star revolving around Sirius A.

Van de Bos (1960) reported the details of the reduction procedure to obtain the orbital parameters of Sirius A/B from observations distributed over more than two orbital periods of the system (i.e., more than 100 years).

Thanks to some recent observations made by the Extreme Ultraviolet Explorer (EUVE) satellite, Holberg et al. (1998) have produced new results concerning the physical (temperature and surface gravity) parameters of Sirius B. By combining the Hipparcos parallax of the Sirius system with the new spectroscopic data, the authors obtained a refined mass estimate of 1.034 ± 0.026 M_{sun} for the white dwarf secondary.

UV Ceti: The orbital elements of the M dwarf binary system L 726-8 composed by UV Ceti and BL Ceti listed in Table 3 and adopted in the course of this study were published by Geyer, Harrington & Worley (1988). By merging observations made at the U.S. Naval Observatory since 1964 with photographic and visual observations of the relative positions of the two components collected since 1948, the authors obtained a parallax of 0.3711 ± 0.0040 arcsec, a proper motion of 3.3299 ± 0.0006 arcsec/yr towards 79.78 ± 0.01 degrees and a mass ratio of 0.4938 ± 0.0031. Then taking 0.375 ± 0.004 arcsec as the absolute parallax, the total mass of the system is 0.200 M_{sun} yielding individual masses for the two components of 0.101 M_{sun} and 0.099 M_{sun}.

Procyon: Several orbit determinations for this double system have been published in recent years. Girard et al. (2000) have made a thorough comparison between their own orbital elements and those published by Strand in 1951 and more recently by Irwin et al. (1992) (Table 9). Together with the redetermined astrometric orbit and parallax, Girard et al. provide new estimates for the component masses: the derived masses are 1.497 ± 0.037 M_{sun} for the primary and 0.602 ± 0.015 M_{sun} for the white dwarf secondary.

Element	Strand (1951)	Irwin et al. (1992)	Girard et al. (2000)
Semi-major axis (arcsec)	1.217±0.002	1.179±0.011	1.232±0.008
Eccentricity	0.40	0.365±0.008	0.407±0.005
Inclination (degrees)	35.7±0.2	31.9±0.9	31.1±0.6
Angle of node (degrees)	104.3±0.3	104.8±1.5	97.3±0.3
Longitude of periastron (degrees)	89.8±0.3	88.8±2.0	92.2±0.3
Period (years)	40.65	40.38±0.15	40.82±0.06
Periastron passage (year)	1927.6	1967±0.16	1967.97±0.05

Table 9: Astrometric orbital elements of Procyon (Girard et al., 2000): comparisons among the data published by Girard et al. (2000) and those determined by Irwin et al. (1992) and Strand (1951).

4.3 Triple systems

We have collected information about the nearest two triple systems listed in our database: Epsilon Indi and EZ Aquarii.

EZ Aquarii: according to the new Sixth Orbit Catalog of Visual Binary Stars, the orbit of stars A and B has a semi-major axis of about 1.22 AU. The orbit has an eccentricity of 0.437, a period of about 2.25

years and an inclination from the perspective of an observer on Earth of about 112.4° (Woitas et al., 2000). In addition, star A is a spectroscopic binary (whose companion has been designated as star C) with an orbit period of only 3.8 days (Delfosse et al., 1999).

Epsilon Indi: this star is the title member of the Epsilon Indi stellar moving group (Kovacs & Foy, 1978). Scholz et al. (2003) identified a brown dwarf as a common proper motion companion (separation of 1459 AU) to ε Indi: as such, ε Indi B is one of the highest proper motion sources outside the Solar System (~4.7 arcsec/yr) and the nearest brown dwarf to the Sun. The separation between the primary and the companion is 402.3 arcsec in the plane of the sky while the separation along the line-of-sight is unknown. Using the age of ε Indi A as a first estimate for the age of ε Indi B, the authors obtained a mass range of 40-60 M_{Jup} for this dwarf. In August 2003, the same as well as another team of astronomers found that the brown dwarf had its own brown dwarf companion (McCaughrean et al., 2004). Since then the two brown dwarfs have been called ε Indi Ba and ε Indi Bb. By analysing optical and IR survey data, McCaughrean and his collaborators determined a more refined proper motion for the combined ε Indi Ba, Bb system (Table 10). The same authors attribute an orbital period of ~15 years to the system, thus estimating that a determination of its orbital parameters will be available within a fairly short time.

Object	$\mu_\alpha \cos\delta$	μ_δ	Source
ε Indi Ba,Bb	+4131 ± 71	-2489 ± 25	Scholz et al. (2003)
ε Indi Ba,Bb	+3976 ± 13	-2500 ± 14	McCaughrean et al. (2004)
ε Indi A	+3961.41 ± 0.57	-2538.33 ± 0.40	ESA (1997)

Table 10: Proper motions for ε Indi Ba,Bb and ε Indi A. The units are mas/year (McCaughrean et al., 2004).

4.4 Planetary systems

Two known planetary systems are present in our star ensemble:

- ε Eridani: the detection of a planet (called "planet b") was first announced by Campbell et al. (1988) after noting a periodicity in the Doppler measurements of the star. Later (Hatzes et al., 2000; Quillen & Thorndike, 2002) modelling of dust ring clumping patterns and RV measurements suggested the presence of a relatively smaller planet ("planet c") with about a tenth of a Jupiter mass. Table 11 summarizes the most widely quoted values for the orbital and physical parameters of the two planets.
- Gliese 876: two planets have recently been discovered around this star with the radial velocity method. The basic orbital data are reported in Table 12 (Marcy et al., 1998 ; Marcy et al., 2001).

	semimajor axis	period	eccentricity	inclination	mass	diameter
	AU	years		degrees	Earths	Earths
ε Eridani	0.0	...	...	...	280,000	94-98
planet b	3.3	6.85	0.61	46?	381	...
planet c	40.0	280.00	0.30	46?	30	...

Table 11: Orbital elements of the planets orbiting Epsilon Eridani (Marcy et al., 1998 ; Marcy et al., 2001).

name	M·sini	semi-major axis	period	eccentricity	inclination	long. ascend. node	Epoch
	M_J	AU	days		sin i	degrees	JD 2450000
Gl 876 b	1.89	0.21	61.02	0.10	0.6 ?	333	106.2
Gl 876 c	0.56	0.13	30.10	0.27	0.6 ?	330	31.4

Table 12: Orbital elements of the planets orbiting GL 876.

4.5 Conclusions

The literature on the nearby stellar systems often contains complementary information and interesting discussions on the dynamical and kinematic properties of these objects. However, our knowledge of the solar neighbourhood remains remarkably sketchy, as often demonstrated by the large uncertainties affecting the determination of many astrometric and physical parameters. In some cases the observations are so imprecise that we are unable to establish the dynamical relationships within stellar systems. Since uncertainties of this kind affect our knowledge of even our nearest stellar system, then the current description of the dynamical evironment that an exploration probe will experience at any other stellar system can only be a very preliminary one.

5 SPACE MISSIONS TO THE NEARBY STARS

From the previous investigations we have learnt that the dynamical envronment in which a spacecraft would travel on an exploration mission to the nearby stars is simpler than expected. Outside the sphere of influence of the departure system, i.e., the Solar System, the S/C is entirely under the influence of the galactic potential, whose gradient is however so small as to let the S/C travel for a small fraction of the galaxy revolution time as if in the presence of no forces at all.

The S/C interacts with other stars, or star systems, only when it enters their spheres of influence. Therefore no Circular Restricted Three-Body Problem (CR3BP) or Two-Fixed Centers (TFC) dynamical paradigms can be sensibly applied to the S/C dynamics during cruise from one star to another. Only when the S/C gets close to a *star system* is it possible to employ such dynamical schemes.

A remarkable consequence of this peculiar dynamical situation is that, by properly imparting velocity impulses, the S/C can be stably positioned anywhere outside the spheres of influence of the nearby stars, irrespective of whether such positions are identifiable with critical points in any of the known dynamical paradigms, like the CR3BP or the TFC paradigms.

It is also worth noting that Lambert-type targeting is also inapplicable. Lambert targeting refers to the determination of the initial velocity of a transfer orbit within the force field of a single primary body. Now, although this role could be played by the axisymmetric galactic potential, the extremely short distance to the nearby stars compared to the typical dimension of our Galaxy makes this approach impracticable. The proper approach to interstellar transfer seems to be a simple straight line orbit.

The fundamental problem of interstellar flight, however, is of course *distance* (Figure 23). Compressing the time of flight of the transfer journey into the scale of human lifetime requires high speeds and these, in turn, require very energetic means of propulsion. Propulsion can be applied as an initial impulse, but more likely as continuous thrust, as will be considered shortly.

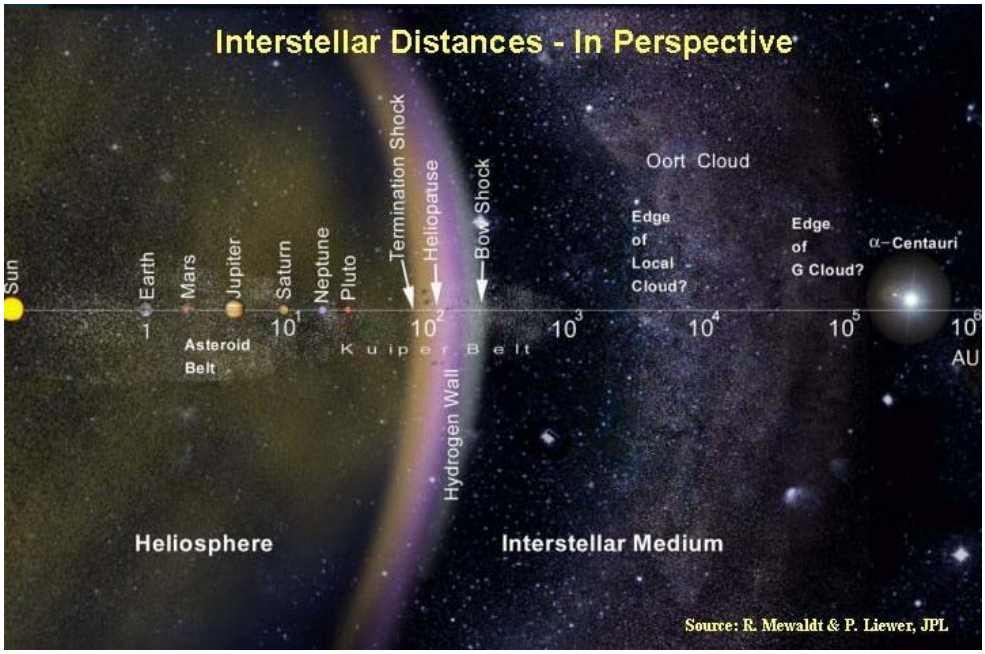

Figure 23: Perspective view of the interstellar distances including the locations of the planets, the boundary between the heliosphere and the interstellar medium, the Oort Cloud and the nearest stars.

In the following subsections we present in summary the outcome of the major past and on-going investigations in the field of interstellar trajectory design. Then we discuss the main issues related to the kinematics of relativistic flight under constant thrust.

5.1 Past and on-going studies

5.1.1 The Daedalus Project

One of the first detailed design studies of an interstellar spacecraft was conducted between 1973 and 1978 by a group of a dozen scientists and engineers of the British Interplanetary Society, led by Alan Bond (Bond et al., 1978): it demonstrated that high-speed, unmanned travel to the stars is a practical possibility. Certain guidelines were adopted: the Daedalus spacecraft had to use current or near-future technology, be able to reach its destination within a human lifetime and be flexible enough in its design that it could be sent to any of a number of target stars. The selected target was Barnard's Star, a red dwarf lying 5.9 light-years from the Sun. Although the Alpha Centauri system is closer, evidence available at the time (now considered unreliable) suggested that Barnard's Star might be orbited by at least one planet. To reach Barnard's Star in 50 years (the flight time allotted in the study), a spacecraft would need to cruise at about 12% of the speed of light, or 36,000 km/s. This being far beyond the reach of a chemical rocket, the Daedalus team had to consider less conventional alternatives. The design they chose was a form of nuclear-pulse rocket, a propulsion system that had already been investigated during Project Orion. However, whereas Orion would have employed nuclear fission, the Daedalus engineers opted to power their starship by nuclear fusion—in particular, by a highly-efficient technique known as internal confinement fusion: the desired cruising speed could be reached during an acceleration phase lasting four years. Since the design made no provision for deceleration upon arrival, Daedalus would carry 18 autonomous probes, equipped with artificial intelligence, to investigate the star and its environs. En route, Daedalus would make measurements of the interstellar medium.

5.1.2 Starwisp

Robert Foward (1985) presented a solution to the interstellar transport problem: an interstellar flyby probe (Starwisp) of wire mesh sail with microcircuits at each intersection. The probe was to be accelerated to near-relativistic speeds by beamed microwave power produced by a solar-power satellite (a Fresnel lens of wire mesh). After a first phase of constant acceleration (as long as the lens can focus on a spot smaller in size than the sail), followed by a phase of decreasing acceleration. In the case of a 4.3 ly transfer (to Alpha Cen), the requirement that Starwisp reaches the target within 21.5 years translates into the following characteristics of the system: sail diameter 1 km, sail weight 16 g, lens mass 50,000 tons, transmitted power 10 GW, maximum spacecraft speed 0.2 *c* reached within one week after launch.

Forward treats the motion of the spacecraft in interstellar space by neglecting the gravitational attractions of the stars. This is correct, since we know that the probe experiences the gravitational accleration caused by the stars only in their immediate proximity. However, the newtonian formalism by which he describes the motion is not adequate when dealing with relativistic speeds. In a later section we shall discuss the rectilinear motion of a relativistic particle subject to costant acceleration in the framework of the theory of Special Relativity.

5.1.3 The Realistic Interstellar Explorer study

The Realistic Interstellar Explorer is a recent feasibility study performed at the NASA Institute for Advanced Concepts (NIAC) by a team led by Dr. Ralph McNutt. The study, documented in a Phase I and a Phase II Final Report (McNutt, 1999; 2003) and in a recent paper by McAdams & McNutt (2002) designed some strategies and considered some propulsion modes for reaching significant penetration into the interstellar medium (> 1000 AU) by considering a variety of science goals and orbital mechanics constraints.

A search for the candidate targets (shown in Table 13) for Solar System escape direction was made by taking into account a number of issues: distance from the Sun, spectral characteristics of the target star, habitable planet probability (according to the criteria proposed by Dole, 1964).

Star name	distance	spectral type	habitable planet probability
	(light years)		
Alpha Cen B	4.3	K1	0.057
Epsilon Eridani	10.8	K2	0.033
Tau Ceti	11.8	G8	0.036
70 Ophiuchi A	16.6	K1	0.057
36 Ophiuchi A	18.2	K2	0.023
Sigma Draconis	18.8	G9	0.036
Eta Cassiopeiae A	19.4	K9	0.057
Delta Pavonis	19.9	G7	0.057
82 Eridani	20.9	G5	0.057
Beta Hydri	24.4	G1	0.037

Table 13: Candidate stars for launch directions including distance, spectral type and habitable planet probability (McNutt, 1999). We reported in grey colour the data concerning Beta Hydri as this star does not belong to our sample, being more than 7 parsecs far from the Sun.

In the typical solar-sail mission design strategy the sail is used first to remove the angular momentum of the Earth and probe about the Sun; the sail is then maneuvered face-on into the Sun at 0.1 to 0.25 AU and solar acceleration pressure accelerates the probe away from the Sun until the sail is jettisoned (at about 5 AU). The approach investigated and proposed by McNutt starts with a Jupiter gravity assist that removes the Earth's angular momentum; then the spacecraft is sent back to the Sun where it reaches a minimum distance of 4 solar radii; there a large propulsive maneuver is applied which puts the probe in a high-energy ballistic escape trajectory from the Solar System. Computations showed that a limiting ecliptic

latitude for the target must be imposed (within ±32.7°) in order to reduce the hyperbolic trajectory turn angle at perihelion. This constraint changes and shortens the list of candidate targets (Table 14). A perihelion ΔV of 14.801 km/s in the spacecraft velocity direction delivers the spacecraft to Solar-System-escape conditions of 20 AU/year for 32.7° ecliptic latitude of the target star.

The author investigated mission trajectories toward a variety of targets matching the desired characteristics. As an example, a probe could be launched toward Epsilon Eridani in 2011 (Figure 24), pass within 653,300 km of Jupiter at 23.527 km/s with a 24.7° approach phase angle and perform a 15.431 km/s perihelion ΔV.

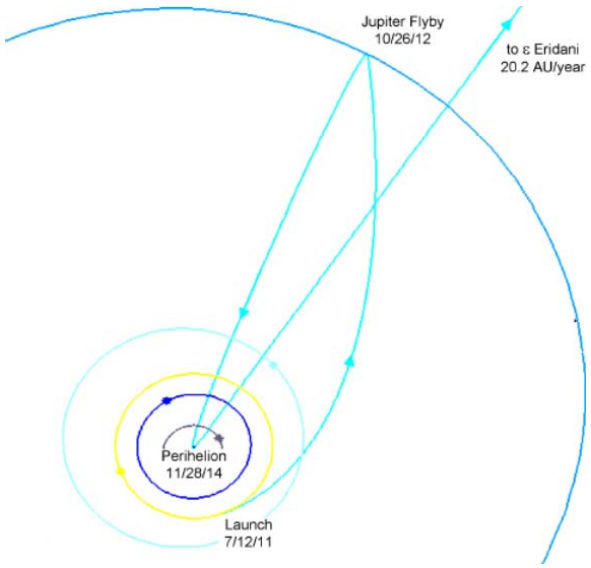

Figure 24: Solar System escape trajectory for a mission toward Epsilon Eridani (from McNutt, 1999).

The Jupiter flyby lowers perihelion from 1.02 AU to 0.02 AU, lowers aphelion from 11.88 AU to 5.04 AU and increases orbital inclination in order to provide the proper orientation for the perihelion burn. Two years later a 15.31 km/s perihelion ΔV 4.6° from the spacecraft velocity drection sends the spacecraft toward Epsilon Eridani at 20.2 AU/year.

A closer look at several technology advances needed for this interstellar precursor mission includes consideration of solar thermal propulsion for the near-Sun maneuvre, although this as well as other solutions require more study.

Star name	spectral type	ecliptic longitude	ecliptic latitude
		deg	deg
Epsilon Eridani	K2	48.29	-27.76
Tau Ceti	G8	17.66	-24.77
Van Maanen 2	DG	13.40	0.11
Procyon 61421	F5	115.79	-16.02
191408	K3	297.06	-15.68
131977 A	K5	237.13	-1.95
36 Ophiuchi	K1	259.96	-3.54

Table 14: Candidate stars for launch directions with ecliptic latitude limits (McNutt, 1999).

5.2 Transfer phase: relativistic interstellar flight under constant thrust

After travelling through space for more than 26 years, Voyager 1 reached 90 AU from the Sun at the end of 2003. With its Solar-System escape speed of 3.6 AU/yr it would take almost 74,000 years to reach the

distance of Proxima Cen. Even at the much higher speed of 20 AU/yr planned by McNutt to bring a spacecraft to 1000 AU in 50 years, Proxima Cen would be approached in more than 13,000 years. In summary, the investigations made so far indicate that interstellar missions with launch in the near future and ending within a few decades can only be targeted to destinations between a few hundred to one thousand AU of the Sun, unless dramatic technological developments enabling relativistic flight occur.

With this in mind and for the sake of completeness we have made some computations based on the assumption that the probe can attain relativistic speeds. Following Banfi (2000), we have computed the characteristics of the flight made by a starship under constant thrust on a rectilinear trajectory: the path s is divided into two equal parts of length $s/2$; in the first half the motion takes place under constant acceleration a, during the second half the spacecraft is subject to a constant and opposite deceleration equal to $-a$. According to the theory of Special Relativity, the relationship between the distance $s/2$ and the coordinated time t measured by an inertial observer is given by

$$\frac{s}{2} = \frac{c^2}{a}\left\{\left[1+\left(\frac{at}{c}\right)^2\right]^{1/2} - 1\right\}. \tag{6}$$

where c is the speed of light. The speed u at time t can be determined by

$$u = \frac{at}{\left[1+\left(\frac{at}{c}\right)^2\right]^{1/2}}. \tag{7}$$

The speed reaches a maximum at $s/2$ and then decreases to the initial value at the end of the flight. The proper time τ (i.e., the time measured by an onboard observer) at mid-course is related to the distance $s/2$ as

$$\tau = \frac{c}{a}\cosh^{-1}\left(1+\frac{as}{2c^2}\right). \tag{8}$$

The relationship between proper time τ and coordinated time t is:

$$\sinh\left(\frac{a\tau}{c}\right) = \frac{at}{c}. \tag{9}$$

With the above formulas and assuming various acceleration levels (between 0.5 and 10 m/s^2), we determined the coordinated and proper time of flight and the maximum ratio $\beta = u/c$ for transfers to the selected 77 stars. The results are illustrated in Figure 25 and in Figure 26. For three acceleration levels the results are also listed in Table 15. By travelling under a constant thrust of 0.5 m/s^2, it takes 17.8 years to the nearest star (Proxima Centauri), 38.7 years to the furthest (GJ 625) according to an on-board clock, while for an observer on Earth the same transfers would last 18.4 years and 45.8 years, respectively. Under a much higher acceleration (10 m/s^2) these values become much shorter: 3.5 years of on-board time (or 5.8 of coordinated time) to get to Proxima Centauri, 6.1 years (23.3 years) to GJ 625 and the speed of the spacecraft at mid-flight would be very close to the speed of light (u/c > 0.9). The total mission duration is obtained by adding the time necessary for the data to be transmitted to Earth, which amounts to 4.3 years for a mission to Proxima and 21.5 years for a journey to GJ 625.

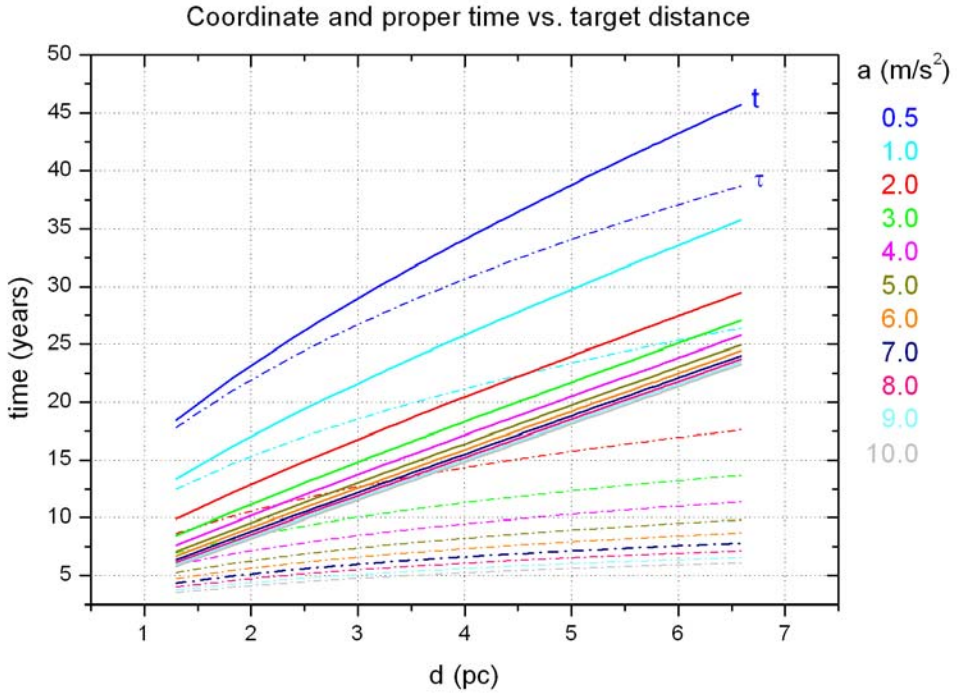

Figure 25: Coordinated and proper time of flight for transfers to the selected 77 stars according to various acceleration levels. Computations have been performed assuming relativistic speed under constant thrust.

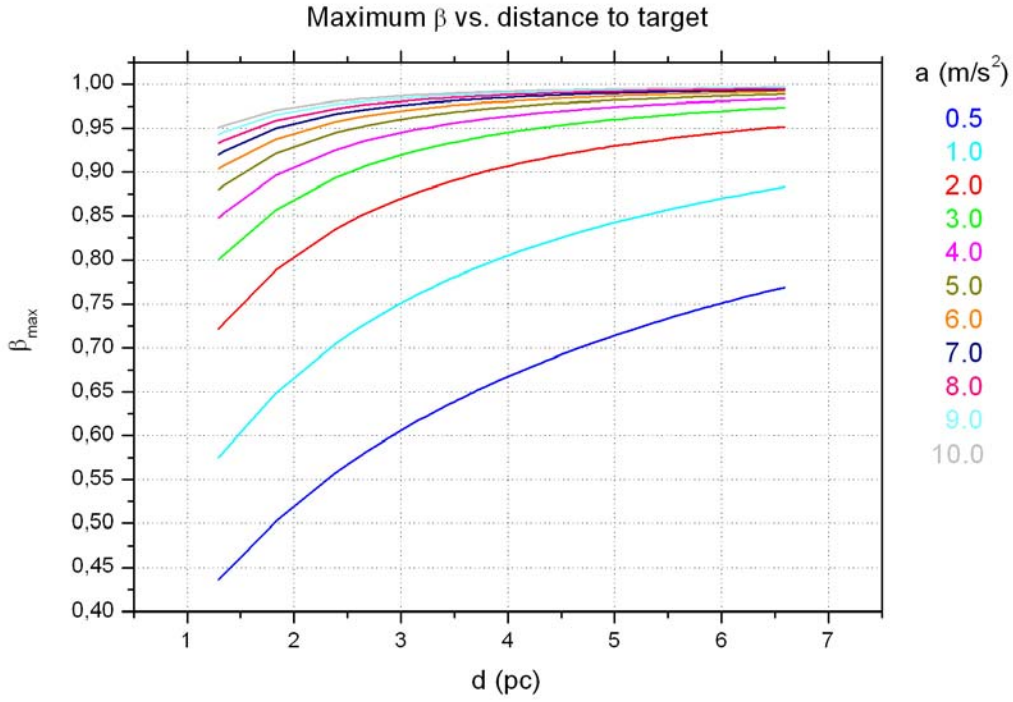

Figure 26: Maximum *u/c* for transfers to the selected 77 stars according to various acceleration levels. Computations have been performed assuming relativistic speed under constant thrust.

Name	a = 0.5 m s^{-2}			a = 3 m s^{-2}			a = 6 m s^{-2}			a = 10 m s^{-2}		
	τ (years)	t (years)	β	τ (years)	t (years)	β	τ (years)	t (years)	β	τ (years)	t (years)	β
Proxima Centauri	17.76	18.41	0.436	6.96	8.45	0.800	4.72	6.68	0.903	3.49	5.82	0.951
alpha Centauri	18.04	18.73	0.442	7.06	8.62	0.806	4.79	6.83	0.907	3.54	5.97	0.953
Barnard's Star	21.02	22.11	0.503	8.12	10.54	0.857	5.45	8.56	0.938	3.99	7.63	0.970
Wolf 359	23.92	25.53	0.557	9.12	12.61	0.894	6.06	10.48	0.957	4.39	9.49	0.981
Lalande 21185	24.67	26.43	0.571	9.37	13.18	0.901	6.21	11.01	0.961	4.49	10.01	0.982
Sirius	25.08	26.94	0.578	9.51	13.50	0.905	6.29	11.31	0.963	4.55	10.30	0.983
UV Ceti	25.29	27.19	0.582	9.58	13.66	0.907	6.33	11.46	0.964	4.57	10.45	0.984
Ross 154	26.58	28.80	0.604	10.00	14.70	0.918	6.58	12.45	0.969	4.74	11.42	0.986
Ross 248	27.41	29.85	0.617	10.27	15.40	0.925	6.74	13.11	0.972	4.84	12.07	0.988
epsilon Eri	27.66	30.17	0.622	10.35	15.61	0.927	6.79	13.31	0.973	4.87	12.27	0.988
Lacaille 9352	27.94	30.52	0.626	10.44	15.85	0.929	6.84	13.54	0.974	4.91	12.49	0.989
Ross 128	28.16	30.80	0.629	10.51	16.04	0.930	6.88	13.72	0.974	4.93	12.67	0.989
EZ Aquarii	28.58	31.35	0.636	10.65	16.42	0.933	6.96	14.07	0.976	4.99	13.02	0.990
Procyon	28.75	31.57	0.639	10.70	16.56	0.934	6.99	14.21	0.976	5.01	13.16	0.990
61 Cygni	28.75	31.57	0.639	10.70	16.56	0.934	6.99	14.21	0.976	5.01	13.16	0.990
DM+59 1915	28.90	31.76	0.641	10.75	16.69	0.935	7.02	14.34	0.976	5.02	13.28	0.990
GX Andromedae	29.01	31.91	0.643	10.78	16.80	0.936	7.04	14.44	0.977	5.04	13.38	0.990
Eps Indi	29.25	32.22	0.646	10.86	17.01	0.937	7.08	14.65	0.977	5.07	13.58	0.990
DX Cancri	29.25	32.22	0.647	10.86	17.01	0.937	7.08	14.65	0.977	5.07	13.59	0.990
Tau Ceti	29.32	32.32	0.648	10.88	17.08	0.938	7.10	14.71	0.978	5.07	13.65	0.990
RECONS 1	29.45	32.48	0.649	10.92	17.19	0.938	7.12	14.82	0.978	5.09	13.75	0.991
YZ Ceti	29.61	32.70	0.652	10.97	17.34	0.939	7.15	14.96	0.978	5.11	13.90	0.991
Luyten's Star	29.88	33.05	0.656	11.06	17.59	0.941	7.20	15.20	0.979	5.14	14.13	0.991
Kapteyn's Star	30.35	33.68	0.663	11.20	18.02	0.943	7.28	15.62	0.980	5.19	14.55	0.992
AX Microscopium	30.45	33.82	0.665	11.24	18.12	0.944	7.30	15.71	0.980	5.21	14.64	0.992
Kruger 60	30.77	34.23	0.669	11.33	18.42	0.946	7.36	16.00	0.981	5.24	14.92	0.992
Ross 614	30.99	34.53	0.672	11.40	18.63	0.947	7.40	16.20	0.981	5.27	15.12	0.992
Wolf 1061	31.50	35.23	0.680	11.56	19.12	0.949	7.49	16.68	0.982	5.33	15.60	0.993
WD 0046+051	31.76	35.59	0.683	11.64	19.38	0.950	7.53	16.93	0.983	5.36	15.84	0.993
GJ 1	31.94	35.83	0.686	11.69	19.56	0.951	7.56	17.10	0.983	5.38	16.01	0.993
Wolf 424	32.02	35.95	0.687	11.72	19.64	0.952	7.58	17.18	0.983	5.39	16.09	0.993
TZ Arietis	32.23	36.23	0.690	11.78	19.85	0.953	7.62	17.38	0.984	5.41	16.29	0.993
GJ 687	32.53	36.64	0.694	11.87	20.15	0.954	7.67	17.67	0.984	5.44	16.57	0.993
LHS 292	32.54	36.66	0.694	11.88	20.16	0.954	7.67	17.68	0.984	5.44	16.59	0.993
GJ 674	32.54	36.67	0.694	11.88	20.16	0.954	7.67	17.69	0.984	5.44	16.59	0.993
GJ 1002	33.06	37.39	0.701	12.04	20.69	0.956	7.76	18.20	0.985	5.50	17.10	0.994
Ross 780	33.09	37.43	0.702	12.04	20.72	0.956	7.76	18.23	0.985	5.50	17.13	0.994
WX Ursae Maj	33.58	38.12	0.708	12.19	21.23	0.958	7.85	18.72	0.986	5.56	17.62	0.994
GJ 380	33.60	38.15	0.708	12.20	21.25	0.958	7.85	18.74	0.986	5.56	17.64	0.994
GJ 388	33.69	38.28	0.709	12.22	21.35	0.959	7.87	18.83	0.986	5.57	17.73	0.994
GJ 832	33.84	38.48	0.711	12.27	21.50	0.959	7.89	18.98	0.986	5.58	17.87	0.994
GJ 682	34.08	38.83	0.715	12.34	21.76	0.960	7.93	19.23	0.987	5.61	18.13	0.995
omicron 2 Eri	34.14	38.91	0.715	12.36	21.81	0.960	7.94	19.29	0.987	5.62	18.18	0.995
EV Lacertae	34.21	39.02	0.716	12.38	21.90	0.961	7.95	19.37	0.987	5.62	18.26	0.995
70 Ophiuchi	34.38	39.26	0.718	12.43	22.08	0.961	7.98	19.55	0.987	5.64	18.44	0.995
Altair	34.46	39.38	0.719	12.45	22.17	0.961	8.00	19.63	0.987	5.65	18.52	0.995
EI Cancri	34.78	39.84	0.723	12.55	22.51	0.963	8.05	19.97	0.988	5.68	18.85	0.995
GJ 445	35.25	40.51	0.729	12.68	23.02	0.964	8.13	20.46	0.988	5.73	19.35	0.995
GJ 1005	35.25	40.52	0.729	12.68	23.02	0.964	8.13	20.47	0.988	5.73	19.35	0.995
GJ 526	35.39	40.73	0.731	12.73	23.18	0.965	8.15	20.62	0.988	5.75	19.50	0.995
Stein 2051	35.72	41.21	0.735	12.82	23.54	0.966	8.20	20.97	0.989	5.78	19.85	0.995
GJ 754	36.23	41.96	0.741	12.97	24.12	0.967	8.29	21.54	0.989	5.84	20.42	0.996
Wolf 1453	36.23	41.97	0.741	12.97	24.13	0.967	8.29	21.54	0.989	5.84	20.42	0.996
sigma Draconi	36.38	42.20	0.743	13.02	24.30	0.968	8.31	21.71	0.990	5.85	20.59	0.996
GJ 229	36.43	42.26	0.743	13.03	24.35	0.968	8.32	21.76	0.990	5.86	20.64	0.996
GJ 693	36.57	42.47	0.745	13.07	24.52	0.968	8.34	21.92	0.990	5.87	20.80	0.996
Wolf 1055	36.64	42.58	0.746	13.09	24.59	0.968	8.35	22.00	0.990	5.88	20.87	0.996
Ross 47	36.70	42.67	0.747	13.11	24.67	0.969	8.36	22.07	0.990	5.88	20.95	0.996
GJ 570	36.75	42.75	0.747	13.12	24.73	0.969	8.37	22.13	0.990	5.89	21.00	0.996
GJ 908	36.89	42.95	0.749	13.16	24.89	0.969	8.39	22.29	0.990	5.90	21.16	0.996
eta Cassiopei	36.90	42.97	0.749	13.17	24.90	0.969	8.40	22.30	0.990	5.90	21.17	0.996
GJ 588	36.90	42.98	0.749	13.17	24.90	0.969	8.40	22.30	0.990	5.90	21.18	0.996
Ross 882	36.99	43.10	0.750	13.19	25.00	0.969	8.41	22.40	0.990	5.91	21.27	0.996
36 Ophiuchi	36.99	43.11	0.750	13.19	25.00	0.969	8.41	22.40	0.990	5.91	21.27	0.996

GJ 783	37.22	43.45	0.753	13.26	25.27	0.970	8.45	22.66	0.990	5.94	21.53	0.996
82 Eridani	37.25	43.50	0.753	13.27	25.31	0.970	8.45	22.70	0.990	5.94	21.57	0.996
delta Pavonis	37.38	43.70	0.754	13.30	25.46	0.970	8.47	22.85	0.991	5.95	21.72	0.996
QY Aurigae	37.47	43.84	0.755	13.33	25.57	0.971	8.49	22.96	0.991	5.96	21.82	0.996
HN Librae	37.48	43.85	0.755	13.33	25.58	0.971	8.49	22.96	0.991	5.96	21.83	0.996
GJ 338	37.56	43.97	0.756	13.35	25.67	0.971	8.50	23.06	0.991	5.97	21.92	0.996
GJ 784	37.66	44.12	0.758	13.38	25.79	0.971	8.52	23.17	0.991	5.98	22.04	0.996
Wolf 562y	37.86	44.44	0.760	13.44	26.04	0.972	8.55	23.42	0.991	6.00	22.28	0.996
EQ Pegasi	38.04	44.71	0.762	13.49	26.25	0.972	8.58	23.62	0.991	6.02	22.49	0.996
GJ 661	38.19	44.95	0.763	13.53	26.44	0.972	8.60	23.81	0.991	6.03	22.67	0.997
Wolf 630	38.35	45.19	0.765	13.58	26.63	0.973	8.63	23.99	0.991	6.05	22.85	0.997
GJ 625	38.72	45.76	0.769	13.68	27.08	0.974	8.68	24.44	0.992	6.09	23.30	0.997

Table 15: Coordinated time, proper time of flight and maximum u/c for transfers to the selected 77 stars according to three acceleration levels. Computations have been performed assuming relativistic speed under constant thrust.

5.3 Exploration phase: orbits around binary systems

For the present case of in situ observations of stars near our Sun, the following privileged locations should be considered when designing the orbit:

a) libration points—and periodic orbits around them—within binary star systems (possibly formed by a star and a planetary companion);

b) (periodic) orbits around stars (and their planetary companions);

c) transfer orbits between any two of the previous sets.

A variety of dynamical acrobatics can be envisioned in relation to these locations. In particular, orbits, possibly of a periodic nature, can be designed around the libration points. Transfers can also be contemplated between the libration points and between orbits around the component bodies and the critical points. Scientific investigation goals will of course determine the desirability of simple or more complicated tours to be designed. Naturally, transfers requiring near null input energy are to be preferred and should be the main goal of the designer.

5.3.1 Lagrange points

The Circular Restricted Three-Body Problem (CR3BP hereinafter) describes the motion of a body with negligible mass under the gravitational influence of two massive bodies, called the primaries, which move in circular orbits about their barycentre. Let (x,y,z) denote the position of the negligible-mass body in a rotating coordinate system with the origin at the barycentre where the x-axis points from the larger to the smaller primary, the z-axis points along the normal to the orbit plane of the primaries and the y-axis completes the right-handed orthogonal triad. The quantity μ represents the ratio of the mass of the smaller primary to the total mass. The units are chosen so that the distance between the primaries, the sum of the masses of the primaries and the angular velocity of the primaries are all equal to one. Therefore the larger and smaller primaries are located at $(-\mu,0,0)$ and $(1-\mu,0,0)$ respectively. The equations of motion for the CR3BP (see also Danby, 1962) are

$$\begin{aligned} \ddot{x} &= 2\dot{y} + x - (1-\mu)(x+\mu)r_1^{-3} - \mu(x-1+\mu)r_2^{-3} \\ \ddot{y} &= -2\dot{x} + y - (1-\mu)yr_1^{-3} - \mu yr_2^{-3} \\ \ddot{z} &= -(1-\mu)zr_1^{-3} - \mu zr_2^{-3} \end{aligned} \tag{10}$$

where r_1 and r_2 are the distances between the third body and the primaries:

$$\begin{aligned} r_1 &= \sqrt{(x+\mu)^2 + y^2 + z^2} \\ r_2 &= \sqrt{(x-1+\mu)^2 + y^2 + z^2} \end{aligned} \tag{11}$$

The well-known integral of motion (i.e., the Jacobi integral) associated to this dynamical system is

$$J = 2U(x,y,z) - (v_x^{\,2} + v_y^{\,2} + v_z^{\,2}) \tag{12}$$

where

$$U(x,y,z) = \frac{1}{2}(x^2 + y^2) + \frac{1-\mu}{r_1} + \frac{\mu}{r_2} \tag{13}$$

is the sum of the centrifugal and gravitational potential at the position of the massless body.

In the barycentric rotating reference system the x coordinates of the three collinear equilibrium points (L_1, L_2 and L_3) are determined by solving the following fifth order equations:

$$u^2[(1-s_1) + 3u + 3u^2 + u^3] = \mu[s_0 + 2s_0u + (1 + s_0 - s_1)u^2 + 2u^3 + u^4] \tag{14}$$

in which u measures the distance from the second primary in normalized units (i.e., in units of the distance between the two primaries), $s_0 = \text{sign}(u)$ and $s_1 = \text{sign}(u+1)$: (s_0,s_1) are equal to (-1,1), (1,1) and (-1,-1), respectively for L_1, L_2 and L_3. (Cornish & Goodman, *lagrange.ps,* document available at http://spiff.rit.edu/classes/phys440/lectures/lagrange/).

The positions of the two equilateral libration points L_4 and L_5 are:

$$\begin{aligned} L_4: &\quad \left(\frac{1-2\mu}{2}, \frac{\sqrt{3}}{2}\right) \\ L_5: &\quad \left(\frac{1-2\mu}{2}, -\frac{\sqrt{3}}{2}\right) \end{aligned} \tag{15}$$

The 13 binary systems of Table 3 are almost all characterized by a large value of the orbital eccentricity. *To such systems the CR3BP does not apply.* The problem is better modelled as an *Elliptical Restricted Three-Body Problem* (ER3BP hereinafter). In the ER3BP the Lagrange critical points still exist, but instead of being fixed (in barycentric rotating coordinates), they pulsate with the distance between the two primaries.

We determined the positions of the five equilibrium points of systems composed by each pair of stars and a third massless body (the spacecraft) at the time when the distance r between the primaries equals the semi-major axis a and assuming zero eccentricity. We solved the fifth-order Lagrange equations (14) by an iterative technique starting from the initial guess u_0 suggested by Brouwer and Clemence (1961):

$$\begin{aligned} L_1: &\quad u_0 = -\alpha\left(1 - \alpha/3 - \alpha^2/9\right) \\ L_2: &\quad u_0 = \alpha\left(1 + \alpha/3 - \alpha^2/9\right) \\ L_3: &\quad u_0 = \beta - 2 \end{aligned} \tag{16}$$

where $\alpha = \left[\frac{\mu}{3(1-\mu)}\right]^{1/3}$, $\beta = -\nu\left(1 + \frac{23}{84}\nu^2\right)$ and $\nu = \frac{7}{12}\mu$. Results for the selected 13 binary systems are shown in barycentric rotating coordinates and physical units in the plots of Figure 27.

The non negligible eccentricity of all the systems (apart from GX Andromedae) causes the three collinear equilibrium points to pulsate along the x-axis around their mean values (i.e., those obtained for r = a) with amplitude $\pm ae$; the two triangular points move both in the x and y directions according to the law:

$$L_4: \quad \left(\frac{1-2\mu}{2}r, \frac{\sqrt{3}}{2}r\right)$$
$$L_5: \quad \left(\frac{1-2\mu}{2}r, -\frac{\sqrt{3}}{2}r\right) \tag{17}$$

where again $a(1-e) \le r \le a(1+e)$ as a function of time.

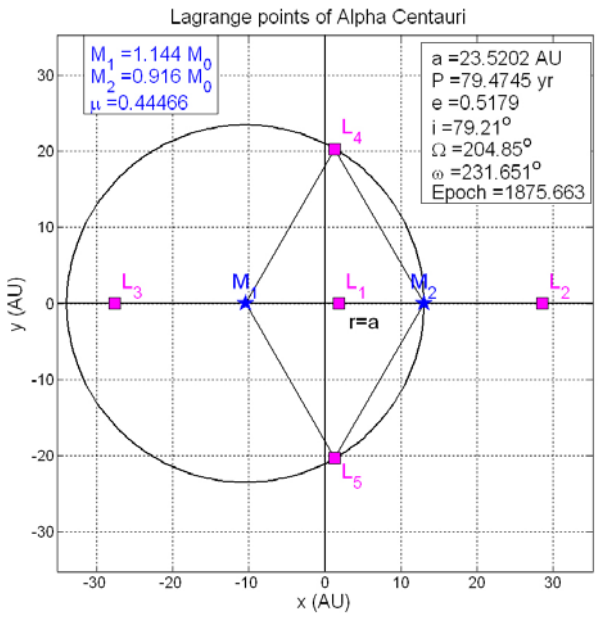

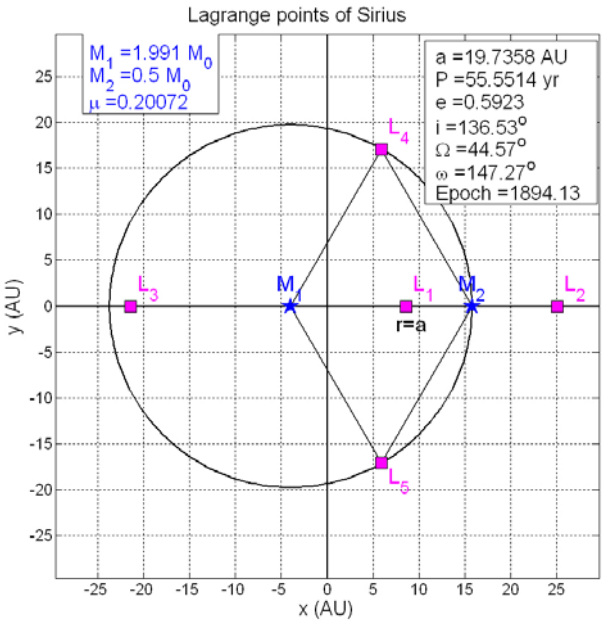

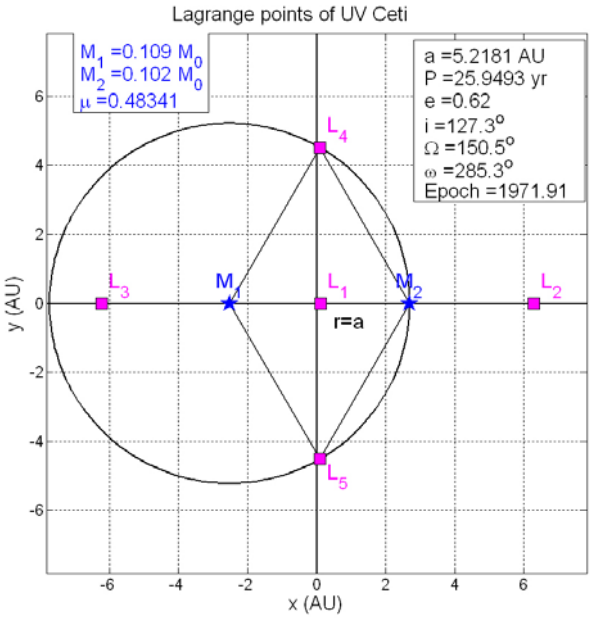

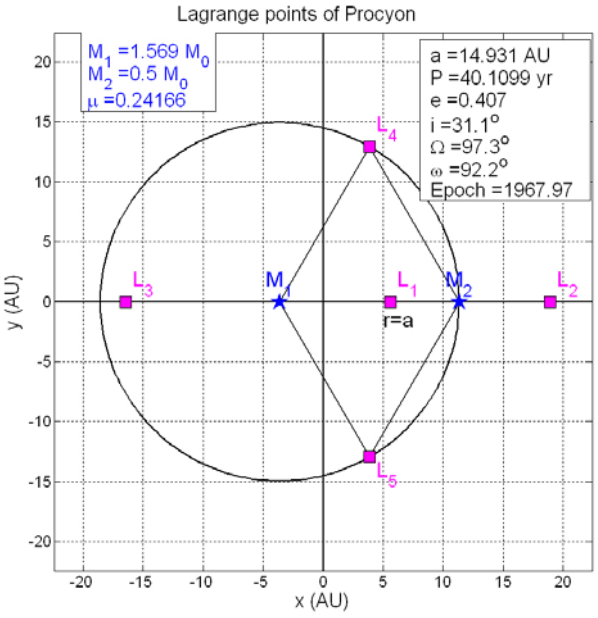

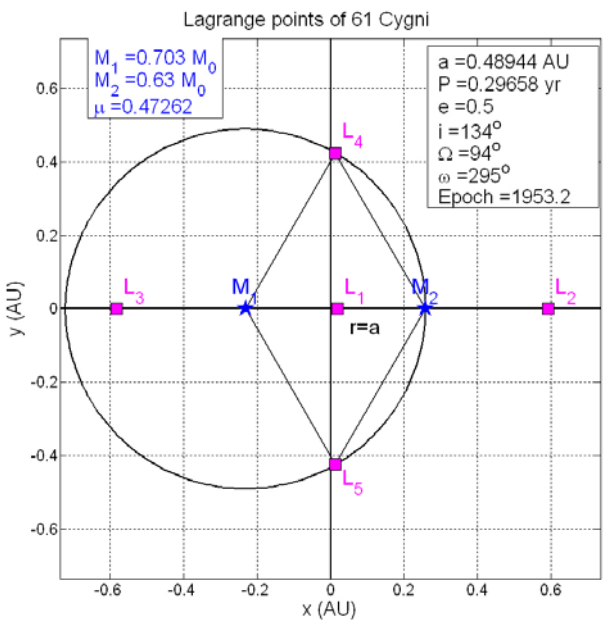
Lagrange points of 61 Cygni
M1 =0.703 M0
M2 =0.63 M0
μ =0.47262
a =0.48944 AU
P =0.29658 yr
e =0.5
i =134°
Ω =94°
ω =295°
Epoch =1953.2
L4
L3
M1
L1
M2
L2
L5
r=a
y (AU)
x (AU)

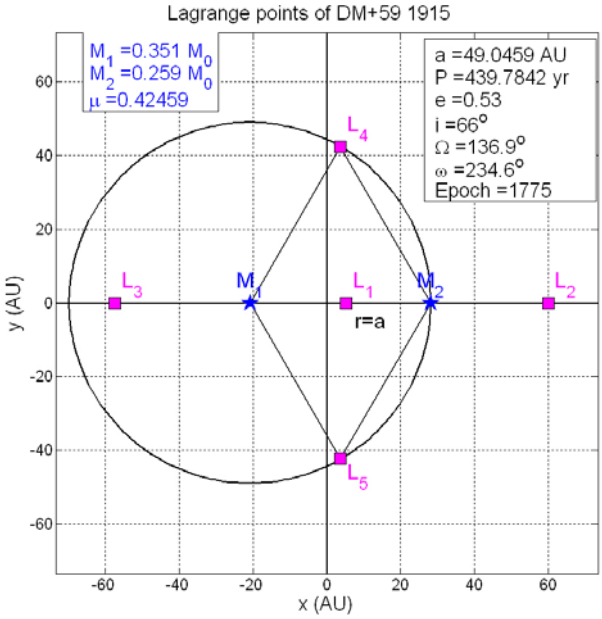
Lagrange points of DM+59 1915
M1 =0.351 M0
M2 =0.259 M0
μ =0.42459
a =49.0459 AU
P =439.7842 yr
e =0.53
i =66°
Ω =136.9°
ω =234.6°
Epoch =1775
L4
L3
M1
L1
M2
L2
L5
r=a
y (AU)
x (AU)

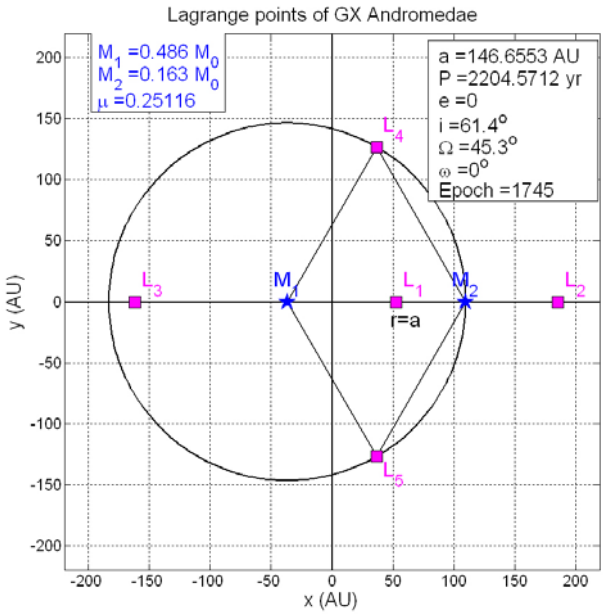
Lagrange points of GX Andromedae
M1 =0.486 M0
M2 =0.163 M0
μ =0.25116
a =146.6553 AU
P =2204.5712 yr
e =0
i =61.4°
Ω =45.3°
ω =0°
Epoch =1745
L4
L3
M1
L1
M2
L2
L5
r=a
y (AU)
x (AU)

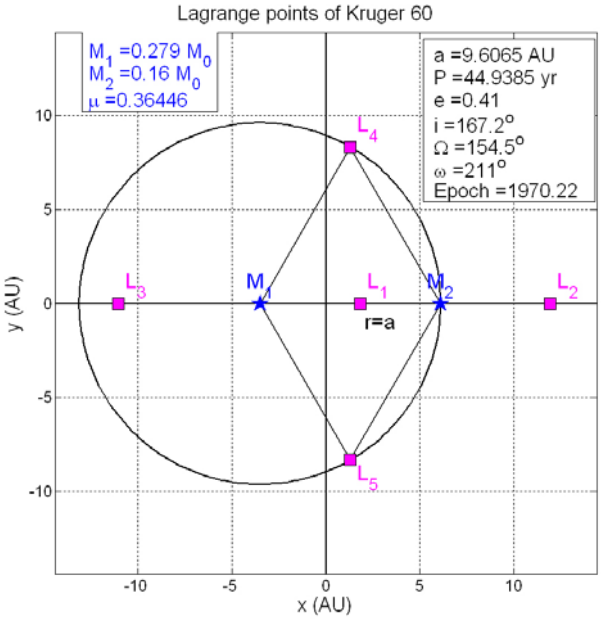
Lagrange points of Kruger 60
M1 =0.279 M0
M2 =0.16 M0
μ =0.36446
a =9.6065 AU
P =44.9385 yr
e =0.41
i =167.2°
Ω =154.5°
ω =211°
Epoch =1970.22
L4
L3
M1
L1
M2
L2
L5
r=a
y (AU)
x (AU)

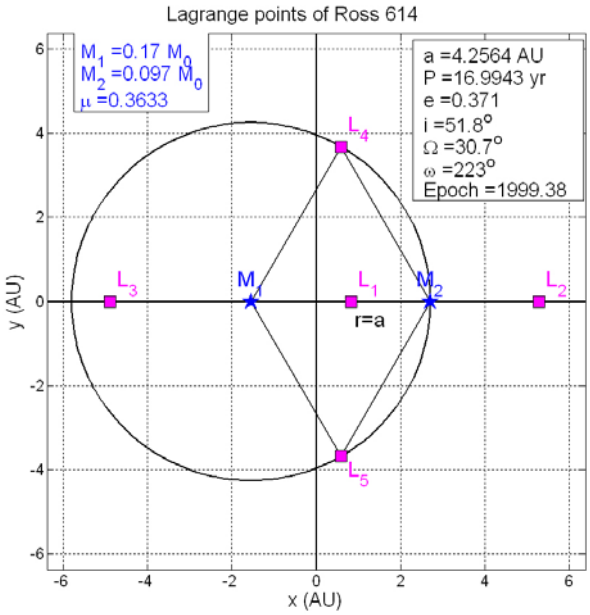
Lagrange points of Ross 614
M1 =0.17 M0
M2 =0.097 M0
μ =0.3633
a =4.2564 AU
P =16.9943 yr
e =0.371
i =51.8°
Ω =30.7°
ω =223°
Epoch =1999.38
L4
L3
M1
L1
M2
L2
L5
r=a
y (AU)
x (AU)

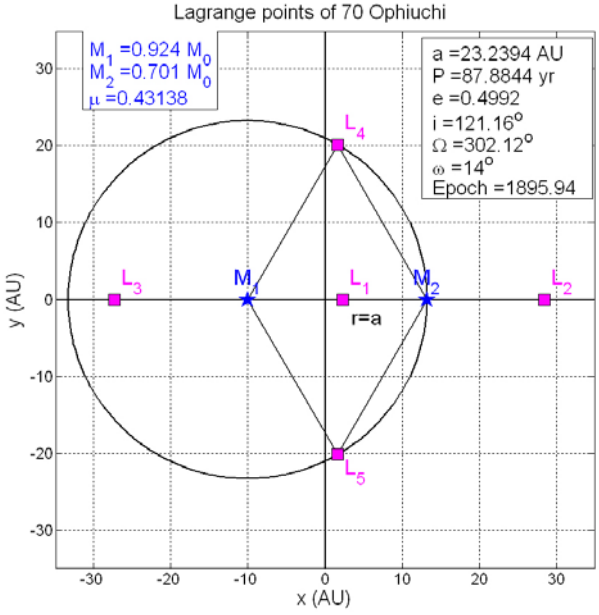
Lagrange points of 70 Ophiuchi
M1 =0.924 M0
M2 =0.701 M0
μ =0.43138
a =23.2394 AU
P =87.8844 yr
e =0.4992
i =121.16°
Ω =302.12°
ω =14°
Epoch =1895.94
L4
L3
M1
L1
M2
L2
L5
r=a
y (AU)
x (AU)

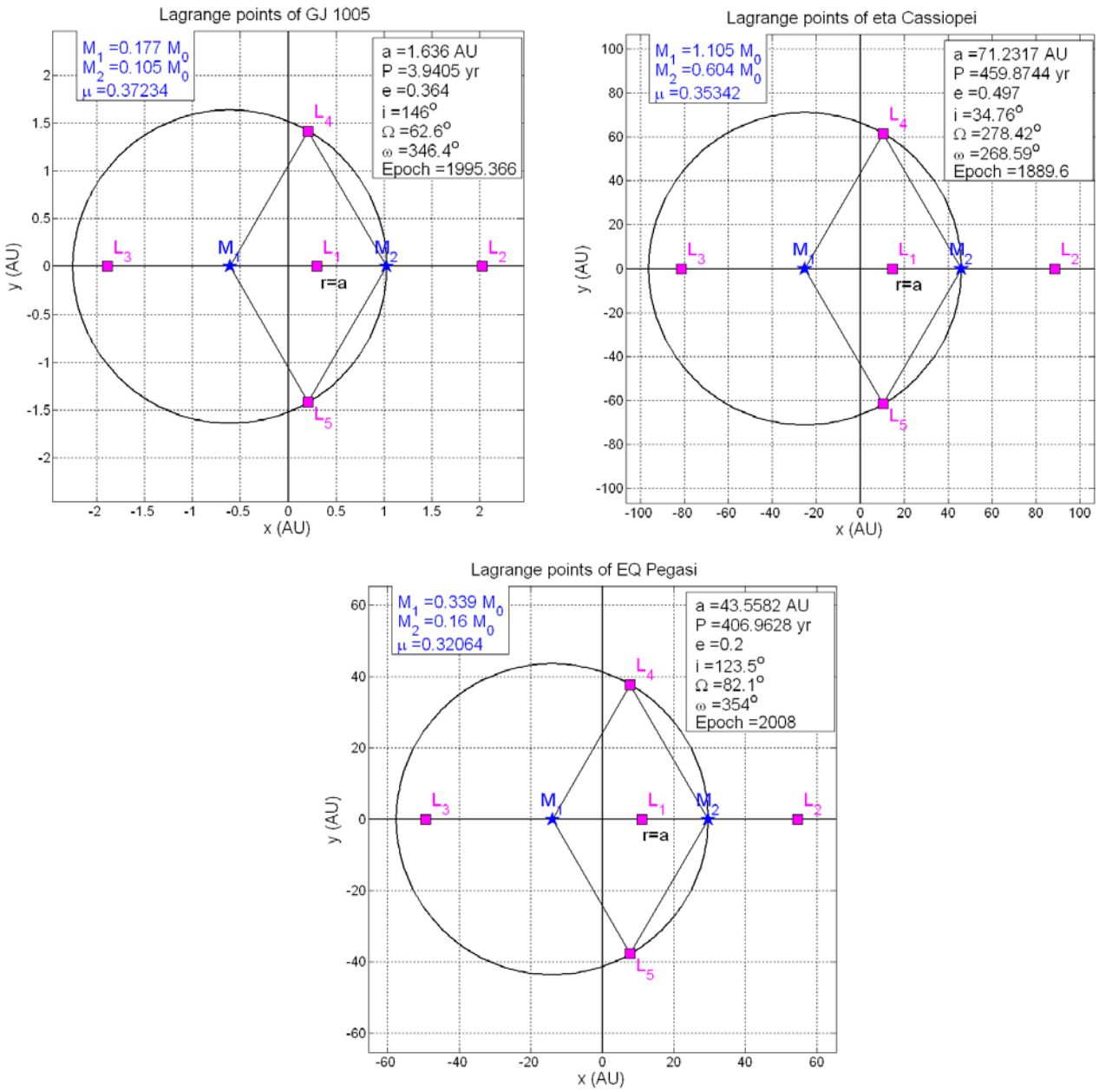

Figure 27: The 13 selected binary systems with their Lagrange points, computed by solving the Lagrange quintic equation under the assumption of zero eccentricity and relative distance between the stars equal to the observed semi-major axis. The plots are drawn in physical units relative to the barycentric rotating reference frame.

Figure 28 shows the orbits of the Lagrangian points for the Alpha Cen A/B system ($e = 0.5179$) as viewed in an inertial reference frame. All critical points follow *elliptical orbits* whose foci coincide with the center of mass of the system.

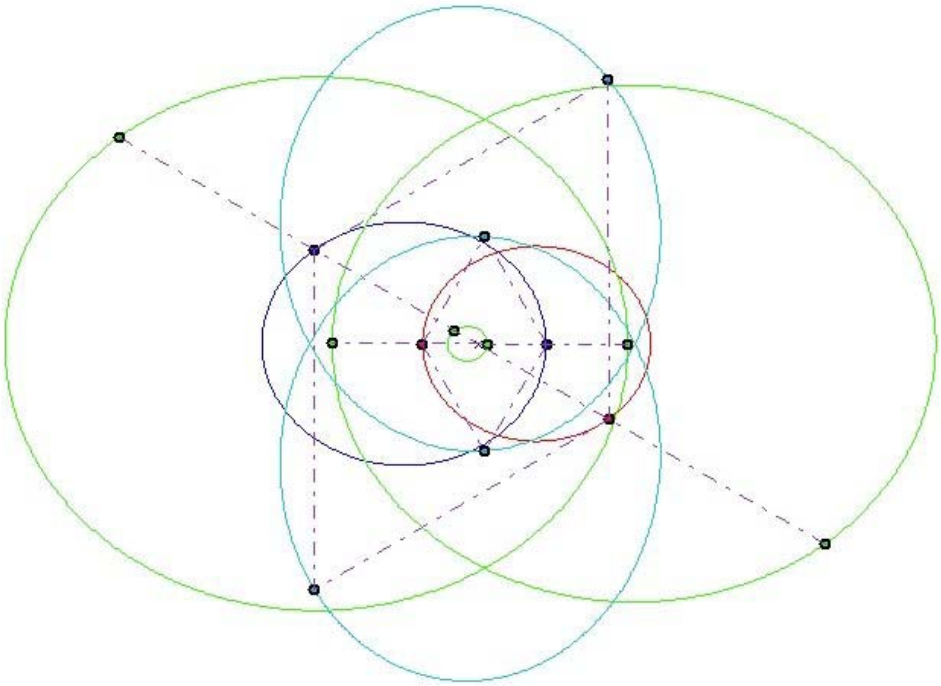

Figure 28: The elliptical paths followed by the Lagrangian points of the Alpha Cen A/B system viewed from an inertial reference frame (two snapshots are shown for true anomalies of 0° and 150°).

5.3.2 Computation of periodic orbits using AUTO2000

AUTO2000 is a software tool for continuation and bifurcation problems in ordinary differential equations developed by R. Paffenroth, E. Doedel and collaborators (Dichmann, Doedel & Paffenroth, 2002; Paffenroth, 2002). The software is free and publicly available from http://auto2000.sourceforge.net/. The problems that may be addressed by numerical continuation methods are those which can be solved as a parameter-dependent system of nonlinear equations. The algorithm starts from a known solution at given parameter values; then a solution is computed at a nearby set of parameter values to generate an initial guess to feed an iterative scheme to compute the solution at a new set of parameter values. Therefore a parameter continuation algorithm can be described as a numerical implementation of a homotopy between solutions of different problems.

Driven by suitable user-defined scripts, AUTO2000 computes families of periodic solutions of conservative systems. In particular, specific scripts, prepared and distributed by the authors, allow to obtain several families of periodic solutions emanating from the libration points.

AUTO2000 uses numerical continuation methods to explore families of three-dimensional periodic solutions of this system that emanate from any of the five libration points. This is done by rewriting Eq. (10) as a six-dimensional first-order system, adding boundary conditions to impose unit periodicity of the solutions and introducing the period T of the orbit as an unknown to be solved for as part of the numerical procedure; finally, a so-called unfolding parameter λ is added and treated as an unknown. The resulting system of differential equations is

$$
\begin{aligned}
\dot{x} &= Tv_x + \lambda \frac{\partial J}{\partial x} \\
\dot{y} &= Tv_y + \lambda \frac{\partial J}{\partial y} \\
\dot{z} &= Tv_z + \lambda \frac{\partial J}{\partial z} \\
\dot{v}_x &= T\left[2v_y + x - (1-\mu)(x+\mu)r_1^{-3} - \mu(x-1+\mu)r_2^{-3} + \lambda \frac{\partial J}{\partial v_x} \right] \\
\dot{v}_y &= T\left[-2v_x + y - (1-\mu)yr_1^{-3} - \mu yr_2^{-3} + \lambda \frac{\partial J}{\partial v_y} \right] \\
\dot{v}_z &= T\left[-(1-\mu)zr_1^{-3} - \mu zr_2^{-3} + \lambda \frac{\partial J}{\partial v_z} \right]
\end{aligned}
\tag{18}
$$

with the following boundary conditions:

$$
\begin{aligned}
&x(1) = x(0), \quad y(1) = y(0), \quad z(1) = z(0), \\
&v_x(1) = v_x(0), \quad v_y(1) = v_y(0), \quad v_z(1) = v_z(0)
\end{aligned}
\tag{19}
$$

5.3.3 The case of GX Andromedae ($e = 0$)

The binary system made up by the two stars GX and GQ Andromedae is characterized by zero orbital eccentricity and therefore is suitable for computation of the periodic orbits in the CR3BP with AUTO2000.

For this mass ratio ($\mu = 0.25116$) AUTO2000 has generated about 15,000 orbits emanating from the three collinear equilibrium positions (L_1, L_2, L_3): each orbit is represented by 201 points and for each point 7 quantities are output (time, 3 position coordinates, 3 velocity components); then, for each orbit the period and the Jacobi integral are also given. The amount of data is huge and therefore difficult to handle. Figure 29, Figure 30 and Figure 31 illustrate a selection (roughly 4%) of the periodic orbits obtained.

The periods of the orbits thus obtained are always a non-negligible fraction of the system's period, equal to 2,200 years; therefore, it would take a very long time to follow the full revolution of any of the periodic orbits associated with the libration points of this system. We regard this as a test case for the exploration of a type of low-cost trajectories within a binary system.

In practice, the revolution period of the primaries is probably long enough to allow application of the Two-Fixed Centers paradigm.

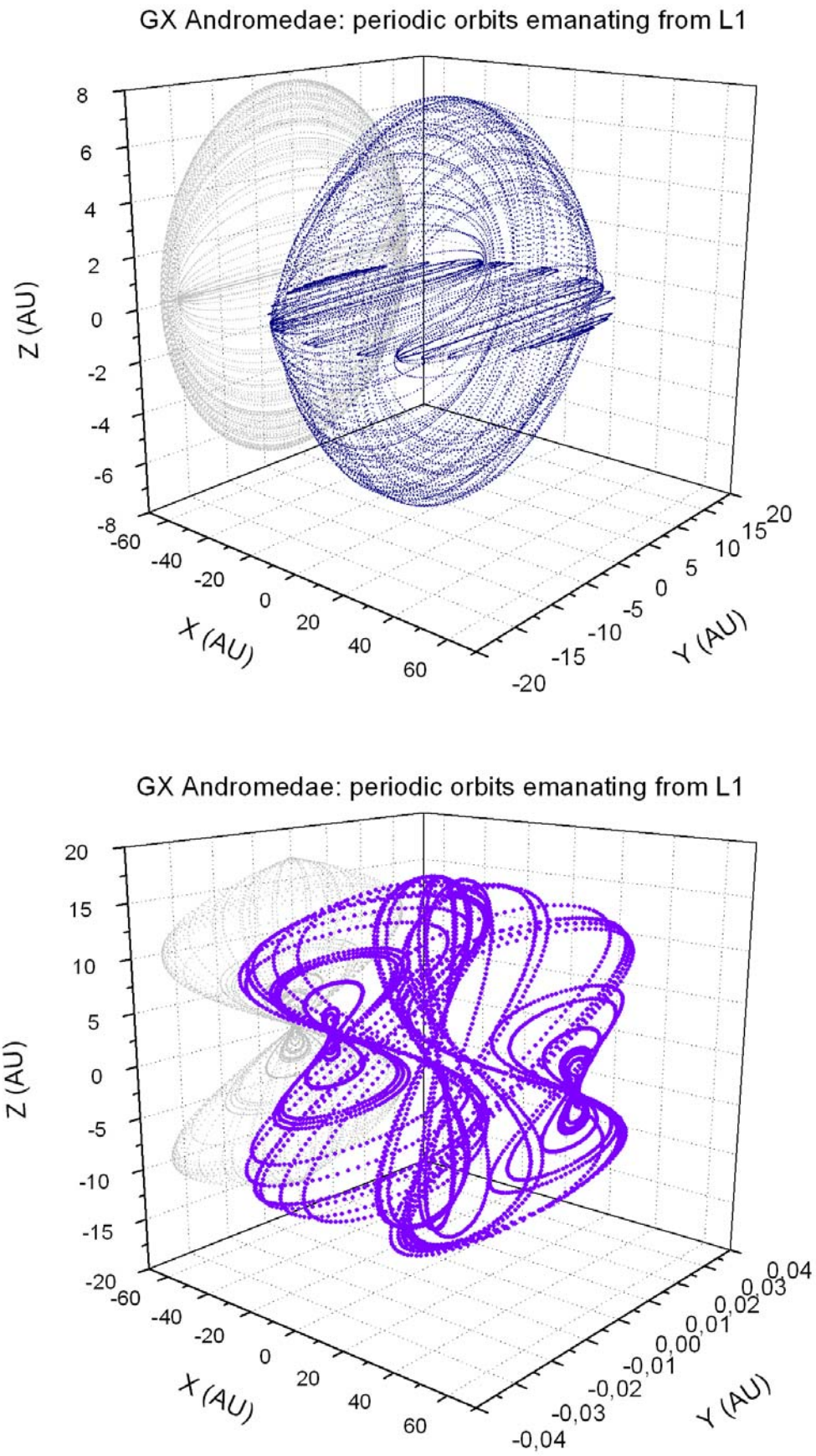

Figure 29: Two sets of periodic orbits emanating from L_1 in barycentric rotating coordinates and physical units. The most meaningful projection of the displayed orbits is shown in grey.

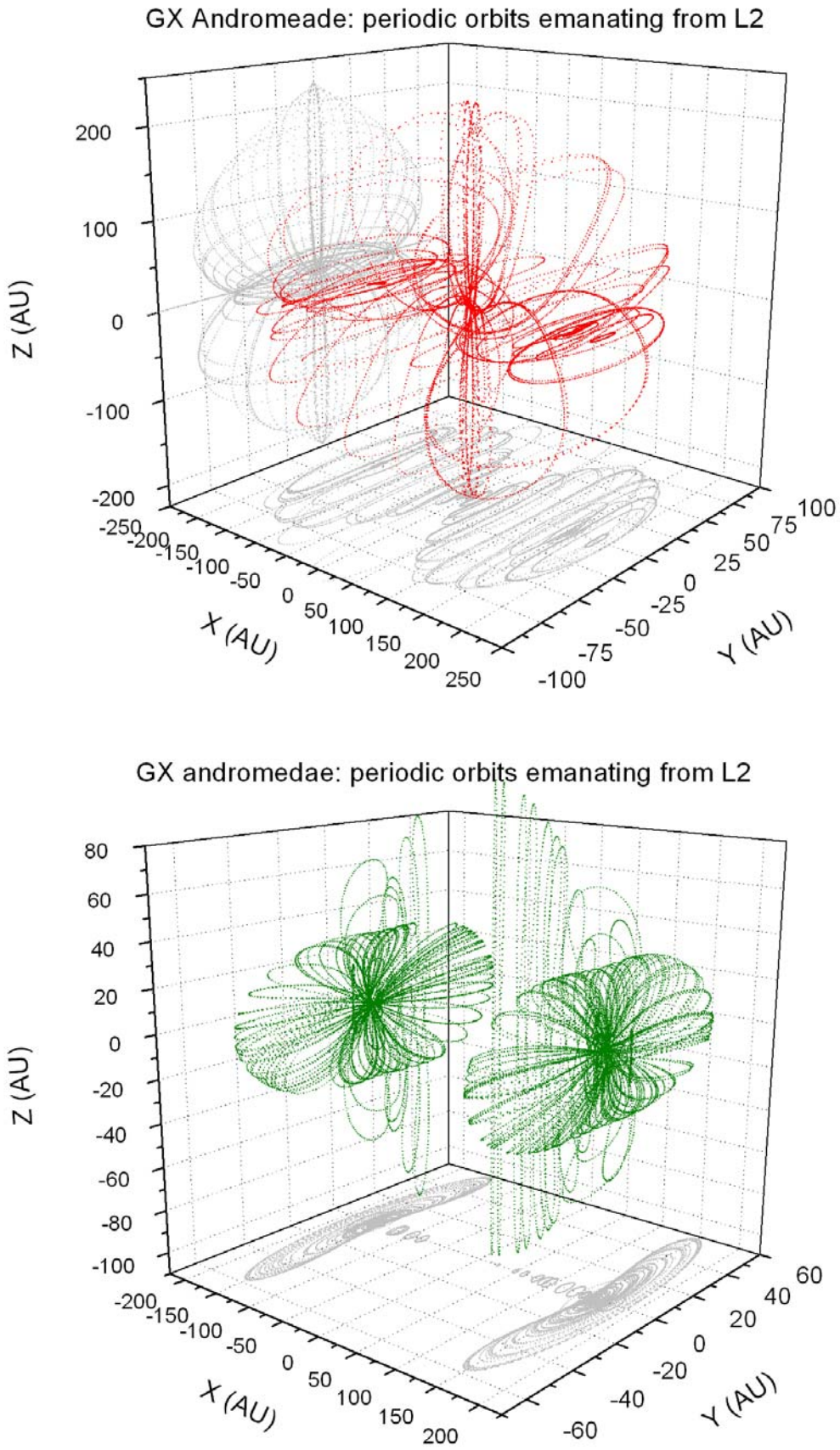

Figure 30: Two sets of periodic orbits emanating from L_2 in barycentric rotating coordinates and physical units. The most meaningful projection of the displayed orbits is shown in grey.

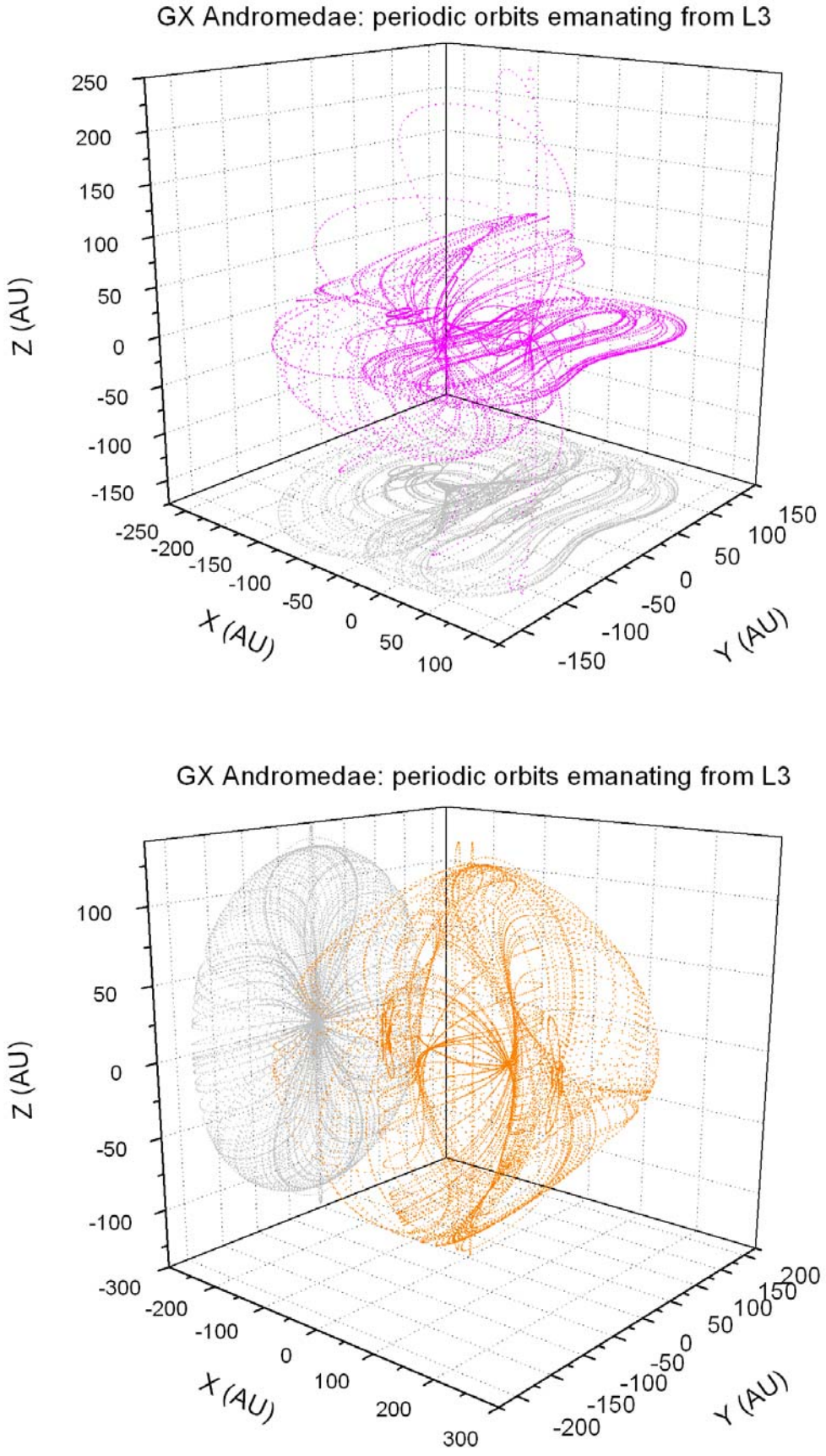

Figure 31: Two sets of periodic orbits emanating from L_3 in barycentric rotating coordinates and physical units. The most meaningful projection of the displayed orbits is shown in grey.

We made a preliminary investigation on the possibility of exploiting this category of natural trajectories in the CR3BP to accomplish low-cost transfers from the first primary to the second primary by travelling through some Lagrange point of the system (most noticeably L_1, which could ensure minimum energy transfers). We selected the periodic orbits by imposing position constraints (maximum distance from L_1, inner and outer radius of a ring of circular orbits around m_1, inner and outer radius of a ring of circular orbits around m_2) and a position tolerance for the intersections. The intersections thus obtained have been graded according to the magnitude of the velocity differences (maneuvres) between the intersecting orbits, the lowest grade being assigned to the most expensive maneuvres. We investigated various sets of constraints and we ended up with two low-cost transfer strategies, shown in Figure 32 and Figure 33.

The first (case A) illustrates 2 solutions, each involving 2 maneuvres, that take the spacecraft from the region around m_1 to the region around m_2 through 3 periodic orbits of the system; the total cost of the transfer is 4.12 km/s and 3.06 km/s respectively.

Case B shows the transfer from a circular orbit around m_1 (13 AU radius) to a circular orbit around m_2 (24 AU radius) through three branches of periodic orbits (the total cost of the maneuvre is 3.27 km/s).

The selection constraints that characterize each strategy are reported in the legends of the two plots.

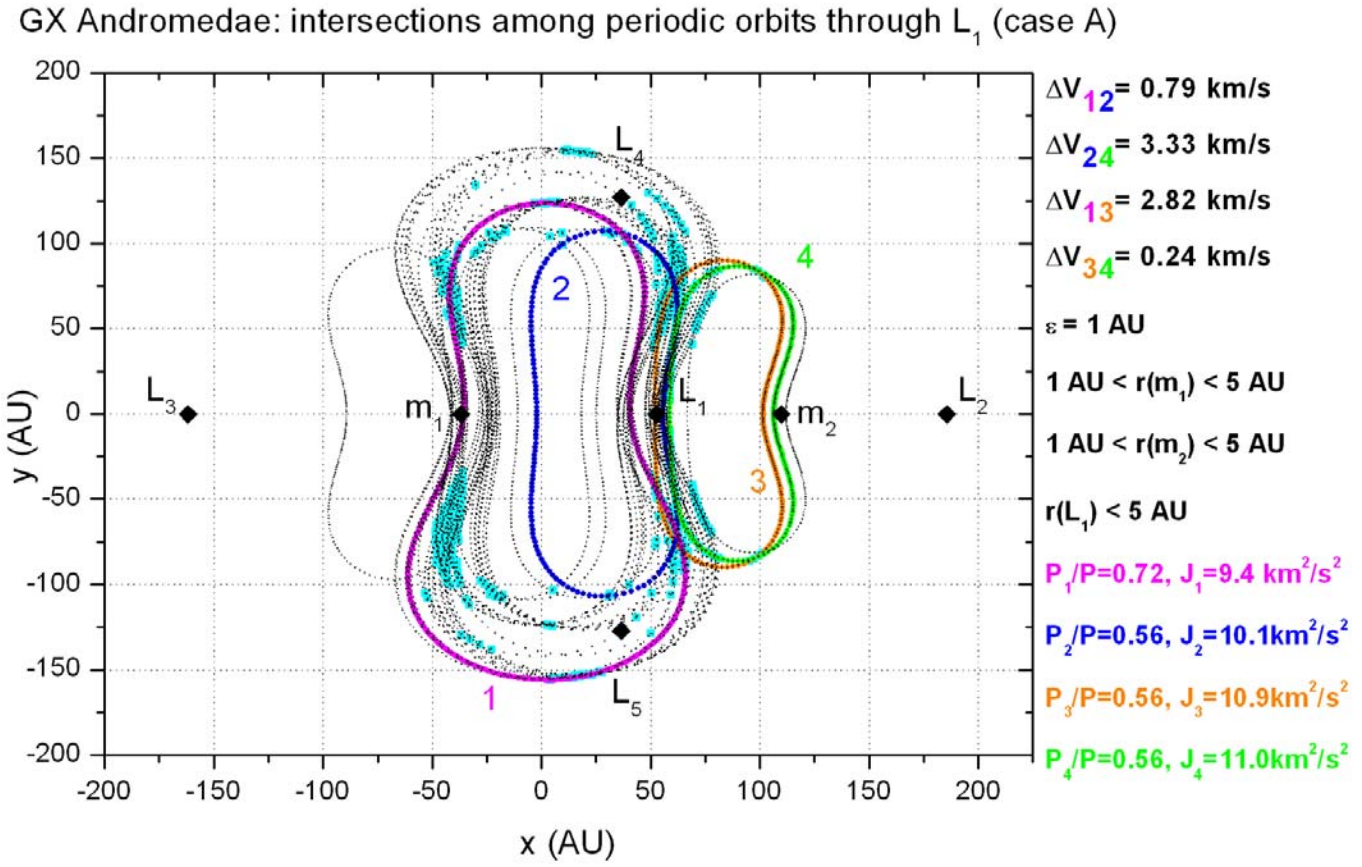

Figure 32: Planar intersecting periodic orbits (black curves) and their intersection points (cyan dots, the intersection tolerance ε equals 1 AU) in the GX Andromedae binary system represented in physical units in the barycentric rotating reference frame. Also shown are the positions of the 5 equilibrium points and the two stars (m_1 and m_2). Four orbits are coloured in magenta, blue, orange and green, indicating one orbit through m_1 (magenta), two orbits through L_1 (orange and blue) and one orbit through m_2 (green) respectively. These intersecting orbits satisfy the position selection criteria described in the legend, namely: the orbits through either of the two stars cross a ring of 1 AU internal radius and 5 AU external radius around the corresponding primary; the orbits through L_1 pass within 5 AU from L_1. A trajectory from the region around m_1 to the region around m_2 through the 1-2-4 chain requires two maneuvres of 0.79 and 3.33 km/s (total ΔV = 4.12 km/s); a trajectory of the same kind through the 1-3-4 connection costs (2.82+0.24) km/s = 3.06 km/s. The lower part of the legend provides the orbital periods of the four orbits in units of the binary system's orbital period and the values of the Jacobi integral.

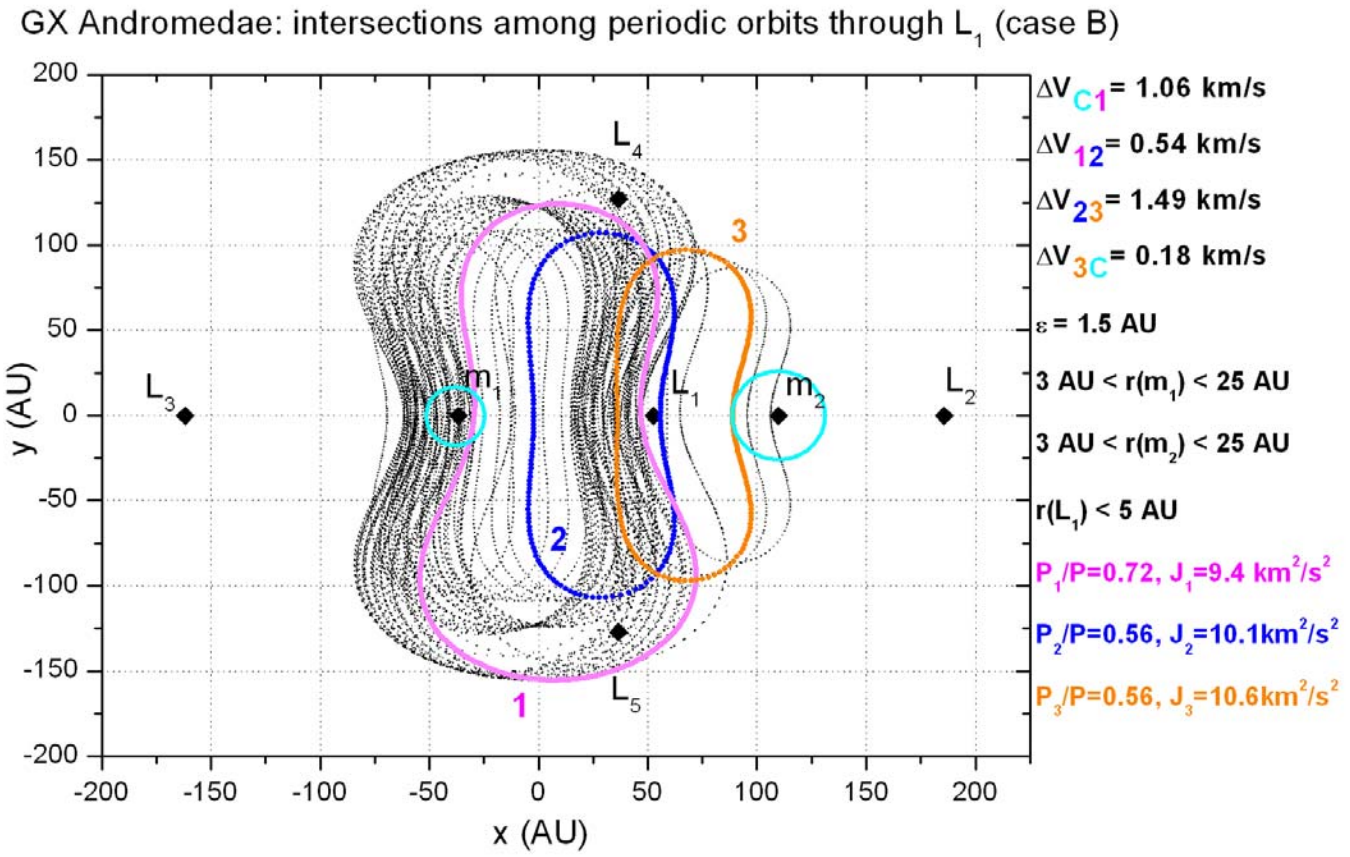

Figure 33: Planar intersecting periodic orbits (black curves) (the intersection tolerance ε equals 1.5 AU) in the GX Andromedae binary system represented in physical units in the barycentric rotating reference frame. Also shown are the positions of the 5 equilibrium points and the two stars (m_1 and m_2). Three orbits are coloured in magenta, blue and orange, indicating one orbit through m_1 (magenta), one orbit through L_1 (blue) and one orbit through m_2 (orange) respectively. These intersecting orbits satisfy the position selection criteria described in the legend, namely: the orbits through either of the two stars cross a ring of 3 AU internal radius and 25 AU external radius around the corresponding primary; the orbits through L_1 pass within 5 AU from L_1. A trajectory from a circular orbit around m_1 (cyan circle) to a circular orbit around m_2 (cyan circle) through the C-1-2-3-C chain requires four maneuvres; the total ΔV is 3.27 km/s. The lower part of the legend provides the orbital periods of the three selected orbits in units of the binary system's orbital period and the values of the Jacobi integral.

Other transfer cases can also be contemplated, for instance between two Lagrangian points. Orbits of this type have been investigated in (Gómez & Masdemont, 2000).

5.3.4 Binary systems with eccentric orbits

The remaining binary systems of our sample are characterized by large orbital eccentricities (between 0.2 and 0.6). In these situations the CR3BP paradigm can only be applied over small fractions of the system's orbital period (Szebehely, 1967). Since the orbits that AUTO2000 computes occupy a significant fraction of the system's orbital period, their use as branches of natural transfers is severely limited in the elliptic case.

The most appropriate framework for studying transfers within elliptic systems is the already mentioned Elliptic Restricted Three-Body Problem (ER3BP). The subject is much less investigated, as indicated by the smaller amount of dedicated papers. The main difference with the circular problem is that the dynamical system is non-autonomous (the Jacobi integral is missing). Then the equations of motion of the third body are coupled with the differential equations describing the pulsation of the distance between the primaries and the independent variable is usually taken to be the true anomaly rather than the time.

Finally, the problem contains two parameters – the eccentricity e and the mass ratio μ of the primaries – in contrast to the single-parameter μ of the circular problem. The extra parameter e adds one degree of freedom to the problem of finding periodic orbits. For given e and μ, only isolated periodic orbits (symmetric with respect to the x-axis) possibly exist in the elliptic problem because the periodicity criterion imposes that the x-axis crossing occurs when the two primaries are at an apse, thus leading to periods which are necessarily integer (hence discrete) multiples of the systems's orbital period (Broucke, 1972).

The computation of periodic orbits emanating from the equilibrium points of the ER3BP with AUTO2000 is not straightforward. Alternative techniques (like that adopted by Broucke (1972): numerical integration with recurrent power series) require nontrivial software development. Some examples of symmetric periodic orbits belonging to a mass-ratio of μ = 0.5 and to various eccentricity levels as obtained by Broucke (1972) are illustrated in Figure 34.

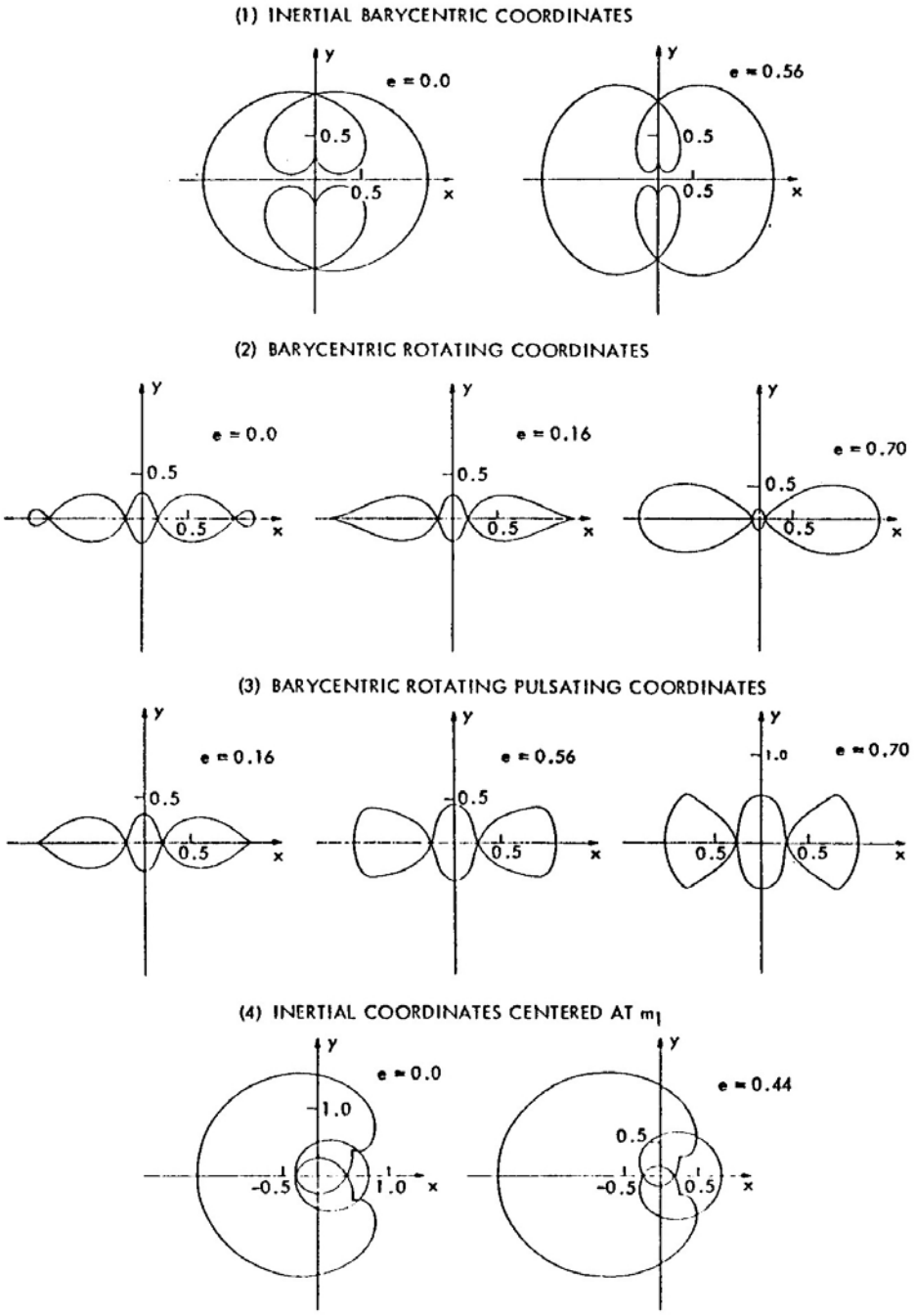

Figure 34: Some examples of symmetric periodic orbits belonging to a mass-ratio of μ = 0.5 and to various eccentricity levels (Broucke, 1972).

Benest (1988) made extensive numerical simulations within the frame of the ER3BP in order to search if stable orbits exist for planets around one of the two components in binary stars. In particular, he showed some results for the Alpha Centauri A/B system (Figure 35 and Figure 36). The existence of such stable orbits could be also exploited to place a spacecraft in orbit around one of the two stars.

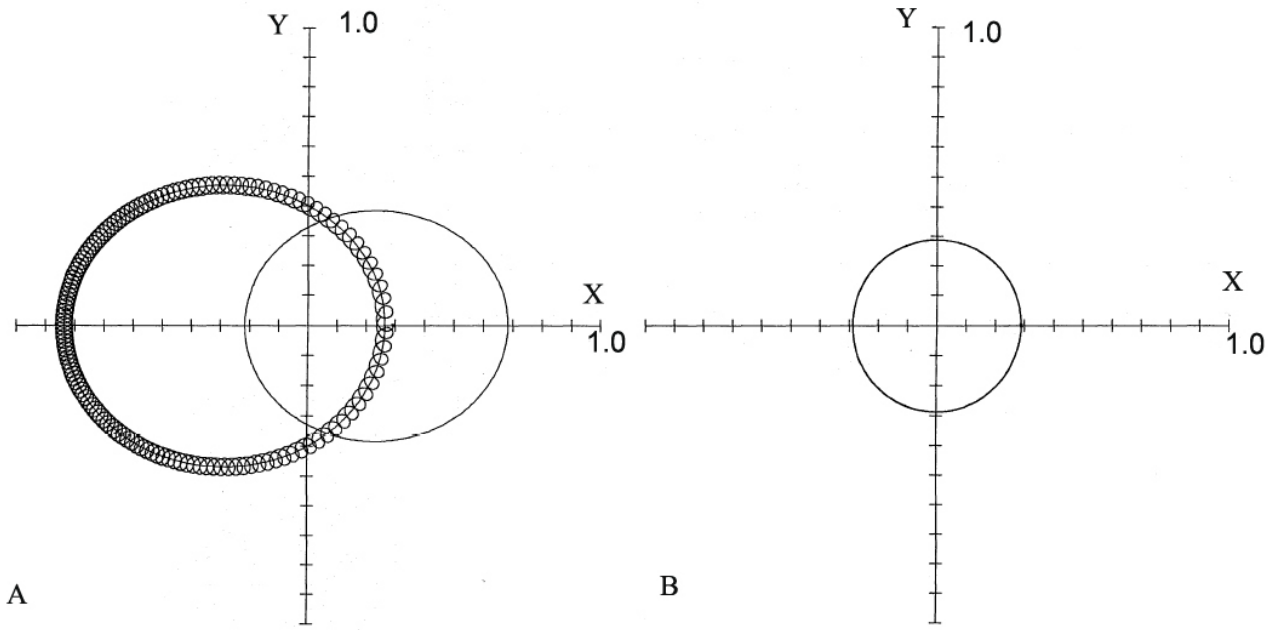

Figure 35: A nearby planetary orbit around Alpha Cen B, represented during one revolution of the binary; A: fixed axes with origin in the binary's barycentre, where the little and large ellipses are the orbits of Alpha Cen A and B; B: rotating frame with origin in Alpha Cen B. (Benest, 1988)

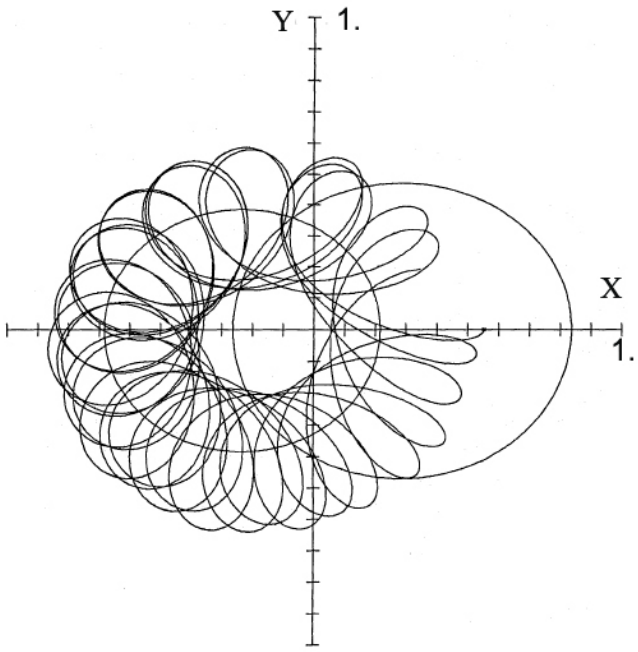

Figure 36: A remote planetary orbit around Alpha Cen A, represented during 5 revolutions of the binary; same notations as for the previous figure, same frame as for Figure 35 B.

5.4 Exploration phase: orbits within triple systems

The following privileged locations should be considered when designing a spacecraft trajectory for in-situ observation of triple systems:

a) trajectories connecting libration points of individual CR3BP or ER3BP—depending on the eccentricity values—known as Weak Stability Boundary transfers (WSB);

b) orbits around one of the component stars (or planetary companion);

c) transfers between solutions of the two types.

5.4.1 Weak Stability Boundary (WSB) transfers

In recent years a new impulse has been given to the design of interplanetary trajectories by the discovery of the so-called "Interplanetary Superhighway System" (IPS) (Lo & Ross, 2001), a system of natural routes that pervade interplanetary space and that can be exploited to accomplish transfers from one planet to another or to one of its moons at low cost. The idea has been already successfully applied to the lunar transfer of the Japanese spacecraft Hiten (1991) thanks to the design and optimization work performed by Miller & Belbruno (1991).

The dynamics of this class of trajectories (also called Weak Stability Boundary (WSB) transfers) has been well explained in the works by Koon et al. (2001) and by Circi & Teofilatto (2001): in principle, the transfer from the Earth to the Moon takes place in the framework of the Sun-Earth-Moon-Spacecraft 4-Body Problem, but can be explained on the basis of two *coupled* Circular Restricted Three-Body Problems (i.e., Sun-Earth-Spacecraft and Earth-Moon-Spacecraft). Within each CR3BP system invariant manifold structures (surfaces of constant energy in phase space) are associated with each libration point. In particular the L_1, L_2 and L_3 libration points are each characterized by one stable and one unstable manifold, respectively leading to, and originating from the periodic Lyapunov orbit (Koon et al., 2001).

Weak Stability Boundary transfers to the Moon exploit the existence of intersections in space and time between invariant manifolds of the two CR3BP problems, allowing the design of low-cost trajectories through the region of the Earth's L_1 and the region of the lunar L_2. Considerable fuel savings (up to 200 m/s) with respect to the classical Hohmann or bielliptic transfers can be obtained with lunar transfer trajectories of this new type because the energy levels of the Earth's L_1 and L_2 differ by little from the energy levels of the lunar counterparts. The price is a longer time of flight: 60-100 days vs. 6-7 days of Hohmann trajectories (Circi & Teofilatto, 2001; Miller & Belbruno, 1991).

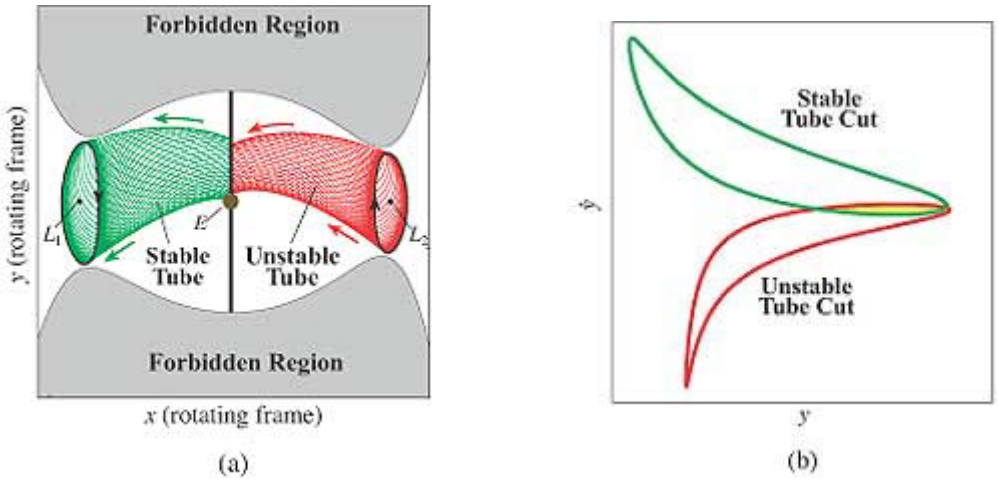

Figure 37: (a) The plane of the Earth's orbit in Sun-Earth synodic coordinates showing the stable and unstable manifolds respectively around L_1 and L_2 and the corresponding halo orbits; the forbidden region cannot be reached with the energy pertaining to the halo orbits. (b) A Poincarè cut passing through Earth in the y-direction: switching from one manifold to another is possible at their intersections.

Further studies have shown that WSB transfers can be found leading to other destinations within our planetary system: to Mars, to the outer planets, to transfers between Jupiter and Saturn. "Petit Grand Tour" (Lo, 2001) is the name given by Martin Lo and collaborators to a system of itineraries that serially tour the satellite system of any planet, to capture into orbit, depart or land onto the various satellites. An example is the transfer from Ganymede to capture around Europa. The trajectory of the Genesis spacecraft, launched in 2001, has used this kind of strategy (Howell et al., 1997) to reach a halo orbit around the Sun-Earth libration point L_1 (Figure 37).

Furthermore, the IPS may constitute a new tool to understand many aspects of the dynamical behaviour of the Solar System (Lo & Ross, 2001): resonance properties of WSB transfers have interesting applications to the motions of Kuiper Belt objects outside the orbit of Neptune. Other studies have shown that comets closely follow IPS paths and, in particular, the temporary capture phenomenon of Jupiter comets seems to be controlled by Jupiter's IPS generated by its Lagrange points. The IPS may also play an important role in the control of the motions of the Asteroid Belt, the Kuiper Belt, the planetary rings and the zodiacal dust tori.

In principle, using one of the periodic orbits computed by AUTO2000 as starting point, the invariant manifolds associated to the corresponding equilibrium position could be found by applying small variations in phase space (position, velocity) to it and by numerically integrating backward and forward in time from the resulting initial conditions. Then, intersections in phase space between invariant manifolds connecting different boundary regions could be searched for and their characteristics investigated with an aim at designing low-cost transfer trajectories.

5.4.2 Are WSB transfers applicable to star systems in the Solar Neighbourhood?

In Section 4 we have presented and discussed the available information on the orbital characteristics of the closest known triple systems of our dataset, namely EZ Aquarii and Epsilon Indi[4]. The list could be extended to include the two known cases of planetary systems (Epsilon Eridani and Gliese 876), since they are both made up of three objects each. The question of the applicability of the WSB orbit design technique to these systems must take into account that their orbits are *highly eccentric*, while the present WSB paradigm has only been applied to coupled *Circular* R3B problems.

It is not clear that this technique is adequate to the cases at hand. It is likely that it must be properly extended to the *Elliptic* R3BP along lines which are yet to be identified.

6 CONCLUSIONS AND IDEAS FOR FUTURE WORK

The investigations performed in this study have clarified a number of issues pertaining to the dynamics of the stars in the Solar Neighbourhood and the design of the trajectories to first reach them and then tour their environs. We have seen that

1. The stars behave as *non-interacting particles*, subject only to the force exerted by the Galaxy as a whole. We have verified this by direct numerical integration of the motion of an ensemble of stars subject only to their mutual gravitational interactions and then subject only to the galactic potential. Over several thousand years (a small fraction of the galactic rotation period which at solar position is about 250 My) their trajectories are effectively identical and with respect to the Sun can be modeled as straight-line orbits.

[4] Following the discussion made in Section 4.1, we prefer to treat Alpha Centauri as a double star experiencing a hyperbolic encounter with Proxima Centauri.

2. The configuration of stars currently constituting the Solar Neighbourhood is bound to disrupt, not being gravitationally bound as a subsystem. Therefore, the picture of the Solar Neighbourhood changes completely over timescales much shorter than the Sun's galactic rotation period.
3. Intersections among stellar spheres of influence are extremely rare events and do not imply that stars that happen to be close to one another are gravitationally bound. As an example, the available measurements suggest that the long-debated relationship between Proxima Centauri and Alpha Centauri A/B is nothing but a hyperbolic passage of the former in the gravitational field of the latter.
4. An exploration probe interacts with the stars only when it enters their spheres of influence, allowing to conclude that the known dynamical paradigms like the Circular Restricted Three-Body Problem (CR3BP) or the Two Fixed Centers (TFC) *do not* apply to the cruise phase of interstellar flight: this implies that no critical points exist between nearby stars.
5. The absence of interactions between nearby stars and between either star and a probe travelling between them has two important consequences: a) that by properly imparting velocity impulses, a spacecraft can be stably positioned anywhere outside the spheres of influence of these stars, and b) that travel between the stars can occur on rectilinear orbits.
6. Limiting the time of flight of the transfer journey to the scale of human lifetime requires high speeds and these, in turn, require high energy propulsion, most likely by means of continuous thrust: under a constant acceleration of 0.5 m/s^2 it takes 18.4 years of (terrestrial) coordinated time (or 17.8 years of proper time) to arrive at Proxima Centauri with a rocket reaching relativistic speeds of the order of 0.4 *c*; adding the 4.3 years necessary for the data to be transmitted back to Earth gives a total mission duration of less than 23 years. As noted above, the transfer trajectory is a rectilinear orbit.
7. Our knowledge of the internal dynamics of the stellar systems that populate the Solar Neighbourhood remains incomplete, as demonstrated by the large uncertainties often affecting the determination of many astrometric and physical parameters. This is especially important when trying to identify the dynamical evironment that an interstellar exploration probe will find when reaching the destination star system.
8. The exploration phase can be separately addressed for single, binary and triple systems.

    8a. In the case of a single star the only option is to put the spacecraft into an orbit around the star. While on the transfer orbit, the star could also be observed, so there appears to be no need to stop in the far distance before proceeding to the rendez-vous, which could be energetically demanding. It is also possible to perform a flyby of the star while on route to another target.

    8b. Binary systems offer several options: orbits around the consituent stars, orbits around the Lagrangian points, transfer orbits between these. For the case of binaries in circular relative orbits the problem can be addressed drawing from a large knowledge base which includes the design of periodic orbits (also by continuation methods) and of transfer orbits between critical points. We made a preliminary design of low-cost ($\Delta V \approx 3$ km/s) transfers between circular orbits around the two primaries of the GX Andromedae system following branches of periodic orbits connecting through the (intermediate) Lagrangian point L_1. The more general and ubiquitous case of non-zero eccentricity requires further development under the Elliptic Restricted Three-Body Problem.

    8c. Triple systems are characterized by highly eccentric orbits and, except for periodic orbits around each of the bodies, other options remain unexplored due to the unavailability of applicable dynamical paradigms.

The analysis carried out within this study has also identified a number of items that deserve further investigation from the viewpoint of trajectory design:

- Solar System escape strategy including attainment of relativistic speed with special regard to the acceleration phase (relationship between proper and coordinated time);
- Verification by simulation of attainability of generic positions (considered wither as final targets of more likely as intermediate stops of longer missions) outside stellar spheres of influence and associated energy consumption;
- In-depth study of the Elliptical Restricted Three-Body Problem in connection with the identification of transfer orbit design between its pulsating critical points. In this respect, new software tools need to be developed due to the inadequacy of those currently, freely available.

7 REFERENCES

Allen, C., Santillán, A. (1991): *An improved model of the galactic mass distribution for orbit computations*, Rev. Mexicana Astron. Astrof., **22**, 255-263.

Anosova, J., Orlov, V. (1995): *Dynamics of the Alpha Cen system*, IAU Symposium no.166.

Axford, W.I., Suess, S.T.: *The Heliosphere*, from:

http://web.mit.edu/space/www/helio.review/axford.suess.html

Banfi, V. (2000): *Relatività e Astrodinamica*, Levrotto & Bella, Torino.

Benest, D., Duvent, J.L. (1995): *Is Sirius a triple star?*, Astron. Astrophys., **299**, 621-628.

Benest, D. (1988): *Planetary orbits in the elliptic restricted problem. I. The α Centauri system*, Astron. Astrophys., **206**, 143-146.

Binney, J., Tremaine, S. (1988): *Galactic Dynamics*, Princeton University Press.

Bond, A., Martin, A. R., Buckland, R. A., Grant, T. J., Lawton, A. T., et al. (1978): *Project Daedalus*, Journal of the British Interplanetary Society, **31** (Supplement).

Broucke, R. (1972): *On the Elliptic Restricted Three-Body Problem*, The Journal of the Astronautical Sciences, **9**, 6, 417-432.

Brower, D., Clemence, G. (1961): *Methods of Celestial Mechanics*, Academic Press, New York.

Campbell, B., Walker, G.A., Yang, S. (1988): *A search for planetary mass companions to nearby stars*, in Bioastronomy - The next steps, Proceedings of the Ninety-ninth IAU Colloquium, Balaton, Hungary, June 22-27, 1987; Dordrecht, Kluwer Academic Publishers, 83-90.

Carraro, G., Chiosi, C. (1994): Galactic orbits of the old open clusters NGC 188, NGC 2682, NGC 2420, NGC 752 and NGC 2506, Astron. Astrophys., **288**, 751-758.

Circi, C., Teofilatto, P. (2001): *On the dynamics of weak stability boundary lunar transfers*, Celest. Mech. & Dyn. Astr., **79**, 41-72.

Cornish, N.J.,Goodman, J.: *lagrange.ps,* document available from:

http://spiff.rit.edu/classes/phys440/lectures/lagrange/

Creze, M., Chereul, E., Bienayme, O., Pinchon, E. (1998*): The distribution of nearby stars in phase space mapped by Hipparcos. I. The potential well*, Astron. Astrophys., **329**, 920-936.

Danby, J.M.A (1962): *Fundamentals of Celestial Mechanics*, Willman-Bell.

Delfosse, X., Forveille, T., Udry, S., Beuzit, J.-L., Mayor, M., Perrier, C. (1999): *Accurate masses of very low mass stars. II. The very low mass triple system Gl 866*,Astron. Astrophys., **350**, 39-42.

Dichman, D.J., Doedel, E.J., Paffenroth, R.C. (2002): *The computation of periodic solutions of the 3-body problem using the numerical continuation software AUTO*, International Conference on Libration Point Orbits and Applications, Aiguablava, Spain, 10-14 June, 2002.

Dole, S.H. (1964): *Habitable Planets for Man*, Blaisdell Publishing Company, New York.

Ducourant, C., Dauphole, B., Rapaport, M., Colin, J., Geffert, M. (1998): *Wide field search for nearby faint stars*, Astron. Astroph., **333**, 882-892.

ESA (1997): *The Hipparcos and Tycho Catalogues*, ESA SP-1200.

Forward, R.L. (1985): *Starwisp: An Ultra-Light Interstellar Probe*, J. Spacecraft, **22**, 3, 345-350.

Geballe, T.R. et al. (2002): *Toward Spectral Classification of L and T Dwarfs: Infrared and Optical Spectroscopy and Analysis*, ApJ, **564**, 466-481.

Geyer, D.W., Harrington, R.S., Worley, C.E. (1988): *Parallax, orbit, and mass of the visual binary L726-8*, ApJ, **95**, 6, 1841-1842.

Girard, T.M., Lee, J.T., Dyson, S.E., van Altena, W.F., Horgh, E.P., Gilliland, R.L., Schaefer, K.G., Bond, H.E., Ftaclas, C., Brown, R.H., Toomwy, D.W., Shipman, H.L., Provencal, J.L., Pourbaix, D. (2000): *A redetermination of the mass of Procyon*, ApJ, 119, 2428-2436.

Gliese, W., Jahreiss, H. (1989): *The Third Catalogue of Nearby Stars. I. General View and Content*, in: Star Catalogues: a Centennial Tribute to A.N. Vyssotsky, Proc. Meeting IAU Comm. 24, Baltimore, MD, USA, 5 August 1988; A.G.D. Philip, A.R. Upgren (eds.), L. Davis Press, Schenectady, NY.

Gliese, W., Jahreiss, H. (1991a): Preliminary Version of the Third Catalogue of Nearby Stars, on: The Astronomical Data Center CD-ROM: Selected Astronomical Catalogs, Vol. I; L.E. Brotzmann, S.E. Gesser (eds.), NASA/Astronomical Data Center, Goddard Space Flight Center, Greenbelt, MD.

Gliese, W., Jahreiss, H. (1991b): *The Third Catalogue of Nearby Stars – Errors and uncertainties*, Astronomisches Rechen-Institut Heidelberg, Mitteilungen, Series A, **224**, 161-164.

Hartkopf, W.J., Mason, B.D., Worley, C.E. (2001): *The 2001 US Naval Observatory Double Star Cd-Rom II. The Fifth Catalog of Orbits of Visual Binaries*, Astron. Journal, **122**, 3472-3479.

Hatzes, A.P., Cochran, W.D., McArthur, B., Baliunas, S.L., Walker, G.A.H., Campbell, B., Irwin, A., Yang, S., Kurster, M., Endl, M., Els, S., Butler, R.P., Marcy, G.W. (2000): *Evidence for a long-period planet orbiting ε Eridani*, ApJ, **544**, 145-148.

Henry, T. J., McCarthy, D.W. (1993): *The mass-luminosity relation for stars of mass 1.0 to 0.08 solar mass*, Astron. Journal, **106**,2, 773-789.

Henry, T. J., Backman, D.E., Blackwell, J., Okimura, T. (2000): *Nearby Stars (Nstars) Research*, Bulletin of the American Astronomical Society, **32**, 1596.

Holberg, J.B., Barstow, M.A., Bruhweiler, F.C., Cruise, A.M., Penny, A.J. (1998): *Sirius B: a new, more accurate view*, ApJ, **497**, 935-942.

Howell, K.C., Barden, B.T., Wilson, R.S., Lo, M.W. (1997): *Trajectory design using a dynamical systems approach with application to Genesis*, AAS/AIAA Astrodynamics Specialist Conference, Sun Valley, Idaho, AAS 97-709.

Irwin, A., Murray Fletcher, J., Yang, L.S., Walker, G.A.H., Goodenough, C. (1992): *The Orbit and mass of Procyon*, PASP, **104**, 489-499.

Jahreiss, H., Gliese, W. (1993): *The Third Catalogue of Nearby Stars - Results and Conclusions*, in: Developments in Astrometry and Their Impact on Astrophysics and Geodynamics. Proc. IAU Symp. 156, Shanghai, China, 15-19 September 1992; I.I. Mueller, B. Kolaczek (eds.), Kluwer, Dordrecht, 107-112

Jahreiss, H., Gliese, W. (1989): *The Third Catalogue of Nearby Stars. II. Applied Methods and Use*, in: Star Catalogues: a Centennial Tribute to A.N. Vyssotsky, Proc. Meeting IAU Comm. 24, Baltimore, MD, USA, 5 August 1988; A.G.D. Philip, A.R. Upgren (eds.), L. Davis Press, Schenectady, NY.

Jahreiss, H., Gliese, W. (1985): *Radial Velocities of Nearby Stars*, Bull. Inf. Cent. Donnees Stellaires, **28**, 19.

Koon, W.S., Lo, M.W., Marsden, J.E., Ross, S.D. (2001) : *Low energy transfer to the Moon*, Celest. Mech. & Dyn. Astr, **81**, 63-73.

Kovacs, N., Foy, R. (1978): *A Detailed Analysis of the Three Stars in the Eggen's ε Indi Moving Group*, Astron. Astrophys., **68**, 27-31.

Kuijken, K., Gilmore, G. (1991): *The galactic disk surface mass density and the Galacti Force K(z) at Z = 1.1 kiloparsecs*, Astrophysical Journal Letters, **367**, 9-13.

Lo, M.W. (2001): *Petit Grand Tour: Mission concepts to outer planets satellites using non-conic low energy trajectories*, Forum on Innovative Approaches to Outer Planetary Exploration 2001-2020, February 21-22, Lunar and Planetary Institute, Houston, Texas.

Lo, M.W., Ross, S.D.: 2001, 'The Lunar L_1 Gateway: Portal to the Stars and Beyond', *AIAA Space 2001 Conference*, August 28-30, Albuquerque, New Mexico.

Marcy, G., Butler, P., Fischer, D., Vogt, S., Lissauer, J., Rivera, E. (2001): *A Pair of Resonant Planets Orbiting GJ 876*, ApJ, **556**, 296-301.

Marcy, G.W., Butler, R.P., Vogt, S.S., Fischer, D., Lissauer, J. (1998): *A planetary companion to a nearby M4 dwarf, Gliese 876*, ApJ, **505**, 147-149.

Matthews, R., Gilmore, G. (1993): *Is Proxima really in orbit about α Cen A/B?*, Mon. Not. R. Astron. Soc., **261**, 5-7.

McAdams, J.V., McNutt, R.L. (2002): *Ballistic Jupiter Gravity-Assist, Perihelion-ΔV Trajectories for a Realistic Interstellar Explorer*, AAS/AIAA Space Flight Mechanics Meeting, San Anonio, Texas, January 2002, Paper AAS 02-158.

McCaughrean, M.J., Close, L.M., Scholz, R.-D., Lenzen, R., Biller, B., Brandner, W., Hartung, M., Lodieu, N. (2004): *ε Indi Ba, Bb: the nearest binary brown dwarf*, Astron. Astrophys., **413**, 1029-1036.

McNutt, R.L. (1999): *A Realistic Interstellar Explorer*, Phase I Final Report, NASA Institute for Advanced Concepts.

McNutt, R.L. (2003): *A Realistic Interstellar Explorer*, Phase II Final Report, NASA Institute for Advanced Concepts.

Mihalas, D., Binney, J. (1981): *Galactic Astronomy*, Princeton University Press.

Miller, J.K., Belbruno, E.A. (1991): *A method for the construction of a lunar transfer trajectory using ballistic capture*, AAS/AIAA Space Flight Mechanics Meeting, Houston, Texas, AAS 91-100.

Murdoch, K., Hearnshaw, J.B. (1993): *The spectroscopic mass ratio of the Alpha CEN system*, The Observatory, **113**, 79-81.

Murray, C.A. (1989): *The transformation of coordinates between the systems of B1950.0 and J2000.0 and the principal galactic axes referred to J2000.0*, Astron. Astrophys., **218**, 325-329.

Paffenroth, R.C. (2002): *Continuation of Periodic Orbits Around Lagrange Points and AUTO2000*, presentation, February 19, 2002.

Quillen, A.C., Thorndike, S. (2002): *Structure in the ε Eridani dusty disk caused by mean motion resonances with a 0.3 eccentricity planet at periastron*, ApJ, **578**, 149-152.

Roy, A.E. (1978): *Orbital Motion*, Adam Hilger, Bristol.

Scholz, R.-D., McCaughrean, M. J., Lodieu, N., Kuhlbrodt, B. (2003): *ε Indi: A new benchmark t dwarf**, Astron. Astroph., **398**, 29-33.

Smart, W.M. (1938): *Stellar Dynamics*, Cambridge University Press.

Söderhjelm, S. (1999): *Visual binary orbits and masses POST HIPPARCOS*, Astron. Astroph., **341**, 121-140.

Spitzer, L. (1985): *Average density along interstellar lines of sight*, ApJ, **290**, 21-24.

Strand, K. (1951): *The Orbit and Parallax of Procyon*, ApJ, **113**, 1-20.

Tinney, C.G. (1996): *CCD astrometry of southern very low-mass stars*, Mon. Not. R. Astron. Soc., **281**, 2, 644-658.

van Altena, W.F., Lee, J.T., Hoffleit, E.D. (1995): *The general catalogue of trigonometric parallaxes*, Yale University Observatory, 4th ed.

van Altena, W., Hoffleit, D. (1996): *Yale Parallax Catalogue*, van Altena, Lee and Hoffleit.

van de Bos, W.H. (1960): *The orbit of Sirius, ADS 5423*, Journal des Observateurs, 43, 10, 145-151.

van Leeuwen, F. (1997): *The HIPPARCOS mission*, Space Sci. Rev., **81**, 3/4, 201-409.

Whittaker, E.T. (1937): *A treatise on the analytical dynamics of particles and rigid bodies*, Cambridge University Press (reissued 1988).

Woitas, J., Leinert, Ch., Jahreiss, H., Henry, T., Franz, O.G., Wasserman, L.H. (2000): *The nearby M-dwarf system Gliese 866 reviseted*, Astron. Astrophys., **353**, 253-256.

Zagar, F. (1984): *Astronomia sferica e teorica*, Zanichelli, Bologna.

Zakhozhaj, V.A. (1998): *Nearest stars until 10 pc, Zakhozhaj (1979-1996)*, VizieR Online Data Catalogue (5101).

8 BIBLIOGRAPHY

Bond, A., Martin, A. R. (1975): *Project Daedalus: The Origins and Aims of the Study*, Journal of the British Interplanetary Society, **28** (3), 147-149.

Gómez, G., Koon, W.S., Lo, M.W., Marsden, J.E., Ross, S.D. (2001): *Invariant Manifolds, the Spatial Three-Body Problem and Space Mission Design*, paper AAS 0-301.

Gómez, G., Masdemont, J. (2000): *Some zero cost transfers between libration points*, Paper AAS 00-177.

Lo, M.W., Rodney, L.A., Whiffen, G., Romans, L. (2004): *The role of invariant manifolds in low thrust trajectory design*, paper AAS 04-288.

Ross, S.D., Koon, W.S., Lo, M.W., Marsden, J.E. (2004): *Application of Dynamical Systems Theory to a Very Low Energy Transfer*, paper AAS 04-289.